

NATIONAL LIBRARY

OTTAWA



CANADA

BIBLIOTHÈQUE NATIONALE

OTTAWA

NAME OF AUTHOR.....SHYAM.....MOHAN.....KHANNA.

TITLE OF THESIS.....Electron Tunneling into.....  
.....Superconducting Lanthanum.....  
.....

UNIVERSITY.....Alberta.....

DEGREE.....Ph.D.....YEAR GRANTED.....1968.....

Permission is hereby granted to THE NATIONAL  
LIBRARY OF CANADA to microfilm this thesis and to  
lend or sell copies of the film.

The author reserves other publication rights,  
and neither the thesis nor extensive extracts from  
it may be printed or otherwise reproduced without  
the author's written permission.

(Signed).....Smkhanna.....

PERMANENT ADDRESS:

Physics Department,  
.....  
Ottawa University,  
.....  
Ottawa 2..  
.....

DATED.....4.2.....1969.

THE UNIVERSITY OF ALBERTA

ELECTRON TUNNELING INTO SUPERCONDUCTING LANTHANUM

BY

SHYAM MOHAN KHANNA

A THESIS

SUBMITTED TO THE FACULTY OF GRADUATE STUDIES IN  
PARTIAL FULFILMENT OF THE REQUIREMENTS FOR THE  
DEGREE OF DOCTOR OF PHILOSOPHY


DEPARTMENT OF PHYSICS

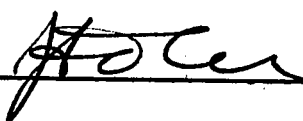
EDMONTON, ALBERTA

JULY, 1968


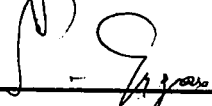
UNIVERSITY OF ALBERTA  
FACULTY OF GRADUATE STUDIES

The undersigned certify that they have read, and recommend to the Faculty of Graduate Studies for acceptance, a thesis entitled "ELECTRON TUNNELING INTO SUPERCONDUCTING LANTHANUM", submitted by Shyam Mohan Khanna in partial fulfilment of the requirements for the degree of Doctor of Philosophy.

  
\_\_\_\_\_  
Supervisor

\_\_\_\_\_  


  
\_\_\_\_\_

  
\_\_\_\_\_  
  
External Examiner

Date 10 Sept. 1968

ABSTRACT

Since the pioneering work of Giaever (1960 a,b), the electron tunneling technique has been successfully applied for studying the properties of superconductors and 'phonon-induced structure' in the tunneling density of states has been observed in several superconductors. It emphasizes that the electron-phonon interaction is responsible for superconductivity of these metals.

It has been suggested that the superconductivity of lanthanum may largely be due to an attractive interaction other than the phonon-mediated electron-electron interaction (Kondo, 1963; Hamilton and Jensen, 1963; Kuper et al., 1964).

We have observed structure in the tunneling density of states of superconducting lanthanum using thin film tunnel junctions which may be attributed to a poorly developed phonon spectrum in the portion of the lanthanum film sampled by the tunneling experiment. These are the first published data on structure in the tunneling density of states of lanthanum. These results are in accord with the present theories of superconductivity and indicate that the electron-phonon interaction may be largely responsible for superconductivity of lanthanum. However, from our results, it is not possible to absolutely exclude the possibility that the superconductivity of

lanthanum may be due to some other mechanism(s).

The energy gap, the transition temperature and the gap ratio of lanthanum have also been measured by this technique. The surface layer of lanthanum adjoining the barrier was found to play an important role in these measurements. There was little evidence of the second energy gap predicted by Kuper et al. More detailed work is, however, necessary to check this aspect.

Zero-bias anomalies have been observed in junctions of thin films of aluminum and lanthanum. These results are the first report of such large anomalies in these junctions. The results for the superconducting properties of lanthanum and the zero-bias anomalies in these junctions are in agreement with other published results. These results suggest that the properties of the metal-metal oxide interfaces in the junction are responsible for the zero-bias anomalies. Large zero-bias anomalies occurred at the same time as marked degradation of the superconducting properties of the lanthanum film sampled by the tunneling experiment.

## ACKNOWLEDGEMENTS

It gives me great pleasure to thank Dr. S.B. Woods, my research supervisor, for his cheerful encouragement and guidance throughout the course of this project. His hopeful attitude has been of much value to me.

Special thanks are due to Dr. J.S. Rogers whose association with this project was of much help.

I also wish to thank Dr. J.P. Franck for many valuable discussions pertaining to this project.

I am also thankful to the Low Temperature technical staff, and in particular, Mr. H. McClung, for supplying the necessary liquid helium and for dealing with my various problems in a co-operative manner.

Financial support, mainly of the National Research Council and partly of the Physics Department, is gratefully acknowledged.

Finally, I am most grateful to my wife Savitri whose interest in this work encouraged me during the difficult stages of the experiment; and also for much help in preparation of this thesis.

# TABLE OF CONTENTS

<u>Chapter</u>	<u>Page</u>
I. INTRODUCTION	1
1.1. Motivation	1
II. MICROSCOPIC THEORIES OF SUPERCONDUCTIVITY	7
2.1. The BCS Theory	7
2.2. The Superconductor at Finite Temperatures	12
2.3. Modifications to the BCS Theory	17
2.4. Two-Band Models of a Superconductor	21
2.5. Theories of a Two-Band Superconductor	25
III. ELECTRON TUNNELING IN METALS	36
3.1. Theory of Electron Tunneling	37
(i) Normal-Normal Case $i_{nn}$	38
(ii) Normal-Superconductor Case $i_{ns}$	39
(iii) Superconductor-Superconductor Case $i_{ss}$	41
3.2. Phonon Density of States and the Tunneling Conductance	43
3.3. Zero-Bias Tunneling Anomalies in the n-n Systems	46
3.4. Appelbaum Magnetic Scattering Model	50
IV. EXPERIMENTAL METHOD	57
4.1. Sample Preparation	57
A. Al-I-La Junction	57
(i) The Base Layer	59
(ii) The Barrier Layer	59

(iii)	The Cover Layer	61
B.	<del>La-I-Al</del> Junction	62
4.2.	General Considerations in Lanthanum Thin Film Preparation	63
4.3.	Electrical Measurements	66
A.	Harmonic Detection Circuit	67
B.	Conductance Calibration	71
4.4.	Production of Low Temperatures	74
4.5.	Description of a Typical Run	77
V.	EXPERIMENTAL RESULTS AND DISCUSSIONS	80
5.1.	Phonon Effects in Tunneling Density of States in Lanthanum	81
5.2.	The Energy Gap in Superconducting Lanthanum.	92
5.3.	Zero-Bias Tunneling Anomalies in the n-n Tunnel Junctions	106
A.	ZBA in Al-I-La Junctions	107
B.	ZBA in La-I-Al Junctions	112
VI.	CONCLUSIONS	118
6.1.	Results for Superconducting Lanthanum	118
6.2.	Results on Zero-Bias Anomalies	120
APPENDIX		
A.	Reprint	
BIBLIOGRAPHY		121



## LIST OF FIGURES

<u>Figure</u>	<u>Page</u>
2.1 Diagram showing the density of states in a superconductor and a normal metal near the Fermi energy.	13
2.2 Temperature dependence of the energy gap in a superconductor.	18
2.3 Energy dependence of the energy gap in a superconductor.	22
(a) Plot of the constant energy gap of the BCS theory.	
(b) Computed real and imaginary parts of the complex gap function $\Delta = \Delta_1 + i\Delta_2$ as a function of energy (after Scalapino et al., 1965).	
2.4 Temperature dependence of the energy gap pairs (after Suhl et al., 1959). The various symbols have the usual meanings.	35
(a) The energy gaps, $\Delta_d$ (solid curve) and $\Delta_s$ (dashed curve), for $v^{ss} = v^{dd} = 0$ , $v^{sd} \sqrt{N_s N_d} = 1/3$ and various ratios of densities of states.	
(b) For $v^{sd} = 0$ , there are two transition temperatures. For small but finite value of $(v^{sd})^2$ , the lower $T_c$ is smoothed out.	
3.1 Energy diagrams, illustrating the density of states near the Fermi level, occupation of	40

states,  $i$ - $v$  characteristic and  $\frac{di}{dv} - v$  characteristic for the normal-superconductor case of a tunnel junction.

- 3.2 Voltage dependence of conductance at different temperatures for a tunnel junction showing ZBA (after Shen and Rowell, 1968). 48
- 3.3 Voltage dependence of  $\Delta g(v)$  (solid line) and temperature dependence of  $\Delta g(0)$  (squares) for a tunnel junction showing ZBA (after Shen and Rowell, 1968). 49
- 3.4 Schematic representing the different tunneling processes that contribute to the theoretical conductance of the Appelbaum model. Here  $G$  corresponds to  $g$  in the text. 51
- 3.5 Schematic representing the same processes of Fig. 3.4 under the influence of an external magnetic field. Here  $G$  corresponds to  $g$  in the text. 54
- 3.6  $g$ - $v$  characteristics for different tunnel junctions at  $1.5^\circ\text{K}$  (after Shen and Rowell, 1968). Here  $G$  corresponds to  $g$  in the text. 55
- 4.1 Diagram showing the Al-I-La tunnel junction pair. A and B are the aluminum films and C is the lanthanum film. Wide evaporated contact pads are also shown. 58
- 4.2 Schematic showing the glow discharge apparatus for the barrier preparation. 60

4.3	Simplified harmonic detection bridge circuits.	68
4.4	The bridge circuit.	72
4.5	The dewar arrangement for the low temperature production.	75
5.1	Normalized first-derivative ( $g = \frac{di}{dv}$ ) and second-derivative results for an Al-I-La tunnel junction at $2.05^{\circ}\text{K}$ . The dashed curve is the BCS density of states for La. $g_s$ and $g_n$ in this diagram correspond to $g_{ns}$ and $g_{nn}$ in the text.	84
5.2	Normalized dynamic conductance $\sigma$ vs. voltage $v$ characteristics at different temperatures for the specimen La-18.	86
5.3	$S$ (as defined in Eqn. (5.1 -1) vs. $\Delta^2$ plot for the specimen La-18.	87
5.4	$g_{ns}$ - $v$ plots for an Al-I-La tunnel junction at two different temperatures. The aluminum probe is normal in trace 1 and superconducting in trace 2.	91
5.5	Normalized dynamic conductance $\sigma$ vs. voltage $v$ in the energy gap region for an Al-I-La tunnel junction. The dashed curve is the calculated curve based upon the Bermon's tables.	95
5.6	Temperature variation of the energy gap for lanthanum. The dashed curve is the BCS prediction	105
5.7	Voltage dependence of conductance for an	110

	Al-I-La tunnel junction showing zero-bias anomaly at different temperatures.	
5.8	Voltage dependence of conductance for an Al-I-La tunnel junction. As the temperature is decreased, the dip in conductance at zero bias changed to a temperature dependent peak in conductance at zero bias as shown earlier in Figure 5.7.	111
5.9	Voltage dependence of conductance for a La-I-Al tunnel junction.	114
5.10	Voltage dependence of dynamic resistance for two La-I-Al tunnel junctions.	115
5.11	Resistance and (resistance) <sup>1/2</sup> vs. $\ln v$ for a La-I-Al tunnel junction.	116

### List of Tables

<u>Table Number</u>		<u>Page</u>
1.	Properties of Superconducting Lanthanum Films.	93
2.	Superconducting Properties of Lanthanum from Different Measurements.	98
3.	Additional Measurements of Superconducting Properties of Lanthanum Films.	100

## CHAPTER I

### INTRODUCTION

#### 1.1. Motivation

The phenomenon of superconductivity was discovered by Kamerlingh Onnes in 1911. It represents a remarkable example of a display of quantum effects on a truly macroscopic scale and many notable physicists have been attracted to this problem. It eluded a successful theoretical description until 1957 when the first microscopic theory, which explains most of its general features, was proposed by Bardeen, Cooper and Schrieffer (1957 a,b) and is usually referred to as the BCS theory. This theory turned out to be indeed a stimulus to further experimental and theoretical investigations and the field is expanding with unabated interest. Since the pioneering experiments of Giaever (1960 a,b), electron tunneling technique has played a leading role in the development of the theory of superconductivity in this decade.

The BCS theory predicts the appearance of a forbidden energy gap about the Fermi level in the density of excited states when a metal turns superconducting. The electron tunneling technique, by which electrons of varying energies may be injected into a superconductor, provides

a direct and simple method of observing this energy gap. One can obtain not only the magnitude of the energy gap but also the variation of the density of excited states with energy in a superconductor.

Small deviations from the BCS density of states at energies of the order of the Debye energy have been observed in many superconductors and are identified as due to the predominant phonon energies in the corresponding metal (see, e.g., Rowell and Kopf, 1965; Adler et al., 1965). Thus, while providing a testing ground for the BCS theory, this simple technique has led to modifications in the theory. It has also permitted investigations of the phonon spectrum of several superconductors and holds promise of providing a great deal of information on the properties of superconductors in general.

A tunnel junction consists of a thin insulating layer sandwiched between two metals, in bulk or in form of thin films or a combination of both. A current can flow through a sufficiently thin barrier layer by quantum mechanical tunneling process on application of a potential across it. If the potential is small, the tunneling current is directly proportional to it so long as the two metals in the tunnel junction are in the normal state. When one or both metals turn superconducting, the dynamic conductance  $g(v) = di/dv$  of the tunnel junction is no longer

constant. In a normal metal-insulator-superconductor system (henceforth referred to as a n-s system), the normalized dynamic conductance  $\sigma(v)$ , which is the ratio of the dynamic conductance  $g_{ns}(v)$  when one of the metallic layers of the tunnel junction is in superconducting state to the dynamic conductance  $g_{nn}(v)$  when both members are in the normal state, is measured as a function of bias voltage  $v$  applied to the junction. The  $\sigma$ - $v$  plot directly reflects the variation in the normalized density of states with energy in the superconductor. The normalized density of states in a superconductor is the ratio of the density of states when a metal is superconducting to the density of states when it is in the normal state.

Matthias has often suggested that the superconductivity of the transition metals may be due to an attractive interaction other than the phonon-mediated electron-electron interaction (see, e.g., Anderson and Matthias, 1964). Such speculations arise mainly from two considerations. Firstly, Matthias (1957) has proposed an empirical rule, giving the dependence of the transition temperature  $T_c$  on the number of valence electrons  $n$  in a superconductor, for superconductivity of transition metals. No such regularities are observed in other superconductors. Secondly, large deviations from the isotope effect,  $T_c \propto M^{-1/2}$ , are observed in the transition metals, where  $M$  is the

isotopic mass of the superconductor. Suhl et al. (1959) proposed a two band model of superconductivity which, in special circumstances, yields independent energy gaps for each band. Experimentally, from the specific heat measurements, there is preliminary evidence that niobium may have two energy gaps (Shen et al., 1965).

Lanthanum and uranium are exceptional with respect to the symmetrical distribution of  $T_c$  in the periodic table. For  $n=3$ , lanthanum is the only element which is superconducting. Kondo (1963) has shown that exchange coupling between the bands enhances superconductivity and he has suggested that this mechanism may be responsible for the relatively high transition temperature of lanthanum. On the other hand, Hamilton and Jensen (1963) have proposed a magnetic interaction as a possible cause of superconductivity in these metals. Kuper et al. (1964) studied this model in detail and predicted large deviations from the law of corresponding states for superconductors viz,  $2\Delta_0 = 3.53 k_B T_c$  where  $2\Delta_0$  is the energy gap of the superconductor at  $0^\circ\text{K}$  and  $k_B$  is the Boltzmann constant. The theory also predicted two energy gaps and little or no isotope effect in these superconductors. Structure in the density of states is also expected due to excitations in the second energy gap.



Indeed a positive isotope effect,  $T_c \propto M^{2.2}$ , was reported in  $\alpha$ -uranium by Fowler et al. (1967) during the later stages of this work. No work on the isotope effect in lanthanum has been done so far. However, the deviations from the isotope effect are not conclusive evidences by themselves of the fact that an electron-phonon interaction is not responsible for superconductivity in these metals (Anderson and Matthias, 1964).

An ideal method to check these theories should be to investigate the density of states in superconducting lanthanum by the electron tunneling technique. As mentioned earlier, the electron-phonon interaction is displayed in a fairly direct manner in these experiments. Thus any variance in the nature of the structure in the tunneling density of states due to a different interaction in lanthanum would be readily recognized. It will also be possible to study the law of corresponding states and check the existence of a second energy gap in lanthanum from these experiments.

The next two chapters briefly review the theories of superconductivity, especially pertaining to lanthanum and the theory of electron tunneling in superconductors. Experimental arrangement and method of junction fabrication are discussed in Chapter IV. Results are presented and discussed in the fifth chapter. The last chapter describes

the conclusions from this work.

The author had written an M.Sc. thesis on 'Recombination Effects on Electron Tunneling into Superconducting Lead' in 1965. In some sections of the present work, results are only mentioned briefly and the M.Sc. thesis is referred to for the details.

## CHAPTER II

### MICROSCOPIC THEORIES OF SUPERCONDUCTIVITY

#### 2.1. The BCS Theory

A brief description of the superconducting ground state has been given by Khanna (1965) and only the pertinent results will be cited here.

The BCS theory evolved from the observation of Cooper (1956) who proved that two electrons excited slightly from the ground state of a Fermi distribution at zero temperature could form a real bound pair provided there was an attractive interaction between them. The energy of this state lies below that of the ground state of the Fermi sea and its wave function is localized. Thus the usual Fermi sea ground state is unstable against the formation of such pair states. The BCS theory provides a method of treating such a state of an electron gas in which a macroscopic fraction of the electrons exists in paired states.

The superconducting condensation energy arises due to strong correlations between these pairs. In real metals, these pair-pair correlations are almost entirely due to Pauli principle restrictions rather than true dynamical interactions. This permits one to treat such a

system in zero order by including dynamical interactions between the mates of a pair only and neglecting all but the Pauli principle restrictions when treating interactions between the pairs. Above the superconducting transition temperature  $T_c$ , the pairing correlations are entirely overcome by thermal fluctuations.

The superconducting ground state will be formed of those paired states which have the largest number of transitions amongst them. For a state carrying no current, the best pairing is between electrons with equal and opposite momentum and opposite spin. The Hamiltonian for this reduced problem is

$$H_{\text{red}} = T + V_{\text{red}} = 2 \sum_k \epsilon_k b_k^* b_k - \sum_{k, k'} V_{k'k} b_{k'}^* b_k .$$

(2.1 -1)

Here  $T$  is the kinetic energy term,  $V_{\text{red}}$  is the interaction energy between the pairs,  $\epsilon_k$  is the Bloch state energy measured from the Fermi level,  $-V_{k'k}$  is the pairing matrix element scattering a pair of electrons initially in the states  $k\uparrow$  and  $-k\downarrow$  into new electron states  $k'\uparrow$  and  $-k'\downarrow$  by exchange of a phonon of momentum  $(k'-k)$  and is assumed to be attractive,  $b_k^*$  and  $b_k$  are pair creation and annihilation operators defined by

$$b_k^* = c_{k\uparrow}^* c_{-k\downarrow}^*$$

and

(2.1 -2)

$$b_k = c_{-k\downarrow} c_{k\uparrow} .$$

$c_{k,\sigma}^*$  and  $c_{k,\sigma}$  are the creation and annihilation operators for electrons in Bloch states with crystal momentum  $k$  and spin index  $\sigma$ .

BCS assume a ground state function  $\Psi_0$  of the form

$$\Psi_0 = \prod_k (u_k + v_k b_k^*) \Phi_0 \quad (2.1 -3)$$

where  $v_k^2$  and  $u_k^2$  are the probabilities that the  $k^{\text{th}}$  pair is occupied or unoccupied respectively and  $\Phi_0$  is the vacuum. We introduce the equivalent parameters

$$v_k^2 = h_k , \quad u_k^2 = 1 - v_k^2 = 1 - h_k . \quad (2.1 -4)$$

In a superconductor, a given pair state  $k$  is partially occupied and partially empty. If an elementary excitation i.e., a quasi-particle with definite  $k$  vector and spin is to be created, this can only be done by partially creating an electron and partially destroying one. This can be achieved by a new set of quasi-particle operators which were introduced by Bogoliubov (1958) and are

defined by

$$\gamma_k^* = u_k c_k^* - v_k c_{-k}$$

and

(2.1 -5)

$$\gamma_{-k}^* = u_k c_{-k}^* + v_k c_k .$$

The BCS ground state is vacuum for these quasi-particle operators.

Treating  $v_k$  as a variational parameter, the condensation energy  $W_c$  corresponding to  $H_{red}$  for the state expressed by Eqn. (2.1 -3) is maximum for the value of  $v_k$  which is given by

$$v_k^2 = \frac{1}{2} \left( 1 - \frac{\epsilon_k}{E_k} \right) , \quad (2.1 -6)$$

$$u_k^2 = \frac{1}{2} \left( 1 + \frac{\epsilon_k}{E_k} \right) ,$$

where

$$E_k = \sqrt{(\epsilon_k^2 + \Delta_k^2)} , \quad (2.1 -7)$$

and

$$\Delta_k = \sum_{k'} V_{k'k} u_{k'} v_{k'} = \sum_{k'} \frac{V_{k'k} \Delta_{k'}}{2E_{k'}} . \quad (2.1 -8)$$

$E_k$  turns out to be the energy required for creating a quasi-particle of momentum  $k$  in the superconducting state and  $\Delta_k$  corresponds to the energy gap parameter for  $k^{\text{th}}$  electron.

Under the BCS assumptions (see, e.g., Khanna, 1965), Eqn. (2.1 -8) yields

$$\Delta = \frac{\hbar\omega_q}{\sinh(1/N(0)V)} \approx 2\hbar\omega_q e^{-1/N(0)V}, \quad (2.1 -9)$$

the latter form being valid in the weak-coupling limit, that is when  $N(0)V \ll 1$ .  $\hbar\omega_q \approx k_B\theta_D$  is cut-off phonon energy,  $\theta_D$  is the Debye temperature,  $k_B$  is the Boltzmann constant and  $N(0)$  is the density of states at the Fermi level.

Although the excitation energy may be associated with one member of the  $k^{\text{th}}$  pair being excited, excited single particles can only be produced in pairs, so that the minimum energy for an allowed excitation is  $2\Delta$ . This finite amount of energy, needed to create an allowed excitation, is known as the energy gap of a superconductor. The difference in energy between having all electrons paired and all but two electrons paired is finite because creating such an excitation not only requires energy to break up a pair, but the occupation of state  $k\uparrow$  and  $-k\downarrow$  by unpaired electrons removes a large amount of pair correlation energy from the system. A large number of pairs which could have interacted so as to occupy the states  $k\uparrow$  and  $-k\downarrow$  can no longer do so. This interaction energy is a large multiple of the single pair correlation energy.

The density of excited states  $N(E)$  in a BCS superconductor is

$$N(E) = 0 \quad |E| < \Delta$$

$$= N(0) \frac{|E|}{\sqrt{(E^2 - \Delta^2)}} \quad |E| \geq \Delta, \quad (2.1 - 10)$$

and is shown in Fig. 2.1.

Giaever et al. (1962) have found quite good agreement between their measurement on Sn, Pb, Al and In and the BCS density of states where a constant energy gap is assumed. However, definite structures (see, e.g., Giaever et al., 1962; Adler and Rogers, 1963; Rowell et al., 1963) in the density of states were observed near the prominent phonon frequencies of the superconductor and shall be discussed later in this thesis.

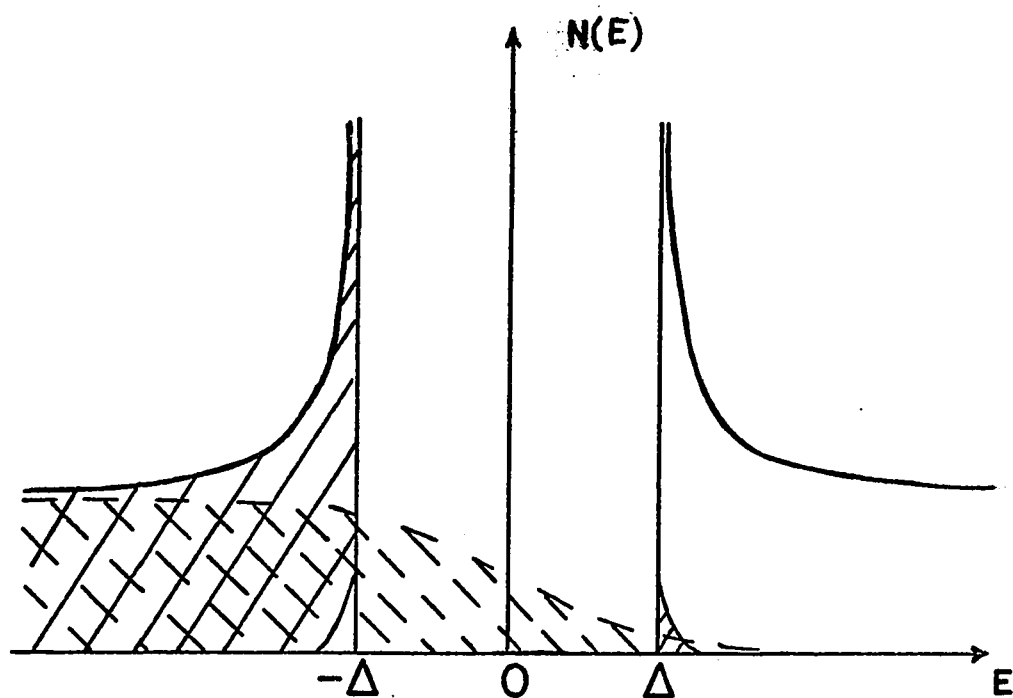
## 2.2. The Superconductor at Finite Temperatures

In a superconductor at  $T > 0^{\circ}\text{K}$ , thermally excited quasi-particles will occur in addition to the Cooper pairs. At any temperature, the number of these excitations will be determined by minimizing the free energy of the system with respect to the occupational probabilities of the excited states and the paired states, both of which will be temperature dependent.



Figure 2.1

Diagram showing the density of states in a superconductor and a normal metal near the Fermi energy.



OCCUPIED  
STATES



$T < T_c$



$T > T_c$

Let  $f_k = f_k(E, T)$  represent the occupational probability of the state  $k\uparrow$  or  $-k\uparrow$  by an excited particle and thus  $1 - 2f_k$  be the probability that neither  $k\uparrow$  nor  $-k\uparrow$  is occupied by this excitation.

The free energy  $F$  is expressed in terms of the internal energy  $U$  and entropy  $S$  by

$$F = U - TS . \quad (2.2 -1)$$

The kinetic energy term is

$$K.E. = 2 \sum_k |\epsilon_k| [f_k + (1-2f_k)h_k]$$

where  $h_k$  has the same meaning as before at  $T=0$  though its value will be different.

The potential energy term is

$$P.E. = - \sum_{kk'} V_{k-k'} [h_k(1-h_k)h_{k'}(1-h_{k'})]^{\frac{1}{2}} \times \\ (1-2f_k)(1-2f_{k'})$$

and the entropy term is

$$-TS = 2k_B T \sum_k [f_k \ln f_k + (1-f_k) \ln (1-f_k)] .$$

Substituting the terms in Eqn. (2.2 -1) and minimizing  $F$  with respect to  $h_k$ , we find

$$2\varepsilon_k - \sum_{k'} v_{k-k'} \sqrt{h_{k'}(1-h_{k'})} (1-2f_{k'}) \frac{1-2h_k}{\sqrt{h_k(1-h_k)}} = 0 .$$

(2.2 -2)

Let 
$$\Delta_k = \sum_{k'} v_{k-k'} \sqrt{h_{k'}(1-h_{k'})} (1-2f_{k'}) .$$

(2.2 -3)

Then the solution of Eqn. (2.2 -2)

$$h_k = v_k^2 = \frac{1}{2} \left( 1 - \frac{\varepsilon_k}{E_k} \right) \quad (2.2 -4)$$

and hence

$$1-h_k = u_k^2 = \frac{1}{2} \left( 1 + \frac{\varepsilon_k}{E_k} \right)$$

where

$$E_k = \sqrt{\varepsilon_k^2 + \Delta_k^2} . \quad (2.2 -5)$$

Thus the forms of  $h_k$  and  $E_k$  are identical to those in (2.1 -6) and (2.1 -7) but the energy gap is now reduced and is temperature dependent.

Minimizing  $F$  with respect to  $f_k$  leads to

$$f_k = \frac{1}{e^{\varepsilon_k/k_B T} + 1} . \quad (2.2 -6)$$

Thus the excitations behave completely like a set of independent fermions whose energies are given by Eqn. (2.2 -5); from ~~Eqns. (2.2 -3)~~ to (2.2 -6), we have

$$\Delta_k = \sum_{k'} V_{k'k} \frac{\Delta_{k'}}{2E_{k'}} \left( 1 - \frac{2}{\frac{E_{k'}}{k_B T} + 1} \right) . \quad (2.2 -7a)$$

Using BCS assumptions, we obtain

$$2\Delta = N(0)V\Delta \int_{-\hbar\omega_q}^{\hbar\omega_q} \frac{\tanh \frac{(\epsilon_k^2 + \Delta^2)^{1/2}}{2k_B T}}{(\epsilon_k^2 + \Delta^2)^{1/2}} d\epsilon . \quad (2.2 -7b)$$

The critical temperature  $T_c$  is defined as the temperature at which all pairs are broken so that  $\Delta(T_c) = 0$ .

In the weak-coupling limit, where  $\hbar\omega_q \gg k_B T_c$ , Eqn.

(2.2 -7b) yields

$$\frac{1}{N(0)V} = \ln \left( 1.14 \frac{\hbar\omega_q}{k_B T_c} \right) \quad (2.2 -8)$$

or

$$k_B T_c = 1.14 \hbar\omega_q e^{-1/N(0)V} . \quad (2.2 -9)$$

Comparing with Eqn. (2.1 -9)

$$2\Delta_0 = 3.53 k_B T_c \quad (2.2 -10)$$

where  $2\Delta_0$  is the energy gap at  $T=0$ .

The temperature dependence of the energy gap is shown in Fig. 2.2.

The isotope effect discovered by Maxwell (1950) and by Reynolds et al. (1950) gives the dependence of  $T_c$  of a superconductor on isotopic mass  $M$ .

$$T_c \propto M^{-\alpha} \quad (2.2 -11)$$

where  $\alpha$  is  $\approx 0.5$ . This follows directly from Eqn. (2.2 -9). Thus

$$T_c \propto \hbar\omega_q \approx k_B \theta_D \propto M^{-1/2}. \quad (2.2 -12)$$

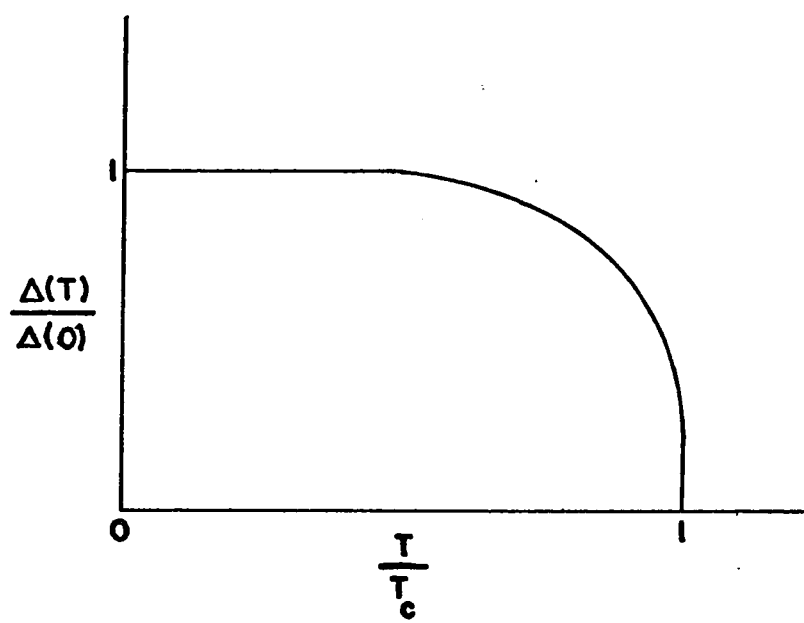
Thus the BCS theory accounted for the available experimental data on the isotope effect at the time when this theory was formulated.  $\alpha$  was found to be  $\sim 0.50$  for Hg, Sn and Tl.

### 2.3. Modifications to the BCS Theory

The predictions of the BCS model, with its one adjustable parameter  $N(0)V$ , have been rather well confirmed by different experiments. Most superconductors follow the law of corresponding states expressed by Eqn. (2.2 -10), indicating that their similarities outweigh their individual characteristics. However, anisotropy in a given metal, differences between metals and structure in

Figure 2.2

Temperature dependence of the energy gap in a super-conductor.





the density of states of a superconductor indicate need for improvement of this theory. In the isotropic model this is achieved by replacing  $V_{\mathbf{k},\mathbf{k}}$  by a kernel  $K(\epsilon, \epsilon')$  which has more accurate convergence properties at larger excitation energies. This leads to an energy gap function that depends on the energy in a complicated manner and which manifests itself in predictions of measurable quantities.

It is necessary to examine the arbitrary cut off for the interaction used in the BCS theory. The wave functions of the quasi-particles are not the exact eigenstates of the system since they interact with each other and the Fermi sea. Thus they have finite lifetimes. The lifetime  $\tau_{\mathbf{k}}$  of the low lying excitations in the immediate vicinity of the Fermi surface is quite long so that the level width  $\Gamma_{\mathbf{k}} = \hbar/2\tau_{\mathbf{k}}$  of these states can be neglected in comparison to their energies. However, for higher energy quasi-particle states, the level width of the states increases due to the increased rate for a quasi-particle decay by phonon emission. If  $\tau_{\mathbf{k}}$  for a quasi-particle of energy  $E_{\mathbf{k}} \approx \hbar\omega_D$  ( $\hbar\omega_D$  is the Debye energy) is so short that the level width is of the order of  $E_{\mathbf{k}}$ , as is the case for the strong-coupling superconductors (e.g., Pb, Hg), the pairing interaction cannot be handled by the BCS approach. For weak-coupling super-

conductors (e.g., Al, Zn), the quasi-particle lifetimes are so long that the level widths are small as compared to  $E_k$  even for  $E_k \sim \hbar\omega_D$  and thus the BCS approach is valid for them.

In addition to the problem of quasi-particle damping and the associated finite lifetime effects, the retarded nature of the phonon-mediated electron-electron interaction in a superconductor has to be taken into account as was emphasized by Eliashberg (1960). The Coulomb interaction is almost instantaneous and has a short range in space. The attractive part of the electron-phonon interaction is also short range in space but is retarded in nature. It is of a complicated nature in time, with rather long range parts. Eliashberg generalized the BCS theory using a potential which depends on both space and time differences. As a first approximation, the differences in space are ignored, resulting in a single integral equation for the gap parameter which is now a complex function of energy only,  $\Delta = \Delta(E)$ . Schrieffer et al. (1963) and Scalapino and Anderson (1964) have developed these ideas using the details of the phonon spectrum of the superconductor. Schrieffer et al. (1963) have shown that the effective tunneling density of states  $N_T(E)$  in a superconductor is given by

$$N_T(E) = N(0) \operatorname{Re} \left\{ \frac{E}{[E^2 - \Delta^2(E)]^{1/2}} \right\}, \quad (2.3 -1)$$

where  $N(0)$  has the same meaning as before and the energy gap

$$\Delta(E) = \Delta_1(E) + i \Delta_2(E), \quad (2.3 -2)$$

where the imaginary part of  $\Delta(E)$  arises from the damping effects.

For  $E \gg \Delta$ , Eqn. (2.3 -1) can be expanded and to the first order in  $\Delta^2(E)$

$$\frac{N_T(E)}{N(0)} \approx 1 + \frac{1}{2} \left[ \left( \frac{\Delta_1(E)}{E} \right)^2 - \left( \frac{\Delta_2(E)}{E} \right)^2 \right].$$

(2.3 -3)

Fig. 2.3b shows  $\Delta_1(E)$  and  $\Delta_2(E)$  for Pb as a function of  $E$  as calculated by Scalapino et al. (1965). Fig. 2.3a depicts the constant energy gap of the BCS theory.

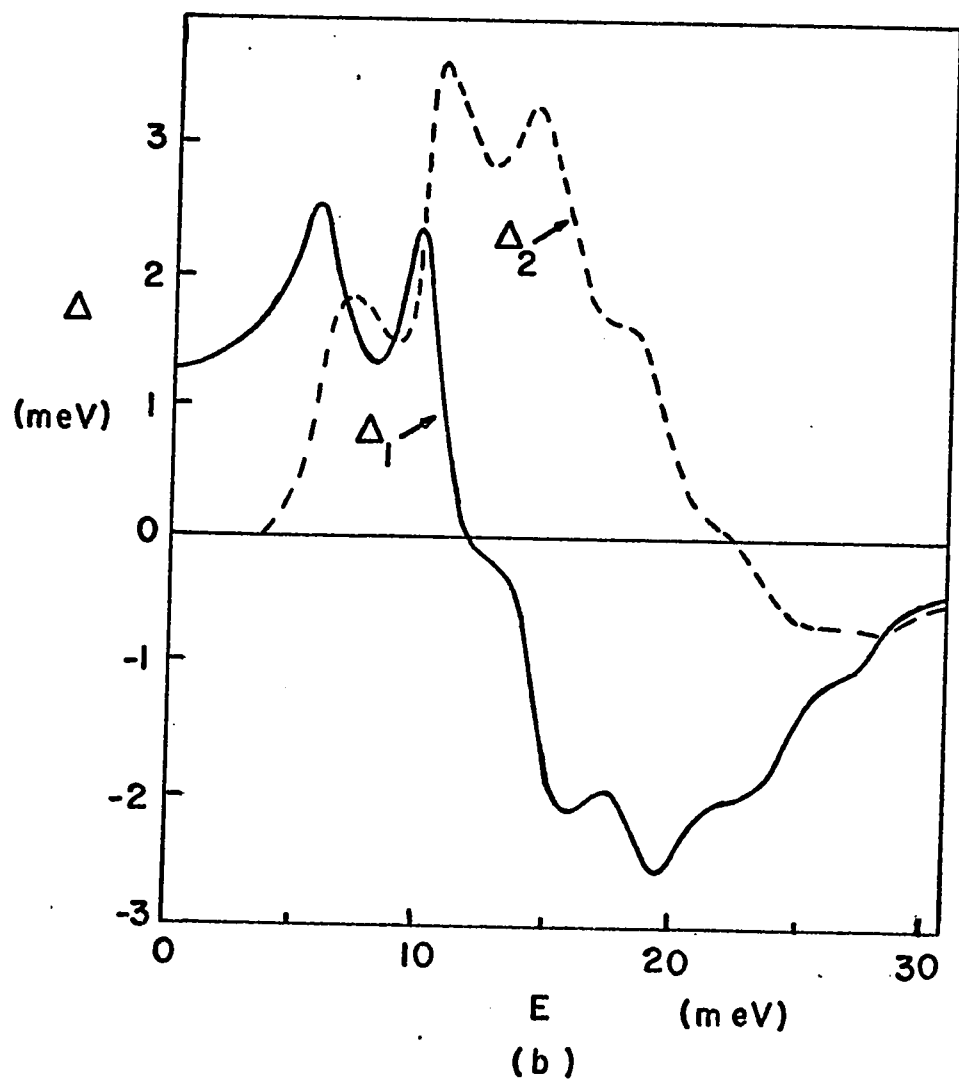
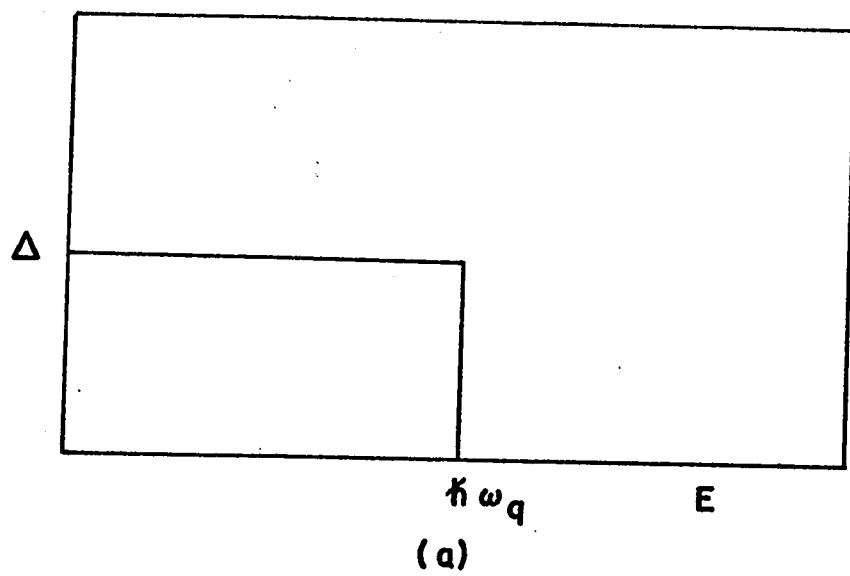
#### 2.4. Two-Band Models of a Superconductor

Matthias has often suggested that an attractive interaction, possibly of a magnetic nature, between electrons could lead to superconductivity (see, e.g.,

Figure 2.3

Energy dependence of the energy gap in a superconductor.

- (a) Plot of the constant energy gap of the BCS theory.
- (b) Computed real and imaginary parts of the complex gap function  $\Delta = \Delta_1 + i\Delta_2$  as a function of energy (after Scalapino et al., 1965) for Pb.



Anderson and Matthias, 1964).

There are two groups of the superconducting metals which behave differently in their superconducting properties. Matthias (1957) has proposed an empirical rule for the occurrence of superconductivity in the transition metals. According to this rule, the transition temperature  $T_c$  is a smooth function of the number of valence electrons  $n$  with sharp maximas at  $n=3, 5$  and  $7$ . Hamilton and Jensen (1963) have modified this rule and have found that the values of  $n$  favorable for superconductivity are  $5$  and  $7$  only and the  $T_c$ , consistent with some other properties of these elements, is quite symmetric about  $n=6$ . Non-transition elements do not have any such regularity in their superconducting properties. The transition temperatures of systems of non-transition elements are not very high; they reach a maximum of  $\sim 9^\circ\text{K}$  in the Pb-Bi system. In comparison, the maximum  $T_c$  for a system containing a transition element is  $\sim 18^\circ\text{K}$ .

While all the non-transition elements investigated to date show the isotope effect expressed by Eqn. (2.2 -11), large deviations from this law are observed in the transition elements and their compounds. For example Ru, Mo, Os,  $\text{Nb}_3\text{Sn}$  have small or almost vanishing isotope effects.

Recent measurements of the isotope effect in  $\alpha$ -uranium, where  $T_c \propto M^{+2.2}$ , are given as the "final proof" that a mechanism other than the electron-phonon interaction leads to superconductivity of this metal (Fowler et al., 1967). There are also varied effects of magnetic impurities on the properties of superconductors. Two-band models of superconductivity attempt to explain some of these interesting superconducting properties.

It should be noted that the isotope effect in the BCS theory is a result of the cut-off of both the Coulomb and the electron-phonon interactions at the same characteristic phonon frequency. When a more realistic criterion for this cut off is employed, it may explain the large deviations from the isotope effect that are observed in some superconductors. The source of the isotope effect is in the retarded part of the interaction caused by ion displacement, since this part will clearly scale in time accurately with the lattice vibration period and hence with the isotopic mass. In some superconductors the Coulomb part of the interaction may be more effective relative to the retarded electron-phonon interaction and they will not exhibit a fully-developed isotope effect. Thus any departure from the isotope effect must measure the effectiveness of the Coulomb part of the interactions which is instantaneous as compared to the

retarded electron-phonon interaction. Thus the deviations from the isotope effect are not by themselves evidence that a phonon interaction is not responsible for superconductivity.

Lanthanum and uranium are exceptional with respect to the symmetric distribution of  $T_c$  in the periodic table. For  $n=3$ , La is the only element which is superconducting ( $T_c \sim 6^\circ\text{K}$  for fcc and  $\sim 4.9^\circ\text{K}$  for d-hcp La). Other elements in Group III B, Sc, Y and Lu, are not superconducting down to  $0.08^\circ\text{K}$ ,  $0.07^\circ\text{K}$  and  $0.35^\circ\text{K}$  respectively. La and U occur at the beginning of the 4f and 5f series respectively without having any occupied f levels. La shows a marked increase of magnetic susceptibility and Knight shift with decreasing temperatures. It also has a large electronic specific heat.

## 2.5. Theories of a Two-Band Superconductor

Several authors have proposed two-band model extensions of the BCS theory to the case where two bands with more or less itinerant electrons overlap (Suhl et al., 1959; Kondo, 1963; Garland, 1963; Kuper et al., 1964). It has also been suggested that the superconductivity in lanthanum is due to such band effects (Kondo, 1963; Hamilton and Jensen, 1963; Kuper et al., 1964). In this



section, some of these theories shall be discussed.

These theories differ only in the nature of interactions within the second band and in between the two bands. In general, these theories treat one band in line with BCS theory and the interaction between this band and a second band is considered as responsible for the 'unusual' properties of a two-band superconductor. We shall first consider Kondo's model because of its emphasis on the enhancement of superconductivity and reduction of the isotope effect.

Kondo considers the problem of superconductivity when two bands are overlapping. Following the BCS theory, the superconducting ground state is still considered to be a linear combination of paired states but the interaction responsible for the pairing is taken to be different from the electron-phonon interaction. The electrons in the conduction band are assumed to interact with each other according to the usual BCS model. The interaction in the second band is assumed to be repulsive. When an interaction between these bands is introduced,  $T_c$  is always found to be raised over that of the single attractive band; also it increases with the density of states in the repulsive band and with the inter-band interaction strength. For convenience, we shall call the conduction band, the s-band, and the repulsive band, the f-band.

Thus there are two kinds of pairs, one in s-band and the other in f-band and there is exchange of pairs between these bands.

The Hamiltonian for such a system is given by

$$\begin{aligned}
 H = & \sum_{k,\sigma} \epsilon_k^s c_{k,\sigma}^* c_{k,\sigma} + \sum_{k,\sigma} \epsilon_k^f d_{k,\sigma}^* d_{k,\sigma} \\
 & + \sum_{k,k'} v_{k'k}^{ss} c_{k'\uparrow}^* c_{-k'\downarrow}^* c_{-k\downarrow} c_{k\uparrow} + \sum_{k,k'} U_{k'k}^{ff} d_{k'\uparrow}^* d_{-k'\downarrow}^* d_{-k\downarrow} d_{k\uparrow} \\
 & + \sum_{k,k'} J_{k'k}^{sf} (c_{k'\uparrow}^* c_{-k'\downarrow}^* d_{-k\downarrow} d_{k\uparrow} + \text{c.c.}), \quad (2.5 -1)
 \end{aligned}$$

$\epsilon_k^s$  and  $\epsilon_k^f$  are the Bloch state energies in the s- and f-bands measured from the Fermi level;  $c^*, c$  and  $d^*, d$  are the corresponding creation and annihilation operators.  $v^{ss}$ ,  $U^{ff}$  and  $J^{sf}$  are the interaction energies between pairs within the s-band, within the f-band and in the s- and f-bands respectively.  $J^{sf}$  is assumed to be repulsive in this model. However, one can gain energy from this interaction by taking the following variational function.

$$\Psi_0 = \prod_k (u_k^s + v_k^s c_{k\uparrow}^* c_{-k\downarrow}^*) \prod_k (x_k^f - y_k^f d_{k\uparrow}^* d_{-k\downarrow}^*) \Phi_0 \quad (2.5 -2)$$

where  $\Phi_0$  is the vacuum;  $(v_k^s)^2$  and  $(u_k^s)^2$  are, respectively, the probabilities that the  $k^{\text{th}}$  pair state is occupied or unoccupied in the s-band;  $(y_k^f)^2$  and  $(x_k^f)^2$  are the corresponding probabilities in the f-band. The sign of  $(-J^{sf})$  before  $y_k^f$  ensures the decrease in the energy of the state through the exchange of pairs between s- and f-bands.

Proceeding on similar lines to those in Section 2.2, we have the two energy gaps

$$2\Delta_k^s = - \sum_{k'} V_{k'k}^{ss} \Delta_{k'}^s (1-2f_{k'}^s) / (\epsilon_{k'}^s{}^2 + \Delta_{k'}^s{}^2)^{1/2} \\ + \sum_{k'} J_{k'k}^{sf} \Delta_{k'}^f (1-2g_{k'}^f) / (\epsilon_{k'}^f{}^2 + \Delta_{k'}^f{}^2)^{1/2} , \quad (2.5 -3)$$

$$2\Delta_k^f = - \sum_{k'} U_{k'k}^{ff} \Delta_{k'}^f (1-2g_{k'}^f) / (\epsilon_{k'}^f{}^2 + \Delta_{k'}^f{}^2)^{1/2} \\ + \sum_{k'} J_{k'k}^{sf} \Delta_{k'}^s (1-2f_{k'}^s) / (\epsilon_{k'}^s{}^2 + \Delta_{k'}^s{}^2)^{1/2} ,$$

where  $f^s$  and  $g^f$  are the occupational probabilities for the quasi-particle in the s- and f-bands.

Following the BCS approximations, Kondo assumes

$$V_{k'k}^{ss} = -V \quad \text{for} \quad |\epsilon_k^s|, |\epsilon_{k'}^s| < \hbar\omega_q , \\ = 0 \quad \text{otherwise.}$$

$U$  and  $J$  are assumed to be constants and repulsive in nature. Densities of states  $N_s$  and  $N_f$  in the bands are also assumed to be constant over the energy ranges  $(-\Delta_1, \Delta_2)$  and  $(-\gamma_1, \gamma_2)$  respectively and zero elsewhere. Henceforth the superscripts on  $U$  and  $J$  have been dropped.

Let  $\ln(1.14 \hbar\omega_q \beta_c) = x$  where  $\beta_c = \frac{1}{k_B T_c}$

or  $k_B T_c = 1.14 \hbar\omega_q e^{-x} . \quad (2.5 -4)$

Using the weak-coupling limit where

$$\hbar\omega_q , \gamma = (\gamma_1 \gamma_2)^{1/2} , \Delta = (\Delta_1 \Delta_2)^{1/2} \text{ are } \gg k_B T_c ,$$

one finds that  $x$  decreases and hence  $T_c$  increases with increase in  $|J|$  and  $N_f$ . Kondo has shown that

$$x \approx \frac{1}{N_s (V + J^2/U')} \quad (2.5 -5)$$

where  $U' = U - N_s J^2 \ln (\Delta/\hbar\omega_q)$

It is easy to show that the isotope effect vanishes when  $|J|$  is large. The deviation from the isotope effect can be defined by a parameter  $\eta$  given by

$$T_c \propto M^{-0.5} (1 + \eta)$$

(cf. Eqn. (2.2 -11)).

$\eta = 0$  in the BCS theory. In this model

$$\eta = - \frac{1}{[1 + \frac{U'V}{J^2}]^2} . \quad (2.5 -6)$$

In the limit  $J^2 \gg U'V$ ,  $\eta \rightarrow -1$  i.e. we have no isotope effect at all.

Kondo considers the case when the f-band is empty and lies close to the Fermi level. This is possibly the case in lanthanum. Assuming that the edges of this band lie at energies  $\gamma_1$  and  $\gamma_2$  above the Fermi level, where  $\gamma_1, \gamma_2 \gg k_B T_C$ , and  $\ln(\gamma_2/\gamma_1) = a$ , one gets

$$x = \frac{1}{N_s [V + J^2 \{U' + (\frac{1}{N_f a})\}^{-1}]} . \quad (2.5 -7)$$

Thus when an empty band lies close to the Fermi level, the interband interaction enhances superconductivity.

$\eta$  is now expressed by

$$\eta = - \frac{1}{\left[ 1 + \frac{V \{U' + (1/N_f a)\}}{J^2} \right]^2} . \quad (2.5 -8)$$

which also approaches  $-1$  when the interband interaction  $J$  dominates.

Kuper et al. (1964) have also proposed a model for the superconductivity of La and U. They postulate a narrow f-band above and very close to the Fermi surface, in agreement with Kondo. La and U do not have any 4f and 5f electrons respectively but the next elements Ce and probably Np have one 4f and 5f electron respectively. They propose that it is the attractive magnetic interaction due to incipient antiferromagnetism (the next element Ce is antiferromagnetic) which leads to pairing of virtually excited electrons in the f-band. Blandin (1961) has shown that the f-f interaction is antiferromagnetic in character near the beginning of the lanthanide series. The f-f interaction has a form

$$H_{ff} = - \frac{1}{2} \int d^3r_i d^3r_j J(\vec{r}_i - \vec{r}_j) \vec{\sigma}(\vec{r}_i) \cdot \vec{\sigma}(\vec{r}_j),$$

where  $\vec{\sigma}(\vec{r}_i)$  is the spin density of the  $i$ th electron, and  $J(a) > 0$ ,  $a$  = interatomic distance. Besides, there is the usual phonon-mediated pairing interaction in the conduction band denoted as s-band. When even a small interband interaction is included, the condensation in the f-band greatly enhances the BCS condensation in the s-band.

The BCS variational approach, has been employed to predict the following results with this model:

1. We have two energy gaps for quasi-particle excitations in the two bands with  $\Delta^s/\Delta^f \lesssim 4$ . 2. Since there will be quasi-particle excitations both in the s- and f-bands, the density of states will depart from the BCS density of states at energies high enough to produce excitations in the f-band. This additional density of states is expected to occur at energy  $\sim 3.5 \Delta^s$  approximately. 3. Strong deviations from the law of corresponding states for the superconductors are expected. 4. Since the condensation in the s-band is greatly dependent on the condensation in the f-band, in the lowest approximation there is no isotope effect. At most, a very small isotope effect is expected.

Garland (1963), in another variation of the two-band model, has shown that superconductivity of the transition metals is due to the electron-phonon interaction, but the Coulomb interaction plays an important role in these superconductors. For the case of 'clean' transition metals, where s- and d-band electrons can be distinctly defined, he obtains two energy gaps similar to those of Suhl et al. (1959). Electrons of high effective mass in the d-band tend not to follow the motion of the s-electrons and thus anti-shield the s-s Coulomb interaction giving rise to a net attraction between s-electrons added to the usual attractive interaction by exchange of

virtual phonons. As both s and d electrons can follow the motion of d electrons, the Coulomb interaction between d-electrons is always repulsive. The net effect is the enhancement of superconductivity in the s-band.

For 'dirty' transition metals, no electrons can be clearly defined to be s- or d- like. As  $N_s(0)/N_d(0) \ll 1$ , where  $N_a(0)$  is the density of states at the Fermi Surface in the  $a^{\text{th}}$  band, the quasi-particles are primarily d-like and their superconductivity arises primarily from d-d interactions. Thus the enhancement of superconductivity is washed out in this case and the usual kind of phonon-mediated single gap superconductivity results. However the Coulomb interaction contributes strongly in these metals, resulting in large deviations from the isotope effect which are in excellent agreement with the experiments. Such a good agreement provides a basis for arguments against the existence of any strong contribution to superconductivity from interactions other than the phonon-mediated electron-electron interaction.

Suhl et al. (1959) have treated a similar problem by assuming that the interactions within s- and d-bands and the inter-band interaction are attractive in nature and arise due to an electron-phonon interaction. In this model, we have two energy gaps which have different temperature dependence depending on the interaction

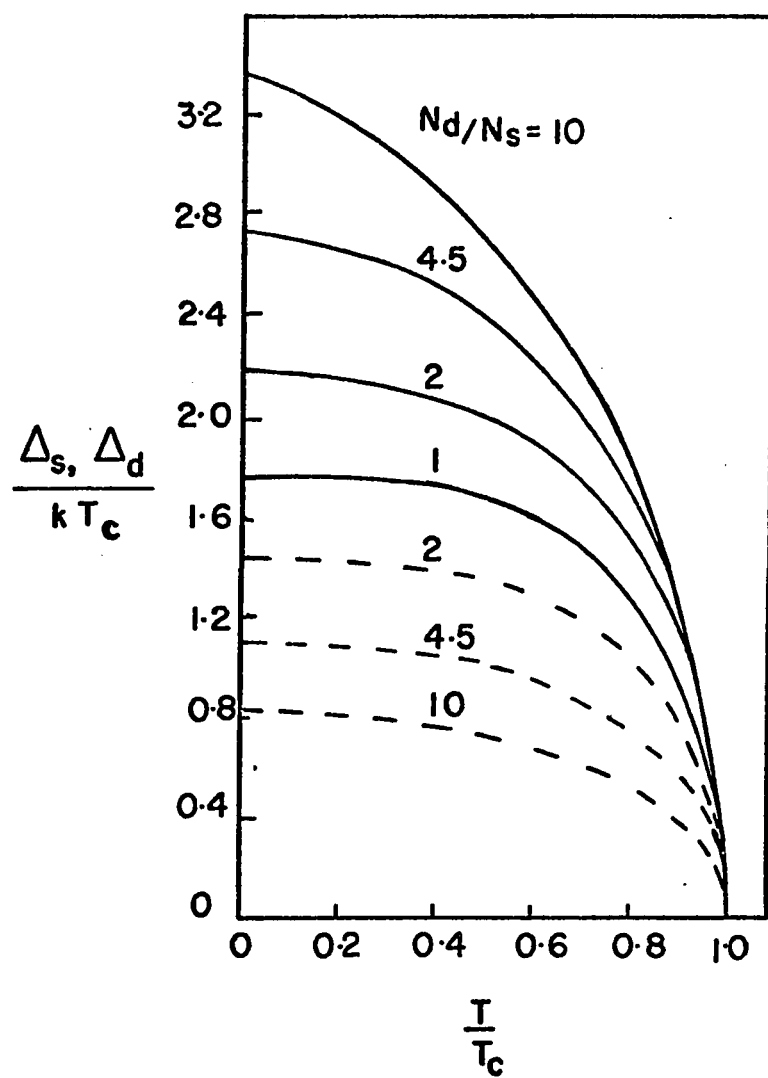


parameters and the densities of states. The gap parameters are shown in Fig. 2.4 for a variety of values of these parameters. These different energy gaps could partly account for the fine structure observed by Ginsberg et al. (1959) in their infrared absorption measurements in superconductors.

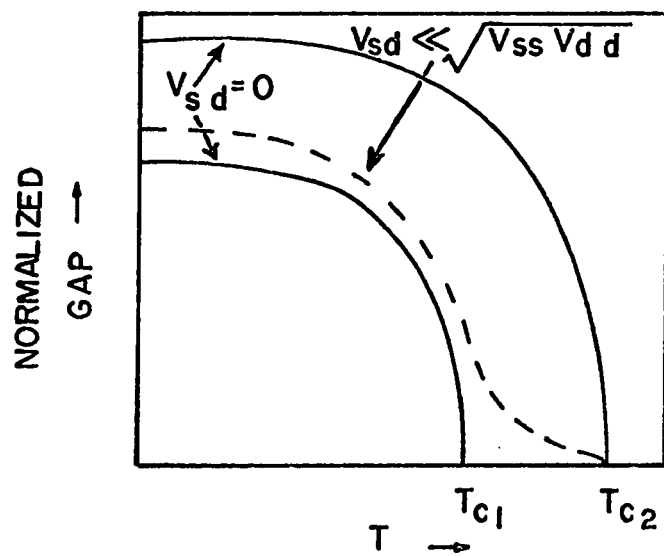
Figure 2.4

Temperature dependence of the energy gap pairs (after Suhl et al., 1959). The various symbols have the usual meanings.

- (a) The energy gaps,  $\Delta_d$  (solid curve) and  $\Delta_s$  (dashed curve), for  $v^{ss} = v^{dd} = 0$ ,  $v^{sd} \sqrt{N_s N_d} = 1/3$  and various ratios of densities of states.
- (b) For  $v^{sd} = 0$ , there are two transition temperatures. For small but finite value of  $(v^{sd})^2$ , the lower  $T_c$  is smoothed out.



(a)



(b)

## CHAPTER III

### ELECTRON TUNNELING IN METALS

In the pioneering experiment in 1960, Giaever showed that a tunneling current can flow by a quantum mechanical tunneling process through a sufficiently thin insulating layer separating two metallic films. If at least one of the metal films was a superconductor, the current voltage  $i$ - $v$  characteristic of the specimen was found to be non-linear at temperatures below the  $T_c$  for the superconducting film and could yield the energy gap value of the superconductor. Since then, this simple, elegant and powerful technique has been increasingly employed to study the microscopic properties of superconductors and has played a very important role in the understanding of the superconducting state and in turn the normal state to some extent. In recent years, it has also been used to study some properties of the insulating layer.

A tunnel junction consists of two metal electrodes, either in the form of evaporated thin films or in bulk, on the opposite sides of a thin insulating layer which is often referred to as the barrier. We will denote a tunnel junction by A-I-B, where A denotes the first metal film, I is the thin insulating layer which is a

few tens of angstrom units thick and is invariably obtained by oxidizing A appropriately, and B is the cover layer that is deposited on the top of the insulating layer.

### 3.1. Theory of Electron Tunneling

The theory of electron tunneling through a thin insulating oxide layer has been discussed by Adler (1963) and by Khanna (1965).

In this theory, the insulating layer in the tunnel junction is considered to be a potential barrier for the electrons. The transmission coefficient for an electron through this barrier depends exponentially on both the square root of the barrier height and its thickness. It is assumed that the barrier height and the thickness remain constant over the range of voltages applied to the tunnel junction which usually does not exceed 50 mv. Here the energies are measured from the Fermi level and henceforth we will take  $\hbar=k_B=e=1$  where the symbols have the usual meanings.

Taking into account the current flow in both directions, the net current for an applied potential  $v$  across the tunnel junction is given by

$$\begin{aligned}
 I &\propto |T|^2 \int_{-\infty}^{\infty} N_1(E) N_2(E+v) [f(E) - f(E+v)] dE \\
 &= c \int_{-\infty}^{\infty} n_1(E) n_2(E+v) [f(E) - f(E+v)] dE .
 \end{aligned}
 \tag{3.1 -1}$$

Here  $c$  is a constant,  $T$  is the matrix element for the transition of an electron between the two metals,  $N_i(E)$  is the effective density of states in metal  $i$ ,  $n_i(E)$  is the reduced density of states in the metal  $i$  and is given by

$$n_i(E) = \frac{N_i(E)}{N_{in}(0)} , \tag{3.1 -2}$$

where  $N_{in}(0)$  is the density of states of the electrons at the Fermi surface in metal  $i$  in the normal state.  $N_{in}(0)$  and  $T$  are assumed to be constant over the energy region of interest. Three important cases arise corresponding to the metals being in the  $n$  (normal) or the  $s$  (superconducting) state.

(i) Normal-Normal Case  $i_{nn}$

When both metals are in the normal state (abbreviated as the  $n$ - $n$  case), Eqn. (3.1 -1) yields a linear  $i$ - $v$  characteristic,  $i_{nn} = cv$ , under the conditions that  $v \ll E_F$  and  $T \ll E_F$ .

(ii) Normal-Superconductor Case  $i_{ns}$ 

When one of the two metals is superconducting (Fig. 3.1), the density of states in the superconductor has an energy gap  $2\Delta_1$  centered at the Fermi level. At  $T=0^\circ\text{K}$ , no electrons can tunnel until  $v > \Delta_1$ .

In this case

$$i_{ns} = c(v^2 - \Delta_1^2)^{\frac{1}{2}}, \quad |v| \geq \Delta_1$$

$$= 0, \quad 0 \leq |v| \leq \Delta_1$$

$$i_{ns}(-v) = -i_{ns}(v)$$

$$\text{and} \quad i_{ns} \approx i_{nn} \quad \text{for} \quad |v| \gg \Delta_1.$$

(3.1 -3)

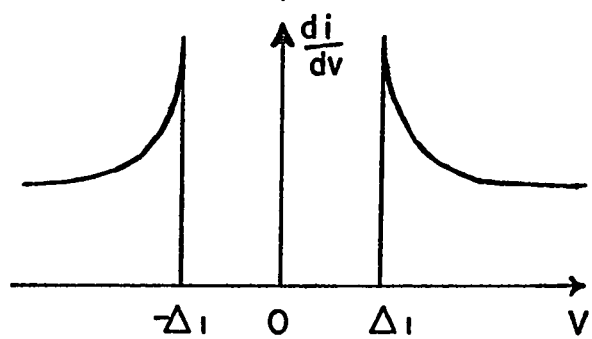
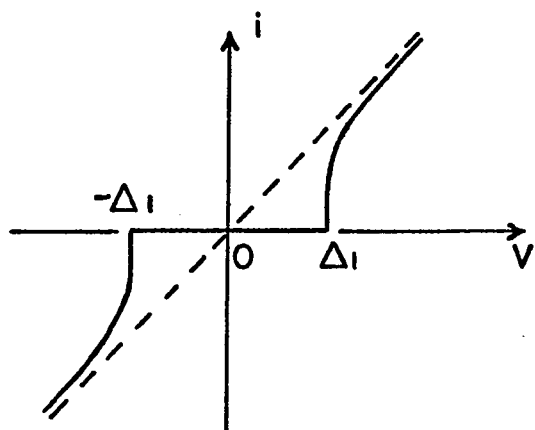
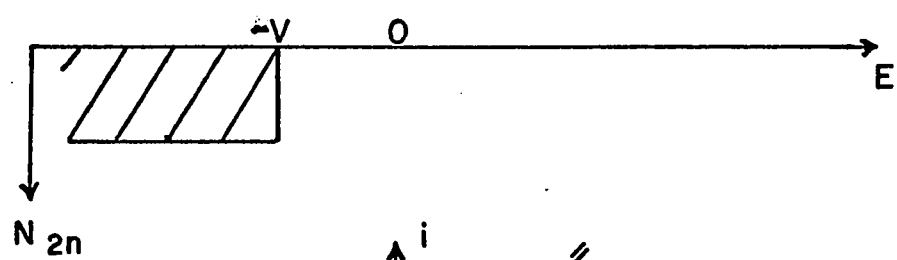
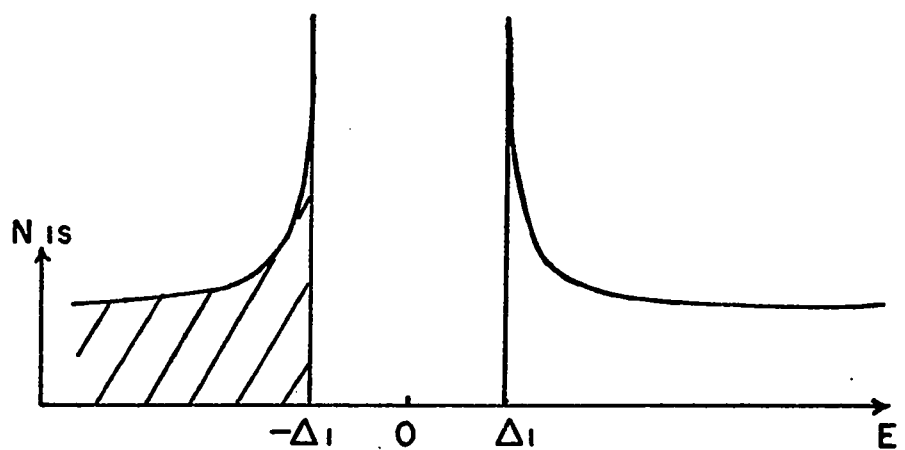
At  $T \neq 0^\circ\text{K}$ , there are always some excited electrons above the energy gap in the superconductor and above the Fermi level in the normal metal. Due to this 'thermal smearing' some current flows even in the gap region  $|v| < \Delta_1$  and smears the  $i$ - $v$  characteristic at  $|v| \sim \Delta_1$  considerably. However, for  $T \ll \Delta_1$ , the energy gap parameter can be easily determined.

Bermon (1964) has computed the normalized conductance  $\sigma = g_{ns}/g_{nn}$  of a tunnel junction as a function of  $\frac{v}{\Delta}$  and  $\frac{\Delta}{T}$  where  $g$  denotes the conductance of the

Figure 3.1

Energy diagrams, illustrating the density of states near the Fermi level, occupation of states,  $i$ - $v$  characteristic and  $\frac{di}{dv}$  -  $v$  characteristic for the normal-superconductor case of a tunnel junction.





tunnel junction,  $g = \frac{di}{dv}$ . From Eqn. (3.1 -1), the conductance

$$g_{ns} = c \int_{-\infty}^{\infty} n_s(E) K(E,v,T) dE \quad (3.1 -4)$$

where the kernel  $K(E,v,T)$  is given by

$$K(E,v,T) = \frac{1}{T} \cdot \frac{e^{(E+v)/T}}{[e^{(E+v)/T} + 1]^2} \quad (3.1 -5)$$

As noted by Bermon,  $K(E,v,T)$  is a bell shaped function symmetrically peaked about  $E=-v$  with full width at half maximum of  $\sim 3.5 T$  and height  $\propto \frac{1}{T}$ . At  $T=0^{\circ}K$ , it becomes a  $\delta$ -function and then  $g_{ns}$  is directly proportional to the density of states in the superconductor. Due to thermal smearing, if  $\Delta$  remains fixed, the peak in conductance moves to higher bias  $v$  as the temperature is increased.

### (iii) Superconductor-Superconductor Case $i_{ss}$

In the s-s case, we have energy gaps  $2\Delta_1$  and  $2\Delta_2$  in the density of states of the two superconductors. At  $T=0^{\circ}K$ , the current  $i_{ss} = 0$  for  $v < \Delta_1 + \Delta_2$  but rises sharply at  $v = \Delta_1 + \Delta_2$  and approaches  $i_{nn}$  at higher voltages. At  $T \neq 0^{\circ}K$ , there are excited electrons in both superconductors and some current flows even for  $v < \Delta_1 + \Delta_2$ . The current first increases up to

$v = \Delta_1 - \Delta_2$  (with  $\Delta_1 > \Delta_2$ ). With further increase in voltage, the current decreases because the same number of 'electrons' are available for tunneling as in range  $v < \Delta_1 - \Delta_2$ , but into a lower density of available states in the opposite superconductor. With further increase in voltage, the current decreases until  $v = \Delta_1 + \Delta_2$  where it abruptly increases and approaches  $i_{nn}$  at higher bias. Shapiro et al. (1962) have computed the current in the s-s case numerically and found a logarithmic singularity at  $v \sim \Delta_1 - \Delta_2$  and a finite discontinuity at  $v = \Delta_1 + \Delta_2$ . There is a region of negative resistance in between these two voltages. In practice, due to lifetime and anisotropy effects, one observes a cusp-like peak at  $v \sim \Delta_1 - \Delta_2$  and a very abrupt current jump spread over a small voltage range at  $v \sim \Delta_1 + \Delta_2$ . However, thermal smearing of the i-v characteristic is much smaller in a s-s case than in a n-s case.

Bardeen (1961) laid the foundation of a Hamiltonian formalism for the problem of electron tunneling and found similar results to those obtained from the semi-phenomenological theory just described, provided the matrix element  $T$  is the same in both the normal and the superconducting state. Harrison (1961) has determined  $T$  using an independent-particle model of a metal. He

found that band structure in the normal metals cannot be observed through tunneling experiments. This is because  $|T|^2$  is proportional to the group velocities of the tunneling electrons in both metals in a direction normal to the barrier. Since  $N_i(E)$  (Eqn. (3.1 -1)) is inversely proportional to the velocity, the current  $i_{nn}$  is completely independent of the density of states. When one of the metals is superconducting, the behaviour of the wave function in the insulating barrier is still almost unchanged and  $|T|^2$  still depends on the group velocity of the normal electrons. The tunneling current would now depend on  $|T|^2 N_s(E) N_n(E) \propto \frac{N_s(E)}{N_n(E)} = n_s(E)$ . However, in a superconductor, one does not have independent 'electrons' and it is the quasi-particles which have to be taken into account. Cohen et al. (1962) have studied this problem and have obtained the same expression for the tunneling current as given by Eqn. (3.1 -1).

### 3.2. Phonon Density of States and the Tunneling Conductance

At  $T = 0^0K$ , the current in a n-s system from normal metal 1 to superconductor 2 is

$$I(v) = \text{Const.} \int_0^v N_{2s}(E) N_{1n}(E-v) dE .$$

Since density of states in the normal metal is assumed to be constant for small voltages compared to the Fermi energy,

$$g_{ns}(v) = \text{Const. } N_{2s}(v) N_{1n}(0) .$$

When both metals are in the normal state,

$$g_{nn}(v) = \text{Const. } N_{2n}(0) N_{1n}(0) .$$

The normalized dynamic conductance  $\sigma$

$$\sigma(v) = \frac{g_{ns}(v)}{g_{nn}(v)} = \frac{N_{2s}(v)}{N_{2n}(0)} = \text{Re.} \left[ \frac{v}{\{v^2 - \Delta^2(v)\}^{\frac{1}{2}}} \right] .$$

(3.2 -1)

Thus in this approximation,  $\sigma$  is identical to the normalized effective tunneling density of states in a superconductor given by Eqn. (2.3 -1). As pointed out in Chapter II,  $\Delta$  is a complex function of energy and both real and imaginary parts exhibit sharp structure at definite energies as shown in Fig. 2.3b. Following the calculations of Schrieffer et al. (1963), as energy approaches  $\Delta_0 + \omega_t$  or  $\Delta_0 + \omega_\ell$ , where  $\omega_t$  and  $\omega_\ell$  are the prominent transverse and longitudinal phonon frequencies respectively in the superconductor and  $\Delta_0$  is the energy gap at the gap edge,  $\Delta_0 = \Delta(\Delta_0)$ ,  $\Delta_1$ , the real part of the energy gap, increases and reaches a

maximum near the predominant phonon energies. Peaks in  $\Delta_1$  arise due to near resonant exchange of large number of phonons at these energies. As the energy is increased,  $\Delta_1$  falls rapidly and beyond the second peak, it becomes negative then finally approaches zero. The imaginary part of the energy gap,  $\Delta_2$ , also reflects the resonant exchange of phonons and exhibits a maximum at energies slightly beyond these characteristic energies.

Thus at energies  $\Delta_0 + \omega_t$  or  $\Delta_0 + \omega_\ell$ ,  $\Delta_1$  gives a peak and  $\Delta_2$  is increasing. Just above these energies,  $\Delta_1$  decreases abruptly while  $\Delta_2$  is increasing to its peak value causing a sharp drop in the effective tunneling density of states following Eqn. (2.3 -3). Thus a peak in the phonon spectrum is reflected as a small peak followed by a rapid drop in the effective density of states which is reflected in  $\sigma - v$  characteristics. The second derivative  $\frac{d^2 i}{dv^2}$  versus  $v$  plot is a still more sensitive measure for locating these structures in  $\sigma - v$  characteristics, where they appear as sharp negative peaks. Structures at  $\Delta_0 + n\omega_t + m\omega_\ell$  ( $n$  and  $m$  integers) also appear due to multi-phonon processes. Further, Scalapino and Anderson (1964) have identified structures in the  $\frac{d^2 i}{dv^2} - v$  plot that arise from the various Van Hove singularities (1953) in the phonon density of states.

### 3.3. Zero-Bias Tunneling Anomalies in the n-n Systems

We now wish to discuss a different kind of structure in the tunneling conductance which is observed as a symmetrical peak or a dip in conductance centered at zero bias and is known as the zero-bias anomaly (here after denoted by ZBA). In some tunnel junctions, the conductance  $g(v)$  shows a temperature dependent peak (or dip) superimposed on a background conductance  $g_0(v)$  which is almost temperature independent. The magnitude of the ZBA which can be expressed as

$$\frac{\Delta g(0)}{g_0(0)} = \frac{g(0) - g_0(0)}{g_0(0)}, \quad (3.3 -1)$$

varies greatly for different types of tunnel junctions. Resistance peaks have been observed in lightly doped Ge, Si (Logan and Rowell, 1964) and III - V semiconductor (Hall et al., 1960; Shewchun and Williams, 1965) tunnel diodes. Generally  $\frac{\Delta r(0)}{r_0(0)} < 0.5$  where  $r(v)$  is the resistance of the junction at bias  $v$ . Heavily doped Si and Ge diodes show a conductance peak where  $\frac{\Delta g(0)}{g_0(0)} \sim 0.05$  (Logan and Rowell, 1964).

Conductance peaks in normal metal junctions were first observed by Wyatt (1964a) in junctions consisting of bulk normal Ta or Nb - the respective oxide-normal

Al, and generally at  $1^{\circ}\text{K}$ , the size of ZBA was  $\sim 0.2$ . In comparison, the size of ZBA in 'well-behaved' tunnel junctions, for example Al-I-(Pb,Sn,In), is  $< 10^{-5}$ . Wyatt also noted that the excess conductance at zero bias,  $\Delta g(0)$ , depended on temperature as  $-\ln T$  and at a fixed temperature,  $\Delta g(v)$  varied as  $-\ln v$  for  $v \gg T$ . Fig. 3.2 shows the variation of conductance of a typical tunnel junction showing ZBA. In Fig. 3.3, the temperature dependence of excess conductance at zero bias,  $\Delta g(0)$ , and voltage dependence of  $\Delta g(v)$  at a fixed temperature have been plotted. Rowell and Shen (1966) have studied tunnel junctions consisting of various kinds of normal electrodes and oxide layers and observed such anomalies of different sizes varying from  $\sim 25\%$  to  $< 1\%$ . In Ta - I - Pb junctions, magnitude of the ZBA was found to vary with surface preparation of Ta and with oxidation procedure. They concluded that the oxide layer or the oxide-metal interface is responsible for the zero-bias anomalies. In addition, they observed anomalous 'giant peaks' in resistance in  $\text{Cr} - \text{Cr}_x\text{O}_y - \text{Ag}$  tunnel junctions, such that the resistance at 100 mv is 0.03 times that at zero bias. Thus the total current appeared to be involved in this anomalous tunneling mechanism and traces of the anomaly seemed to persist even at room temperature. In all other cases, the ZBA could be



Figure 3.2

Voltage dependence of conductance at different temperatures for a tunnel junction showing ZBA (after Shen and Rowell, 1968).

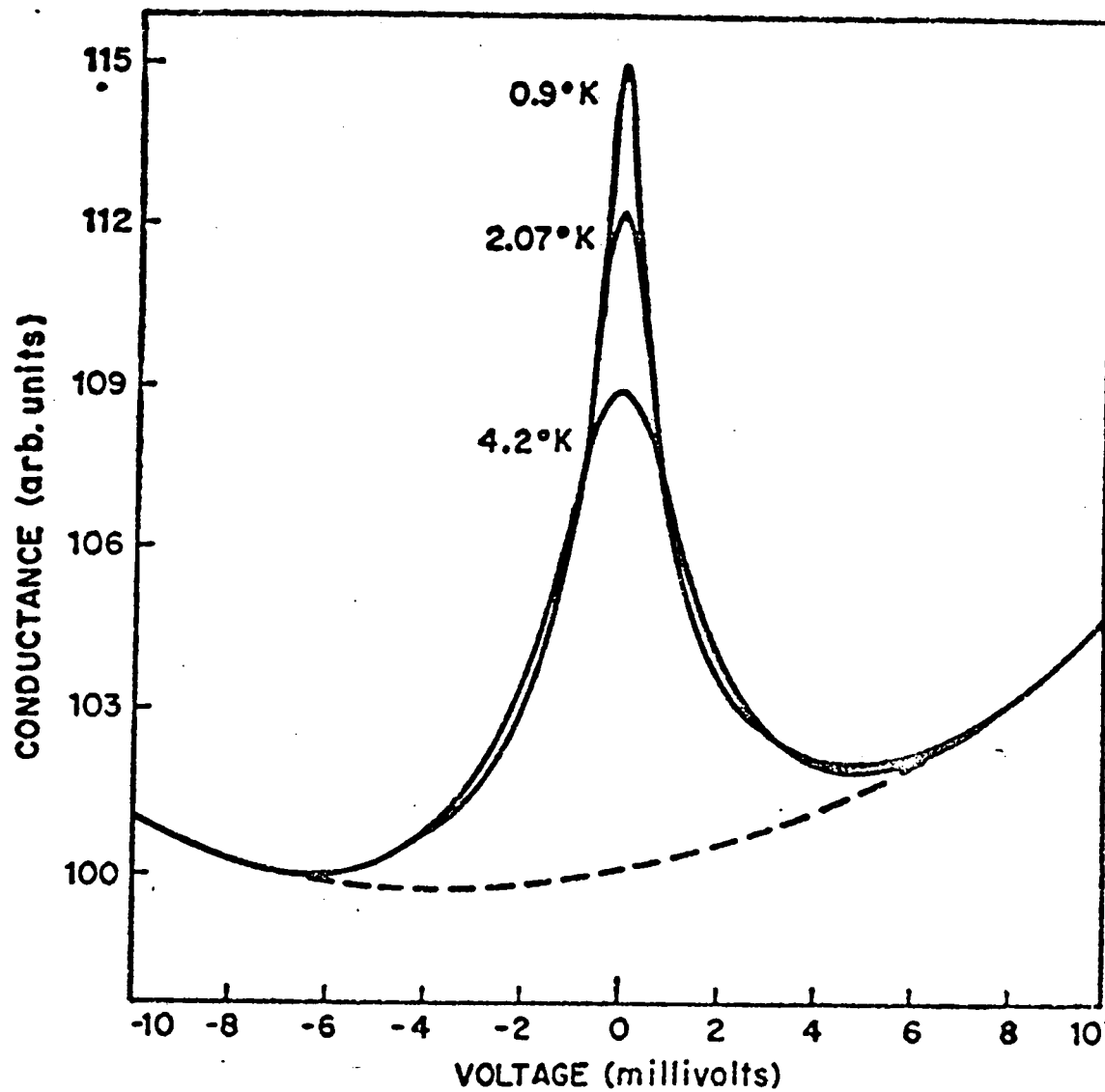
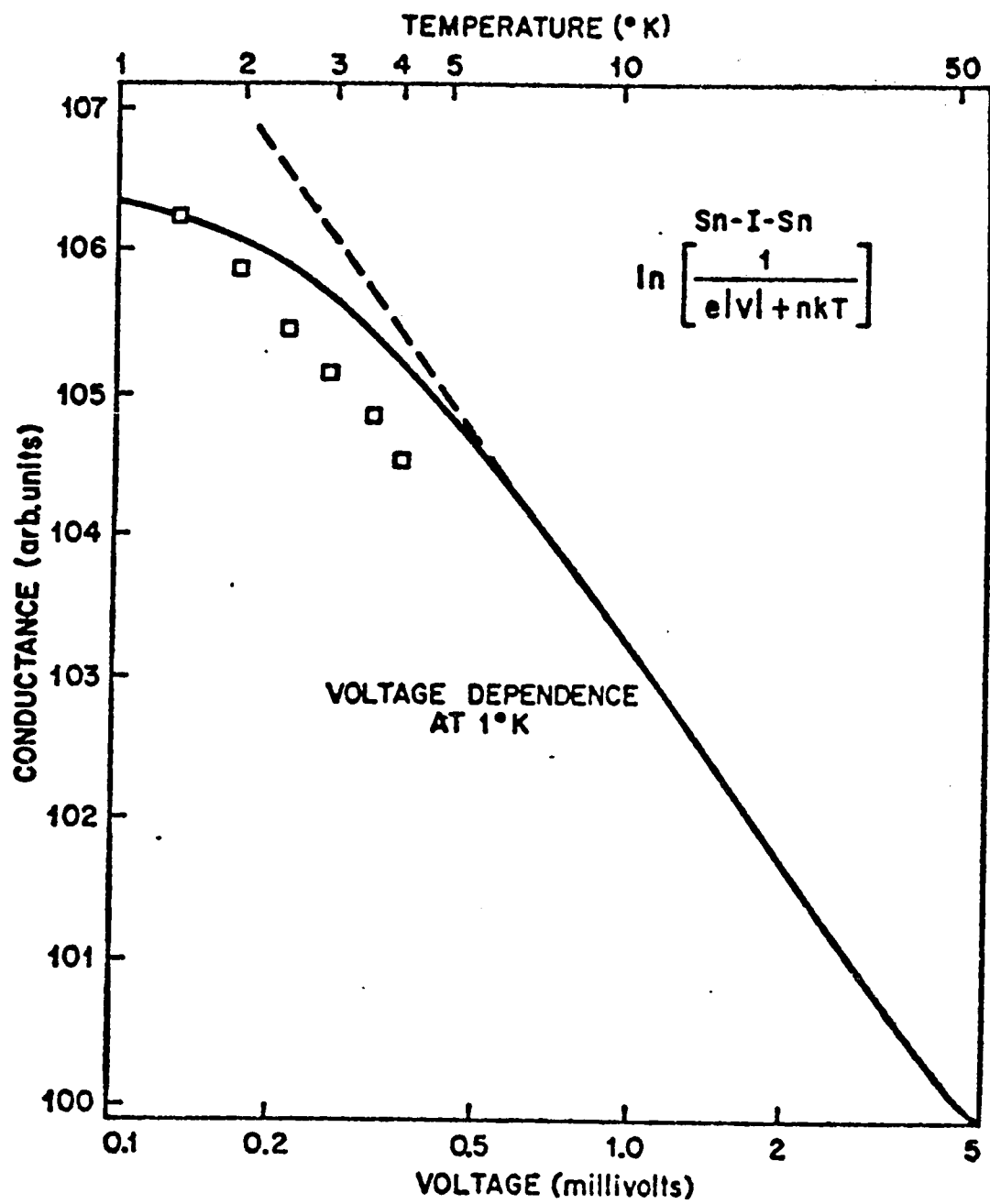


Figure 3.3

Voltage dependence of  $\Delta g(v)$  (solid line) and temperature dependence of  $\Delta g(0)$  (squares) for a tunnel junction showing ZBA (after Shen and Rowell, 1968).



observed only in the temperature region  $T < 10^0 \text{K}$  .  
 $r(0)$  varied approximately as  $-\ln T$  and at a fixed temperature,  $\sqrt{r(v)}$  varied as  $-\ln v$  in contrast to results in other normal metal tunnel junctions (Rowell and Shen, 1966; Shen and Rowell, 1968; Wyatt, 1964).

### 3.4. Appelbaum Magnetic Scattering Model

Following a suggestion by Anderson that the ZBA may be caused by magnetic impurities in the oxide layer, Appelbaum (1966, 1967) evaluated the tunneling current through an oxide layer which contains a number of non-interacting localized magnetic impurities, particularly at the metal-metal oxide interface. We will consider an oversimplified picture, due to Shen and Rowell (1968) of the Appelbaum model of electron tunneling from metal A to B as shown in Fig. 3.4. The tunneling conductance  $g$  of a junction can be regarded as a sum of three components,

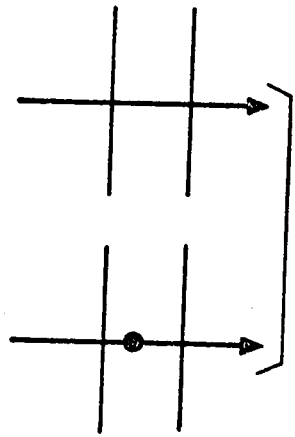
$$g = g^{(1)} + g^{(2)} + g^{(3)} . \quad (3.4 -1)$$

$g^{(1)}$  is due to electrons which can tunnel without interacting with the impurities or are simply scattered by the impurities without any spin exchange with them. This term is independent of any applied magnetic field.

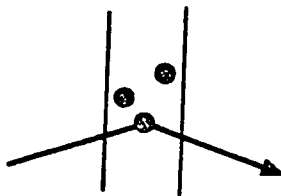
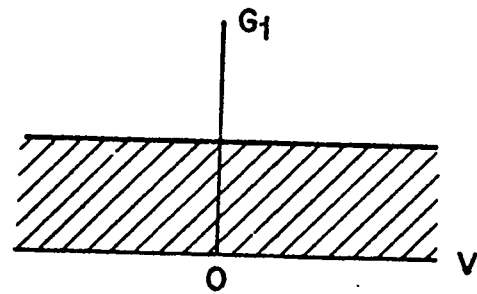
Figure 3.4

Schematic representing the different tunneling processes that contribute to the theoretical conductance of the Appelbaum model. Here  $G$  corresponds to  $g$  in the text.

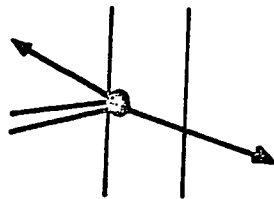
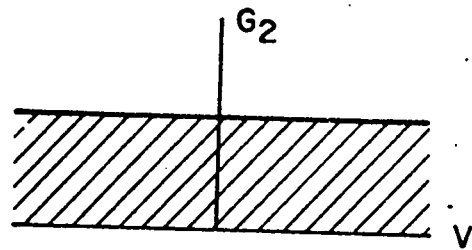
# APPELBAUM - ANDERSON MODEL H = 0   T = 0



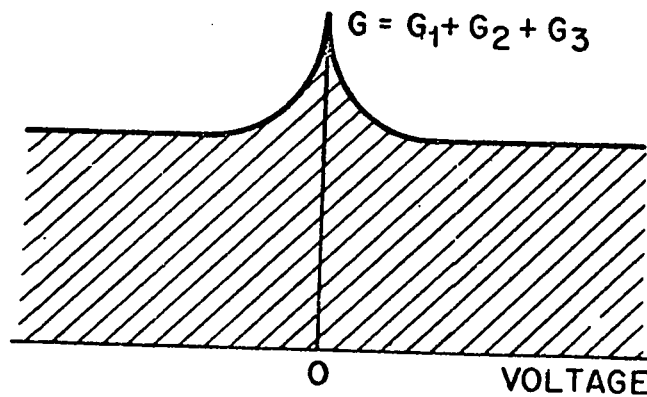
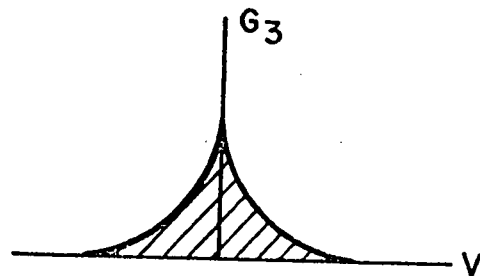
$G_1$



$G_2$



$G_3$



$g^{(2)}$  is due to electrons which scatter from A to B and in doing so exchange spin with the impurity. Obviously impurities anywhere in the oxide will contribute to this process.  $g^{(2)}$  will depend on the magnetic field but will be independent of voltage in zero magnetic field. The electron in A, as it approaches the barrier, can also be scattered back to A by exchange interaction. This reflected electron interferes with the transmitted electrons and this results in the third component  $g^{(3)}$ . Applebaum showed that it is this component which has the anomalous behaviour. He showed that for  $|v| \gg T$ ,  $g^{(3)}(v)$  (which is identical to  $\Delta g(v)$  of the earlier notation) varies as  $-\ln[(|v| + nT)/E_0]$ , where  $E_0$  is a cut off energy and  $n$  is a constant. This is similar to the result obtained by Wyatt (1964). It also depends on the nature of the exchange interaction  $J$  between the conduction electron and the localized spin. Antiferromagnetic coupling should result in a peak in conductance while ferromagnetic coupling should cause a dip.

This theory can be critically examined by comparing the observed and the predicted magnetic field dependence of the ZBA. The applied field  $H$ , will split the Zeeman levels of the impurity by  $g\mu_B H$ . Since the tunneling electron flips the spin of the impurity, it will have to lose energy  $g\mu_B H$ . Thus a hole of width  $2g\mu_B H$



will appear in the  $g^{(2)}$  term. Finally, Appelbaum has shown that the logarithmic peak due to  $g^{(3)}$  will also be split into two peaks  $2g\mu_B H$  apart. Thus at  $T = 0^\circ K$ , in this oversimplified model, the peak in total conductance  $g$  in zero field should change to a well of width  $2g\mu_B H$  with side peaks as the field is applied. This behaviour is shown in Fig. 3.5. Fig. 3.6. shows the  $g(v) - v$  plots of different tunnel junctions in different magnetic fields as found by Shen and Rowell. They conclude that the main effect of the field is to reduce  $g^{(2)}$  and thus decrease the total conductance near zero bias. The thermal smearing even at  $T \sim 1.5^\circ K$  is sufficient to smear the expected well in  $g^{(2)}$  to a dip. From the results at higher biases it is apparent that there is little field dependence of the  $g^{(3)}$  term, contrary to the calculations of Appelbaum. At most there is a slight increase in conductance for  $v > 1.5$  mv. Thus the observed twin peak behaviour of  $g(v)$  in the presence of a field is not due to splitting of  $g^{(3)}$ , but is due, almost entirely, to reduction in  $g^{(2)}$ .

From detailed analysis of their results, Shen and Rowell conclude that localized magnetic impurities are the cause of the ZBA and the scattering model of Appelbaum explains these tunneling characteristics. The 'giant anomaly' in  $Cr - Cr_x O_y - Ag$  junctions

Figure 3.5

Schematic representing the same processes of Fig. 3.4  
under the influence of an external magnetic field.

Here  $G$  corresponds to  $g$  in the text.

FIELD H APPLIED T=0

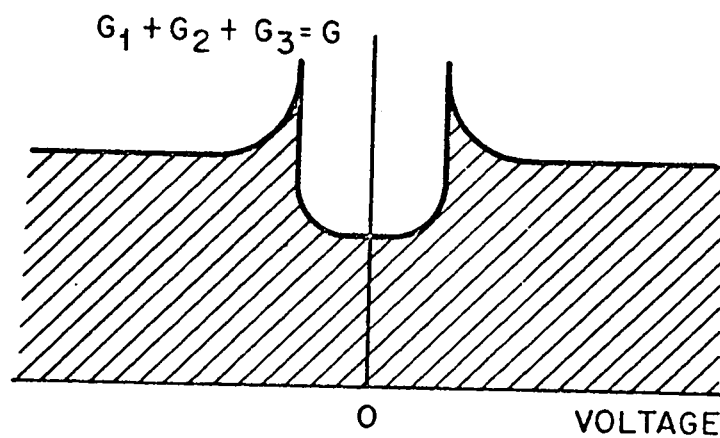
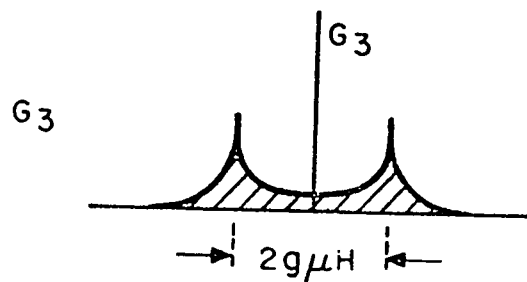
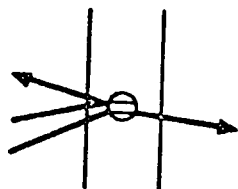
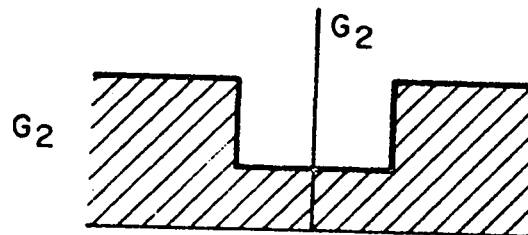
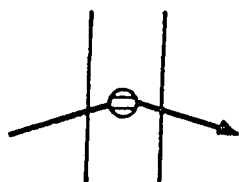
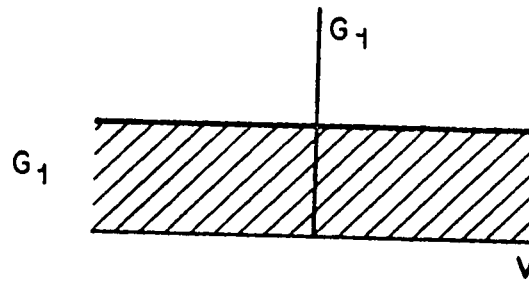
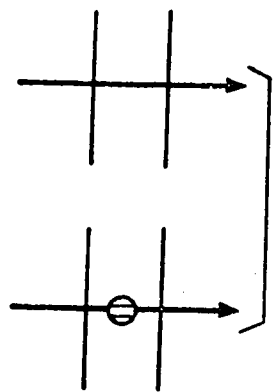
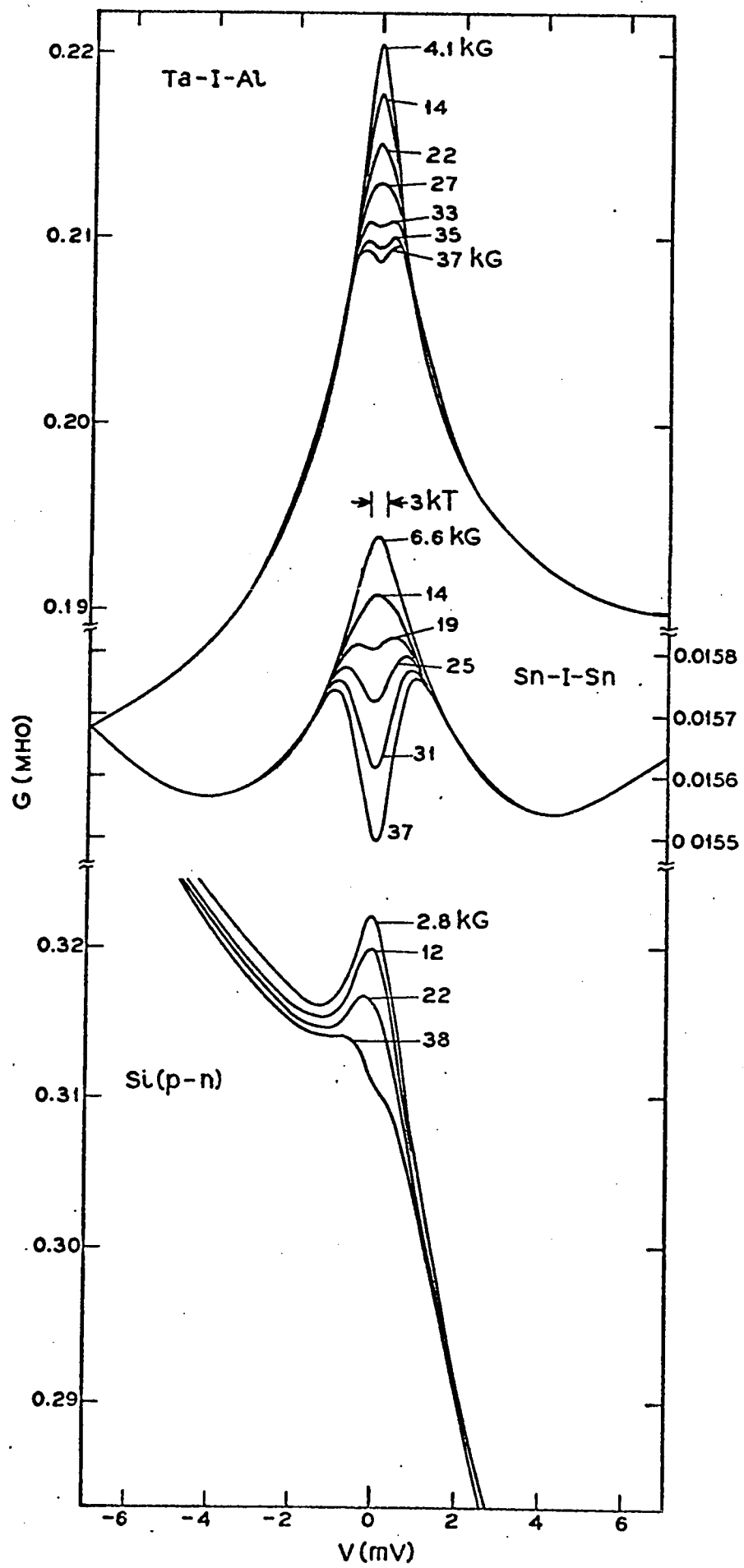


Figure 3.6

$g - v$  characteristics for different tunnel junctions at  $1.5^{\circ}\text{K}$  (after Shen and Rowell, 1968). Here  $G$  corresponds to  $g$  in the text.



remains unexplained, though attempts have been made to explain it in terms of strong-coupling between the tunneling electrons and the impurities (Appelbaum et al., 1967). Shen and Rowell also noted the following important effects of the zero-bias anomalies.

1. When the ZBA is large, the background conductance at high bias voltages is large.
2. ZBA appears to effect the superconducting properties of the tin films. Ratio of the current flowing at 0.2 mv (i.e.,  $v < \Delta_{\text{sn}}$ ) to that at 1.4 mv ( $v$  just above  $2\Delta_{\text{sn}}$ ) was considered as a measure of the departure from the 'ideal' behaviour of a s-s case. This ratio was large in tunnel junctions showing larger ZBA. However, no effect of ZBA was found on the energy gap or transition temperature of tin films (Rowell, 1968).
3. There is no effect of the chromium oxide on the energy gap of Pb in Cr - I - Pb junctions, but drastic reduction in the size and sharpness of the phonon-induced structure in the density of quasi-particle states in Pb was observed.

## CHAPTER IV

### EXPERIMENTAL METHOD

#### 4.1. Sample Preparation

It is generally the difficulties in the preparation of a tunnel junction which have hindered extensive exploitation of the basically simple technique of electron tunneling. While it is relatively easy to make tunnel junctions involving metals such as aluminum, lead, tin and indium, severe complications arise in the preparation of thin film tunnel junctions of metals such as the transition metals which have high melting and boiling points. Some of these problems will be discussed later in this chapter.

Al-I-La junctions were prepared for studying the superconducting properties of lanthanum. A few La-I-Al junctions were also studied. Junction preparation will be described in some detail in view of the extreme variability of the results with various fabrication parameters.

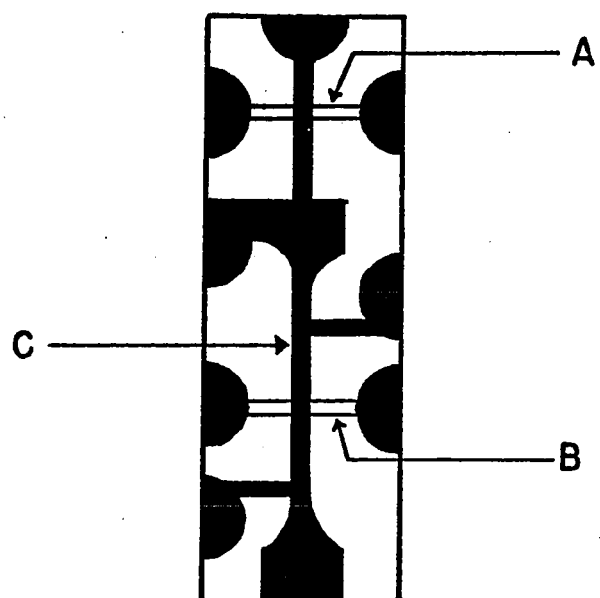
#### A. Al-I-La Junction

The tunnel junctions were always prepared in pairs. Fig. 4.1 shows a typical tunnel junction pair. A 1"x3" microscope slide was used as the substrate. The slide was first cleaned in the manner described by Adler (1963).

Figure 4.1

Diagram showing the Al-I-La tunnel junction pair. A and B are the aluminum films and C is the lanthanum film. Wide evaporated contact pads are also shown.





Nine leads of 36 B&S gauge copper wire were soldered on suitable areas of the glass slide using pure indium metal. All the evaporated films terminated in wide contact pads that overlapped the indium and provided contact with the leads. The slide was next placed on an appropriate mask inside the evaporator. The substrate was at room temperature at the beginning of all evaporations.

(i) The Base Layer

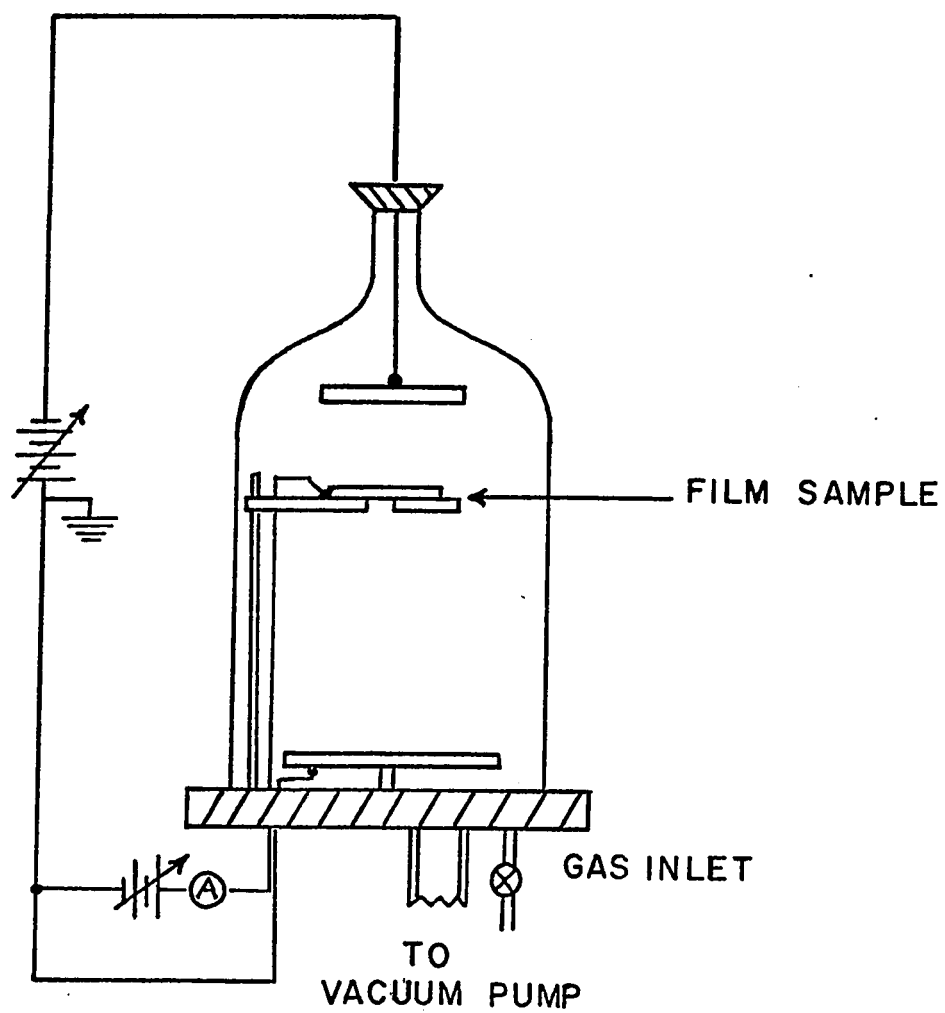
A pair of aluminum films and all the contact pads were evaporated from a 0.060" diameter tungsten wire carrying a charge of 99.999% pure aluminum.

(ii) The Barrier Layer

Al-I-La junctions, in which the barrier layers were prepared by thermally growing the oxide layer (see, e.g., Khanna, 1965) were found to be unstable. Stable oxide layers were prepared by a gaseous anodization process (Miles and Smith, 1963). For this purpose, the substrate was removed from the evaporator after the aluminum films had been deposited and was placed in a suitable plastic holder in another vacuum system shown in Fig. 4.2. The bell jar was filled with oxygen gas to a pressure of about 150  $\mu$  Hg. A glow discharge was initiated in the system by applying about 400 volts negative potential to a circular aluminum disc hanging from the top of the bell

Figure 4.2

Schematic showing the glow discharge apparatus for the barrier preparation.



jar. A metal plate in the base of the bell jar served as the ground electrode. The aluminum films were maintained at a small positive potential, about 0-6 volts, with respect to ground. The anodizing current was  $\sim 100 \mu\text{a}$  and was maintained almost constant by adjusting the pressure, the discharge potential in the bell jar and the potential of the aluminum films. The glow near the aluminum films was visible when the anodizing current was increased above about  $\sim 200 \mu\text{a}$ . The resistance of the junctions depended on the oxidation time, which was typically about 10 minutes. Though a junction suitable for tunneling measurements could be prepared with each attempt by this method, junction prepared in the same way could have resistances that differed by a factor of five. This was probably due to slight differences in the discharge conditions in the vacuum system.

### (iii) The Cover Layer

The substrate was then replaced in the evaporator and a cross strip of lanthanum about  $10,000 - 30,000 \text{ \AA}^0$  thick was deposited from a tantalum boat using 99.9+% pure lanthanum. The pressure inside the bell jar was about  $5 \times 10^{-7}$  torr at the start of evaporation while during the evaporation, a pressure of  $< 1 \times 10^{-5}$  torr could be maintained. Liquid nitrogen was circulated through a Meissner trap located about 4 cms above the base plate

around the periphery inside the bell jar. Lanthanum was first deposited on the large surface area inside the bell jar and then the substrate was exposed to the lanthanum vapour stream. High deposition rates of about  $300\text{--}600 \text{ \AA}^0/\text{sec}$  were used. The thickness of the edges of evaporated film may be slightly different from the rest of the film. The tunnel junctions were checked under a microscope and it was estimated that the edges of lanthanum and aluminum films over the junction region did not constitute more than 10% of the junction area which was about  $2.25 \text{ mm}^2$ . The substrate temperature increased to about  $80^\circ\text{C}$  during the evaporation. This completed the Al-I-La junction preparation.

It was possible to make four-terminal resistance measurements on two tunnel junctions and a portion of the lanthanum film. The evaporated films could be annealed by passing a current through them. For this purpose, it was necessary to have wide evaporated contact pads overlapping the indium metal to reduce the current density over this overlapping region.

#### B. La-I-Al Junction

La-I-Al junctions were also prepared in pairs. Lanthanum was first evaporated on a  $0.5 \times 1.8$  glass slide. It was oxidized at room temperature for about 8 minutes

either in air or in oxygen which has been passed through a trap immersed in liquid nitrogen. One junction was completed by depositing a cross strip of aluminum. The lanthanum film was further oxidized in the same manner for a period depending on the resistance of the first junction. Finally, a second cross strip of aluminum was deposited. Thus two tunnel junction  $2.25 \text{ mm}^2$  each were prepared. As lanthanum films oxidize quickly in air, there was insufficient time to replace the boats or the masks after each evaporation. Suitable boats were mounted in the evaporator at the start and the glass slide and rotating mask were held in different supports. Such junctions, however, often developed shorts at helium temperatures and the chances of getting a good junction were about one out of ten.

#### 4.2. General Considerations in Lanthanum Thin Film

##### Preparation

Lanthanum metal is an active reducing agent and reacts with oxygen, hydrogen and water vapours even at room temperature. Lanthanum films totally decompose at room temperature if they are exposed to air for a period that depends on the film thickness and the humidity content of air. The best method of storing bulk lanthanum was to keep it in vacuum. Lanthanum melts at  $920^\circ\text{C}$  and boils at about  $3470^\circ\text{C}$ . It has a vapour pressure of  $1 \times 10^{-3} \text{ mm}$  and

1 mm of Hg at 1535°C and 2331°C respectively. It is difficult to prepare thin films of this metal that have properties similar to the bulk material due to its extreme chemical activity and relatively high melting and boiling points. In this regard, lanthanum is similar to the transition metals, e.g. Nb, V and Ta. Superconducting properties of thin films of these metals have been studied by different workers. De Sorbo (1963) has studied the effect of dissolved impurities on the transition temperature  $T_c$  of bulk niobium. It was found that one atomic percent of oxygen in niobium lowered its  $T_c$  by about 1°K.

It is difficult to prepare oxygen free films of these elements because of their great affinity for oxygen. Lanthanum is even worse in this respect. Gaseous impurities are incorporated in a film during the deposition when gas molecules are absorbed on the surface of the film and are buried by metal atoms arriving later. The concentration of these impurities depends on (i) the partial pressure of the residual gases in the vacuum system, (ii) the ratio of the gaseous impurity atoms and the evaporating metal atoms striking the substrate and (iii) the sticking probability of the gas atoms when they hit the substrate. Ultra high vacuum,  $\sim 10^{-9}$  torr, is thus needed to prepare thin films of these metals (Gerstenberg and Hall, 1964),



though low critical temperatures have been reported even for films prepared in ultra high vacuum (London and Clark, 1964).

In relatively poor vacuo of  $\sim 10^{-7}$  torr, deposition of these metals on the large surface area inside the bell jar serves to reduce the partial pressure of oxygen by their gettering action. High deposition rates increase the ratio of the evaporating metal atoms to the gas atoms striking the substrate. As gettering continues at all times during the evaporation, the partial pressure of oxygen will continuously decrease as the deposition progresses depending on the leak rate of the vacuum system. Thus as the thickness of the evaporated film increases, the successive layers of the film have lesser oxygen concentration. Thus the transition temperatures of thick films of these metals are close to the corresponding bulk values. Rairden and Neugebauer (1964) have further shown the effect of substrate temperature on the properties of evaporated niobium films. They found that niobium films with transition temperature and lattice parameter similar to bulk niobium could be prepared by evaporating on a substrate at about  $400^{\circ}\text{C}$ . The resistance ratios of these films  $(R_{300^{\circ}\text{K}} - R_{10^{\circ}\text{K}})/R_{10^{\circ}\text{K}}$  increased from about 3.5 to 12.0 when the substrate temperature for evaporation was increased from room temperature to  $400^{\circ}\text{C}$ .

Four-terminal resistance measurements could be made on a portion of the lanthanum film while it was still in the evaporator. The resistance of the lanthanum film was measured at room temperature,  $R_{300^{\circ}\text{K}}$ , at liquid nitrogen temperature,  $R_{77^{\circ}\text{K}}$ , and at just above its transition temperature,  $R_0$ . The resistivity ratio,  $(R_{300^{\circ}\text{K}} - R_0)/R_0$ , of a film is a good measure of its purity and was used to compare the different lanthanum films. Bulk resistivity of lanthanum was used in the estimation of the film thickness from the film resistance measurements (Toxen et al., 1965).

#### 4.3. Electrical Measurements

Two-terminal resistance and capacitance measurements of the tunnel junctions were done with a RC bridge described by Rogers (1964). The signal from this bridge can be displayed on an oscilloscope as a function of voltage across the specimen over a range of about 0-300 mv and thus the non-linearity of the tunneling characteristic can be checked. Four-terminal resistance measurements of the lanthanum films were carried out with a bridge which is a simplified modification of the circuit described by Rogers, Adler and Woods (1964); it permits one 4-terminal measurement of the film resistance, three 2-terminal measurements of resistances of the films and one 4-terminal tunnel junction resistance measurement with an accuracy

of  $\pm 3\%$  without a change of lead connections.

#### A. Harmonic Detection Circuit

The structure in the tunneling density of states due to phonon effects varies widely among different superconductors. It is desirable to determine the normalized dynamic conductance  $\sigma = g_{ns}/g_{nn}$  to better than 1 part in  $10^4$  over the range of junction bias voltage from nearly 1 or 2 to 40 mv. Both  $\sigma$  and  $dg_{ns}/dv$  can be obtained by using harmonic detection techniques.

The principle of the harmonic detection method can be understood by considering Fig. 4.3a. It is an ac Wheatstone bridge in which the tunnel junction of resistance  $r$  may be treated as a slightly non-linear passive element. It provides nearly identical currents through its two branches if it is assumed that the junction is only weakly non-linear. If the current modulation amplitude  $\delta$  is kept constant, the voltage  $v$  across the tunnel junction can be written in terms of a Taylor's series,

$$v(i) = v(I_0) + \left(\frac{dv}{di}\right)_{I_0} \delta \cos \omega t + \frac{1}{2} \left(\frac{d^2v}{di^2}\right)_{I_0} \delta^2 \cos^2 \omega t +$$

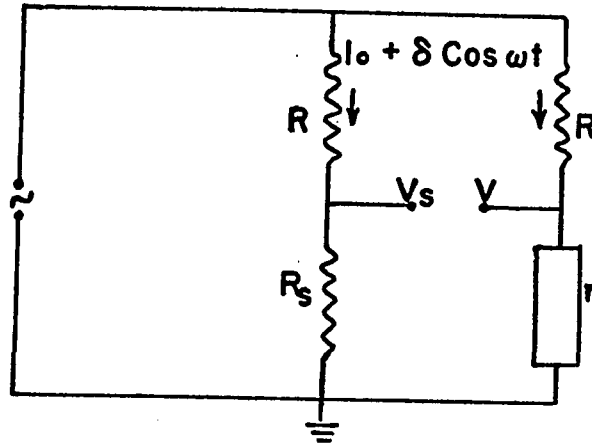
higher order terms,

(4.3 -1)

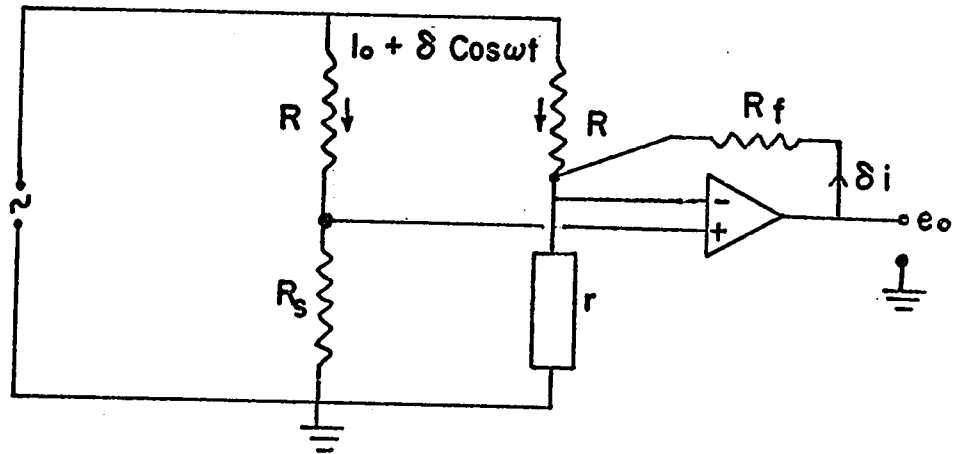
where  $v(I_0)$  is the dc bias across the tunnel junction and  $\omega$  is the modulating angular frequency. The voltage

Figure 4.3

Simplified harmonic detection bridge circuits.



(a)



(b)

$v_s$  across  $R_s$  which has linear  $i-v$  characteristic is given by

$$v_s(i) = (I_0 + \delta \cos \omega t) R_s . \quad (4.3 -2)$$

The ac part of  $(v-v_s)$  is

$$(v-v_s)_{ac} = \left[ \left( \frac{dv}{di} \right)_{I_0} - R_s \right] \delta \cos \omega t + \frac{1}{2} \left( \frac{d^2v}{di^2} \right)_{I_0} \delta^2 \cos^2 \omega t +$$

higher order terms. (4.3 -3)

If  $\delta$  is kept constant, the first harmonic component in  $(v-v_s)_{ac}$  is proportional to the departure of the dynamic resistance  $(dv/di)_{I_0}$  from  $R_s$  and the second harmonic component is proportional to  $(d^2v/di^2)_{I_0}$  of the tunnel junction. It is clear that the bridge circuit provides rejection of a large signal voltage across the junction and the drifts of oscillator and amplifier will affect only the difference rather than the full signal voltage.

It is, however, appropriate to measure  $g-v$  and  $(dg/dv)-v$  for the studies of the superconducting properties of the tunnel junctions. Fig. 4.3b shows a simplified bridge circuit which was used for this purpose. The essential feature of this circuit is to maintain  $v = v_s$ . The differential input to the high gain ( $\sim 50,000$ ) operation-

al amplifier is maintained essentially equal to zero by the negative feedback loop and to a first approximation  $v = v_s$ . Thus  $(v)_{ac} = (v_s)_{ac} = R_s \delta \cos \omega t = \epsilon \cos \omega t$  say. The alternating component of the current through  $r$  is given by

$$\delta \cos \omega t + \delta i = (di/dv)_{V_0} \epsilon \cos \omega t + \frac{1}{2} (d^2 i / dv^2)_{V_0} \epsilon^2 \cos^2 \omega t + \dots \quad (4.3 - 4)$$

where  $V_0$  is the dc potential across  $r$ .

$$\text{Thus } \delta i = [(di/dv)_{V_0} - 1/R_s] \epsilon \cos \omega t + \frac{1}{2} (d^2 i / dv^2)_{V_0} \epsilon^2 \cos^2 \omega t + \dots \quad (4.3 - 5)$$

and the output signal is

$$\begin{aligned} e_o &= \epsilon \cos \omega t + R_f \delta i \\ &= R_f [(di/dv)_{V_0} - 1/R_s + 1/R_f] \epsilon \cos \omega t \\ &\quad + \frac{1}{2} (d^2 i / dv^2)_{V_0} \epsilon^2 \cos^2 \omega t + \dots \end{aligned} \quad (4.3 - 6)$$

$$\text{Let } (di/dv)_{V_0} = g ; 1/R_s = G_s ; 1/R_f = G_f .$$

$$\begin{aligned} \text{Then } e_o &= R_f [(g - G_s + G_f) \epsilon \cos \omega t + \frac{1}{2} (dg/dv)_{V_0} \epsilon^2 \cos^2 \omega t \\ &\quad + \dots] . \end{aligned} \quad (4.3 - 7)$$

$G_f$  is generally small and hence can be neglected. Thus the first harmonic in the output voltage  $e_o$  is linear in  $g$  and is sensitive to  $(g - G_s)$ . The second harmonic in  $e_o$  is proportional to  $dg/dv$  of the tunnel junction. The complete bridge circuit diagram is shown in Fig. 4.4.\* The output signal from the bridge circuit is detected by a PAR HR-8 phase sensitive lock-in amplifier in which the signal is mixed with a reference signal of the fundamental or higher harmonic of the signal giving a dc output. This is fed to the Y input of a Mosley 7000 AMR X-Y recorder while the dc bias across the junction is plotted along the X-axis. The dc bias across the junction is swept by an electronic sweep circuit or a motor driven potentiometer.

#### B. Conductance Calibration

Linearity of the bridge was checked by using known resistances from  $10\ \Omega$  to  $1K\ \Omega$ , with a variable capacitor across them, in place of the junction in the bridge circuit. Lead resistances of  $50\ \Omega$  were used in this test. The bridge was found to be linear in conductance and the changes in conductance could be measured with an accuracy 1 part in  $10^4$  with a modulation voltage of

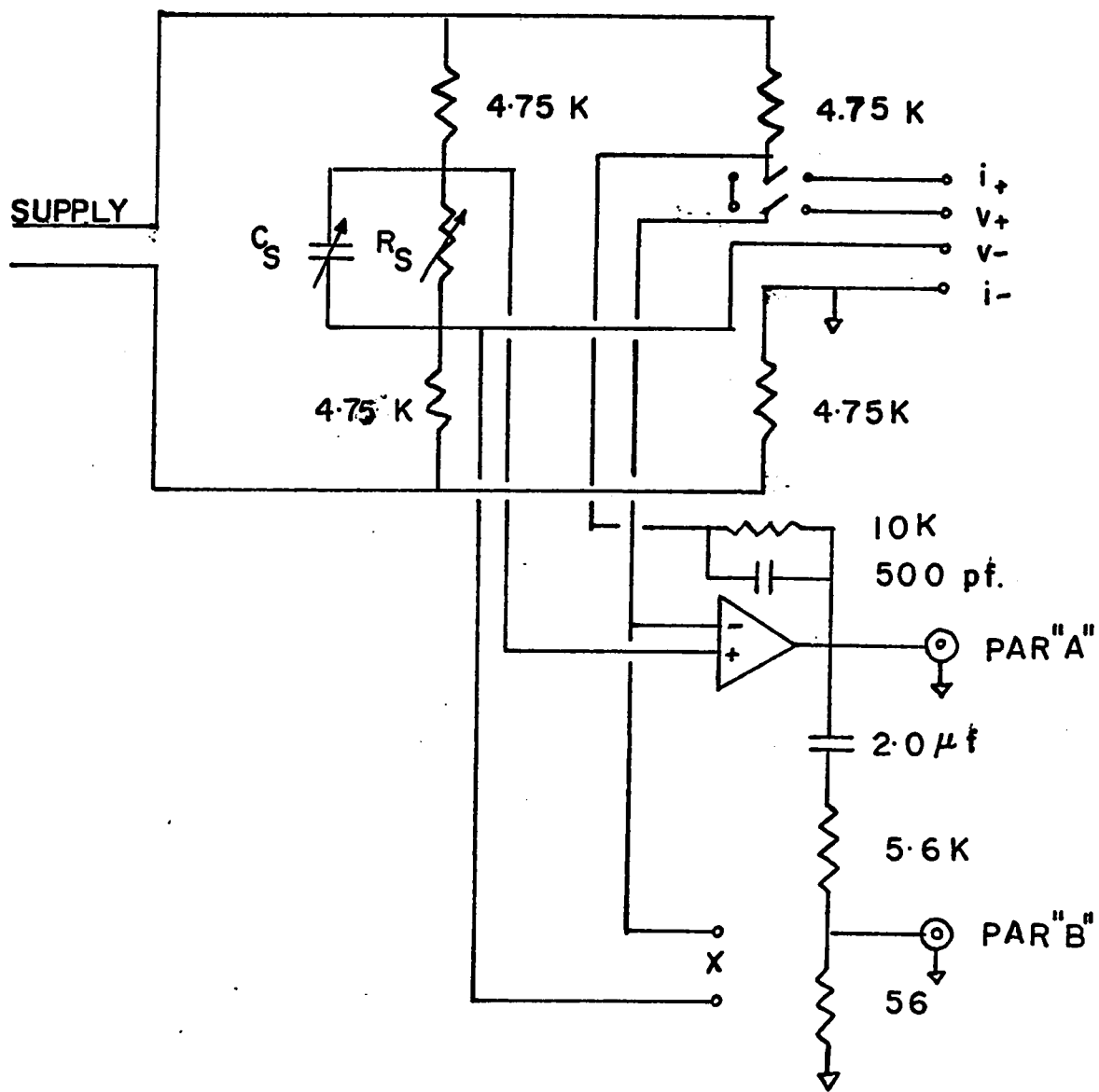
---

\* It is a pleasure to thank Dr. J.S. Rogers for his designing this bridge. Further details regarding the bridge are given in "Rogers J.S., 1967 Tunneling Curve Tracer Manual, University of Alberta, 1968".



**Figure 4.4**

**The bridge circuit.**



about 100  $\mu\text{V}$  rms.

A modulation voltage of about 70-100  $\mu\text{V}$  rms was used for the phonon studies while it was about 20  $\mu\text{V}$  rms for the conductance plots over the energy gap region. The lowest temperature used in this work  $\sim 1.75^\circ\text{K}$  and the thermal smearing ( $k_B T = 86 \mu\text{V}$  at  $1^\circ\text{K}$ ) was always more than the smearing due to the modulation voltages used in this work.

The bridge was first balanced at  $\sim 15$  mV bias voltage. Both reactive and resistive balances of the bridge were obtained by using the phase sensitive lock-in amplifier. The phase between the reference signal and the input signal to the lock-in amplifier was properly adjusted so that any capacitative imbalance did not affect the resistive balance. It was then desirable to calibrate the Y gain of the recorder display. For this purpose, the junction was open circuited resulting in  $g=0$ . The difference in  $g=0$  and  $g=1$  was adjusted to 10 cms y-deflection of the X-Y recorder by suitably adjusting the recorder and the lock-in amplifier sensitivities. Higher Y-axis sensitivities could be directly dialed through the lock-in amplifier.  $\frac{dg}{dv} - v$  traces could be plotted by using a reference frequency of  $2\omega$ . Since there was relatively weak structure in the junctions of aluminum and lanthanum, modulation levels from about 170 to

350  $\mu\text{v}$  rms were used for the second derivative plots.

$\sigma$ -v is calculated by superimposing the  $g_{\text{ns}}$ -v and  $g_{\text{nn}}$ -v plots. The difference between the two traces directly gives  $(\sigma-1)$  to a good approximation. For energy gap analysis, it is, however, preferable to divide the two conductance values for the n-s and the n-n cases to obtain  $(\sigma-1)$ .

It is important to emphasize that the  $g_{\text{nn}}$ -v plot should be measured with the same sensitivity as the  $g_{\text{ns}}$ -v plot for proper normalization, particularly when the normal state conductance  $g_{\text{nn}}$  varies appreciably with bias as in the tunnel junctions showing the ZBA. It is also necessary to ascertain that  $g_{\text{nn}}$ -v characteristic does not change between the temperatures at which  $g_{\text{nn}}$ -v and  $g_{\text{ns}}$ -v are studied.

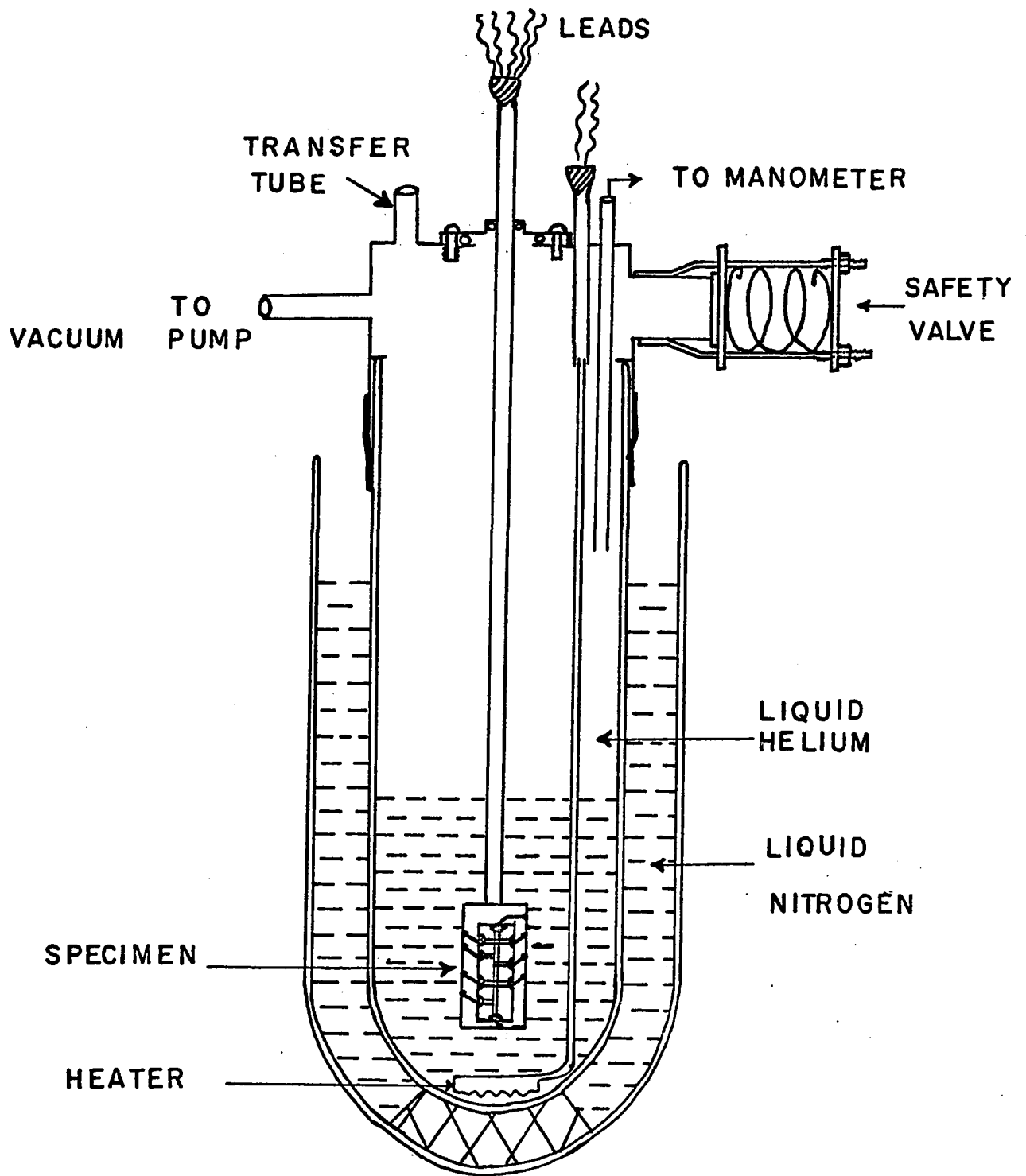
#### 4.4. Production of Low Temperatures

The experimental arrangement used in this work is shown in Fig. 4.5. It permitted quick ( $\sim 10$  minutes) cooling of the tunnel junction to liquid  $\text{N}_2$  temperature after it was removed from the evaporator. This was important as the junction deteriorates with time at room temperature. It can, however, be maintained at liquid  $\text{N}_2$  temperature without any further deterioration for long periods.

W 21

Figure 4.5

The dewar arrangement for the low temperature production.



The sample was removed from the evaporator soon after the cover layer of lanthanum had been deposited. For this purpose, helium gas which has been passed through a trap immersed in liquid  $N_2$  was first allowed to enter the evaporator. The specimen was then quickly mounted on a plastic board at the end of a dip stick and lowered into the inner dewar containing liquid  $N_2$ . The junction was not removed from this dewar until all the measurements had been taken. Liquid  $N_2$  was next siphoned out by pressurizing it to about 80 cms of Hg. Liquid helium was then transferred in the inner dewar.

Liquid helium in the inner dewar could be pressurized to about two atmospheres. Temperatures lower than  $4.2^{\circ}\text{K}$  were obtained by pumping over liquid helium. The temperature was obtained by measuring the vapour pressure of liquid helium. A 15 mm I.D. and an 8 mm I.D. Hg manometers were used in conjunction with a Wild cathetometer to measure the pressure in the range from 0 to 2 atmospheres. The vacuum side of the large manometer was maintained at a vacuum  $\ll 0.01$  mm Hg with a charcoal trap at  $\sim 80^{\circ}\text{K}$ . The vacuum was checked occasionally with a mechanical pump. A manostat with a flexible membrane permitted temperature regulation to better than 5 mdeg. Since the specimen was immersed in liquid helium bath, it was in good thermal contact with the bath. Thus it was

possible to determine the temperature of the specimen from  $\sim 1.8^{\circ}\text{K}$  to  $5.1^{\circ}\text{K}$  with an accuracy of 5 mdeg. Its temperature could be raised above  $5.1^{\circ}\text{K}$  by pulling it out of the liquid helium bath. A Westinghouse superconducting solenoid with a rated field of 21 kG was used to apply magnetic fields parallel to the films of the junction.

#### 4.5. Description of a Typical Run

The selection of a good tunnel junction is important. There are a few tests that can be used to select a 'good' junction before it has been cooled to helium temperature. Firstly, its resistance and capacitance could be measured at room temperature. A tunnel junction having a uniform barrier layer of  $\text{Al}_2\text{O}_3$  could be subjected to a voltage of about 250 mv for short periods without damage and the non-linearity of the tunneling characteristic could be checked. This may not be possible with tunnel junctions having other barrier layers. Poor tunnel junctions were generally noisy at higher bias values and invariably developed metallic shorts when cooled to helium temperatures. Further the junction resistance should remain essentially the same on cooling from room temperature to helium temperature. The essential criterion of a good junction is that at sufficiently low temperatures  $T \ll T_c$ , it should show the characteristic



energy gap(s) of the superconductor(s) constituting the junction and that the tunneling current dominates over any other conduction mechanism.

After the junction was successfully mounted, the resistances of the junctions and the films were measured at liquid  $N_2$  temperature.  $g-v$  was then measured at this temperature at bias voltages between -30 mv and +30 mv to determine the asymmetry in the tunneling conductance. By pumping over liquid helium, the lowest possible temperature was attained; the bridge was suitably balanced and calibrated and  $g_{ns}-v$  was plotted in the energy gap region. The modulation level was then increased; the bridge was recalibrated and  $g_{ns}-v$  was plotted from 1 or 2 mv to about 40 or 50 mv. The temperature of the liquid helium was then raised to about  $5.1^{\circ}K$ ; the bridge was rebalanced and calibrated and  $g_{nn}-v$  was plotted over the same voltage region with the same sensitivity. Alternatively, a magnetic field was applied to obtain the normal state of the superconductor and  $g_{ns}-v$  and  $g_{nn}-v$  were plotted at the same temperature.  $g-v$  was then measured in the energy gap region from about  $5.1^{\circ}K$  to  $1.7^{\circ}K$ . Tunneling transition temperature  $T_{c\Delta}$  of the superconductor is defined as the temperature at which the energy gap first appears in these curves. At  $T_{c\Delta}$ , there is a sudden decrease in  $\sigma$  at

zero bias that indicates the transition from normal to superconducting state.

Resistive transition temperature  $T_{cr}$ , where the resistance of the lanthanum thin film becomes zero, was always higher than its  $T_{c\Delta}$ . For the ZBA studies, the  $g_{nn}-v$  was measured at different temperatures. Finally, the residual resistance of the lanthanum film was also measured.

## CHAPTER V

### Experimental Results and Discussions

There has been considerable speculation concerning the mechanism for superconductivity in lanthanum which was discussed in Section 2.5. In recent years, this led to many experimental investigations of its superconducting properties by various techniques. The energy gap  $2\Delta_0$  at  $T = 0^\circ\text{K}$ , the transition temperature  $T_C$  and hence the ratio  $2\Delta_0/k_B T_C$  were generally the principal parameters that were determined in these studies. Varied results were reported by different workers (Leslie et al., 1964; Edelstein and Toxen, 1966; Hauser, 1966; Thompson, 1967; Levinstein et al., 1967) in the beginning and the problem was not clear from the experimental standpoint.

Lanthanum can occur in two phases, fcc and d-hcp, at room temperature. The d-hcp structure is the stable phase at room temperature but the phase transition is rather sluggish. Thus it has not yet been possible to prepare a sample having only one structure. Johnson and Finnemore (1967) have successfully prepared samples containing either 96% d-hcp or 91% fcc lanthanum.

Four research articles (Edelstein and Toxen, 1966; Hauser, 1966; Levinstein et al., 1967; Edelstein, 1967), dealing mainly with the energy gap measurement in La by electron tunneling techniques, have been published since July 1966 and the results differ considerably from one another. We obtained the results on the energy gap in La thin films almost simultaneously with these reports and we now understand to some extent the reasons for the differences in the results.

The results of the phonon effects on the tunneling density of states will be discussed first and the results on the energy gap measurements will be given in the following section. All the junctions studied in this work showed zero-bias anomalies and only those junctions which had  $ZBA^* \sim 2\%$  were selected for superconducting studies.

#### 5.1. Phonon Effects in Tunneling Density of States in Lanthanum

The primary object of this work was to study the tunneling density of states in La with a view to determine if any alternate interaction, other than the phonon-mediated electron-electron interaction, could be mainly

---

\* Magnitude of a ZBA is defined in Section 3.3.

responsible for its superconductivity. Any variation from the nature of the tunneling density of states in a phonon-mediated superconductor should be observable directly and the origin of the attractive interaction might then be traceable.

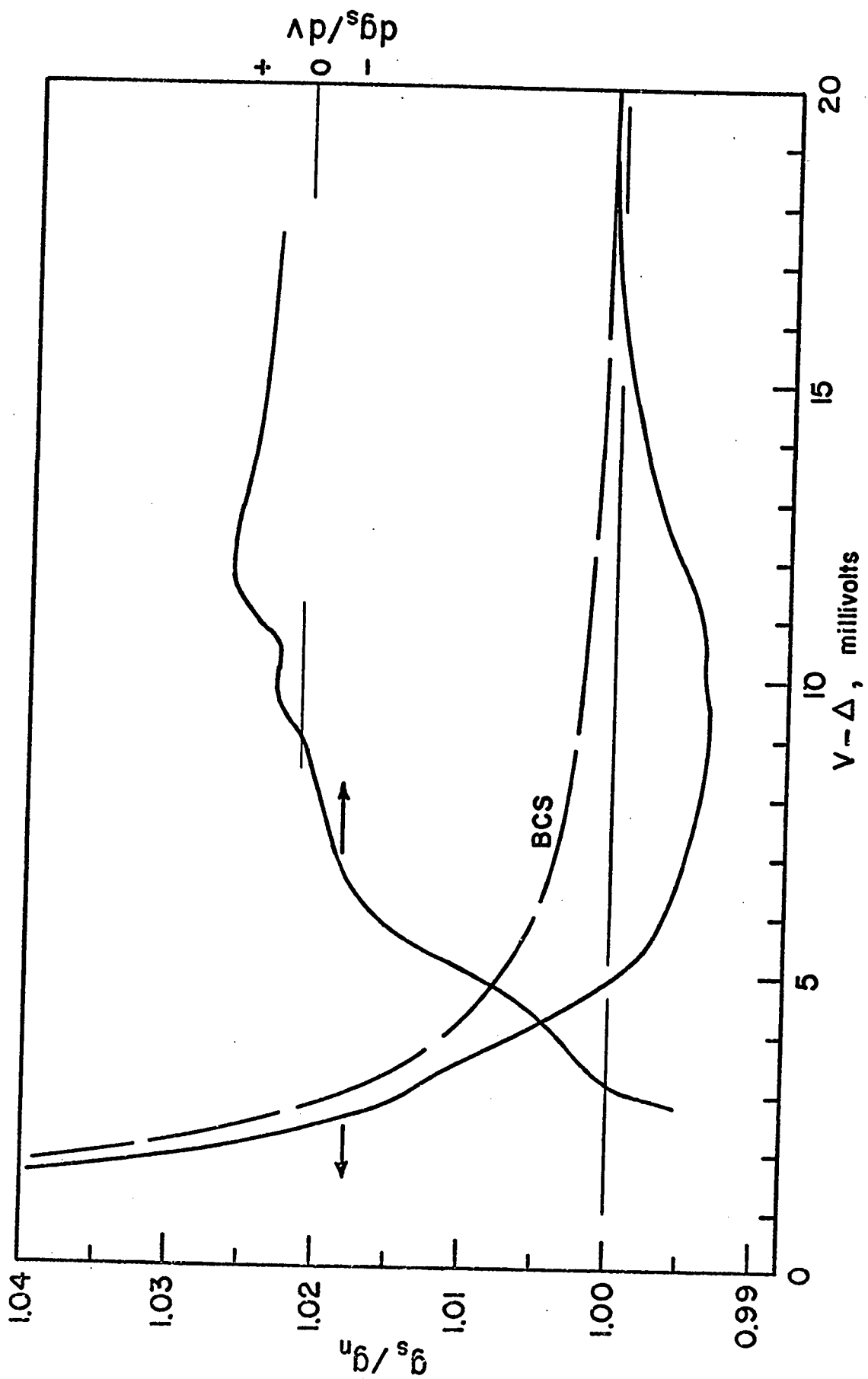
The phonon effects on the tunneling density of states of a superconductor have been discussed in Section 3.2. Each predominant phonon peak in a superconductor appears as a small peak followed by a rapid drop in its effective tunneling density of states which is reflected in the normalized dynamic conductance  $\sigma$  vs. voltage  $v$  characteristic of a tunnel junction. Thus  $\sigma - v$  curves have points of inflection at energies corresponding to the predominant phonon peaks in the superconductor. Phonon effects have been observed in many superconductors, e.g., the strong-coupling superconductors like Pb (Rowell and Kopf, 1965), Hg (Bermon and Ginsberg, 1964), and the weak-coupling superconductors like Al (Woods and Rogers, 1966), In (Adler et al., 1965). Wyatt (1964b) has also demonstrated these effects in two of the superconducting transition metals, Ta and Nb. These results emphasize that the superconductivity of these metals is largely due to electron-phonon interaction.

Fig. 5.1 shows the  $\sigma - v$  characteristic of a typical  $\text{Al}-\text{Al}_x\text{O}_y-\text{La}$  junction at  $2.05^\circ\text{K}$ . Reproducible results, which were polarity independent, were observed for six successive junctions. These junctions had  $\sim 2\%$  zero-bias conductance anomalies and hence for normalization, the normal state conductance  $g_{nn}-v$  was also obtained with the help of a magnetic field rather than increase in temperature. This was done to eliminate the temperature dependence, if any, of the  $g_{nn}-v$  plot. There was practically no magnetic field dependence of the  $g_{nn}-v$  characteristic at these energies. The second derivative plot  $\frac{dg_{ns}}{dv} - v$  was also obtained at the same temperature. The BCS density of states for La is shown for comparison.

Thus while no sharp structure of  $\sim 0.1\%$  amplitude is present, there is a definite overall departure of the observed curve from the BCS density of states, and it has a marked resemblance to typical corresponding results that would be expected of a phonon-mediated superconductor, in which the phonon spectrum is poorly developed. Sharpness of the structure would also be lost if the La did not exhibit a single energy gap over the entire junction area. Also the transition from normal to superconducting behaviour would be broad.

Figure 5.1

Normalized first-derivative ( $g = \frac{di}{dv}$ ) and second-derivative results for an Al-I-La tunnel junction at 2.05° K. The dashed curve is the BCS density of states for La.  $g_s$  and  $g_n$  in this diagram correspond to  $g_{ns}$  and  $g_{nn}$  in the text.





The amplitude of the gross structure is of the order of magnitude ( $\sim 1\%$ ) which one would expect from the value of  $T_c / \theta_D$  of La if it were a phonon-mediated superconductor. Fig. 5.2 shows this structure in the  $\sigma - v$  plots at different temperatures for specimen La-18.

The strength of the phonon structure,  $S(T)$ , may be defined as

$$S(T) = 1 - \sigma_{\min} \quad (5.1 - 1)$$

where  $\sigma_{\min}$  is the minimum value of the normalized dynamic conductance outside the gap region. Adler et al. have shown that  $S(T)$  varies linearly as  $\Delta^2(T)$  approximately. Fig. 5.3 shows a plot of  $S$  vs.  $\Delta^2$  for specimen La-18 and the results are in agreement with these calculations.

Levinstein et al. have reported seeing phonon effects of amplitude intermediate between those of Sn and Pb during the course of preliminary point contact tunneling measurements in bulk La. However, the results were not reproducible due to the unstable nature of these junctions (Kunzler, 1968). Edelstein has reported seeing no such effects with La thin film tunnel diodes. The lack of structure due to the phonon spectrum was attributed to lattice disorder in these films. This explanation would be more convincing if phonon effects could be destroyed by deliberately distorting the lattice of

Figure 5.2

Normalized dynamic conductance  $\sigma$  vs. voltage  $v$   
characteristics at different temperatures for the  
specimen La - 18.

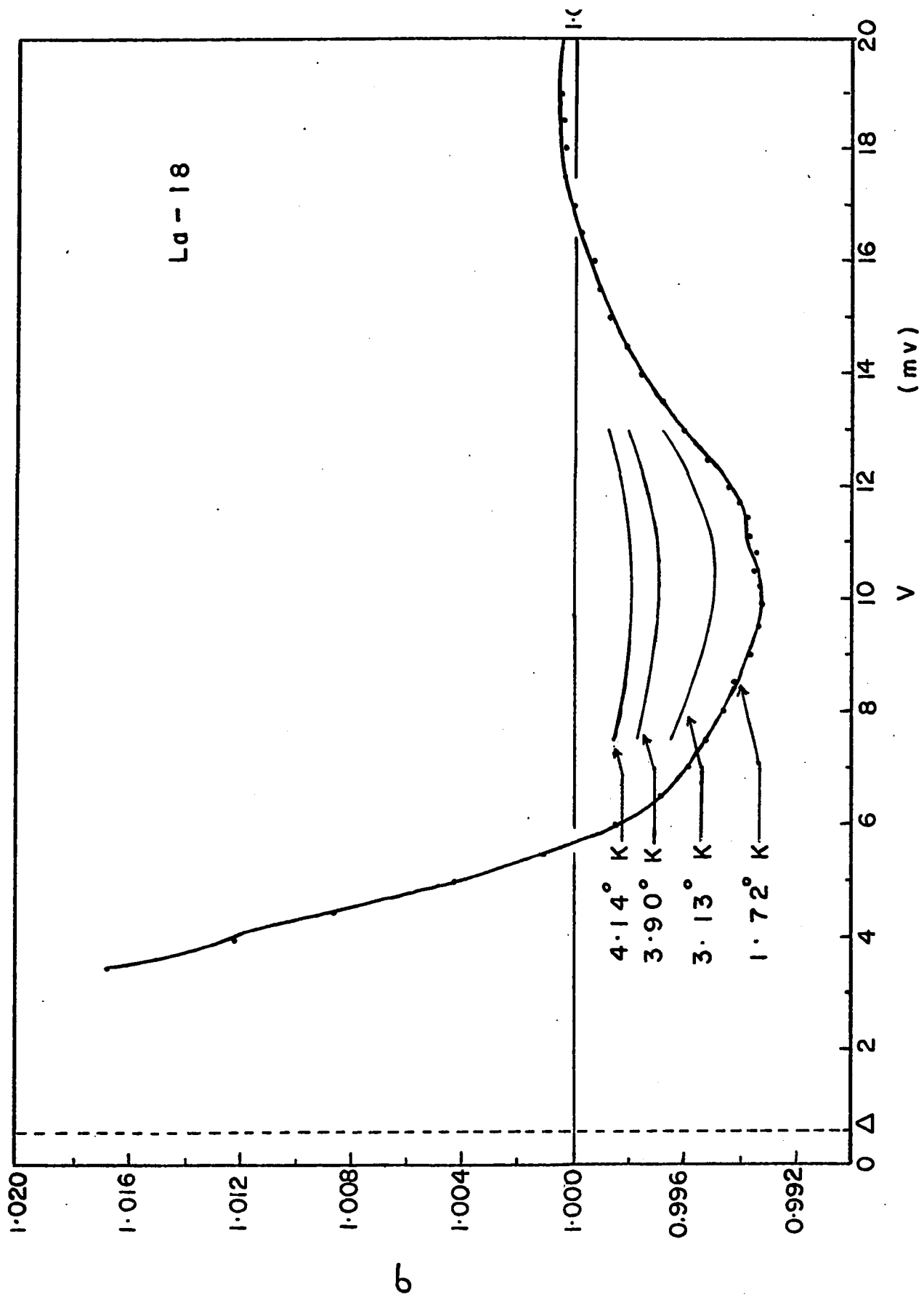
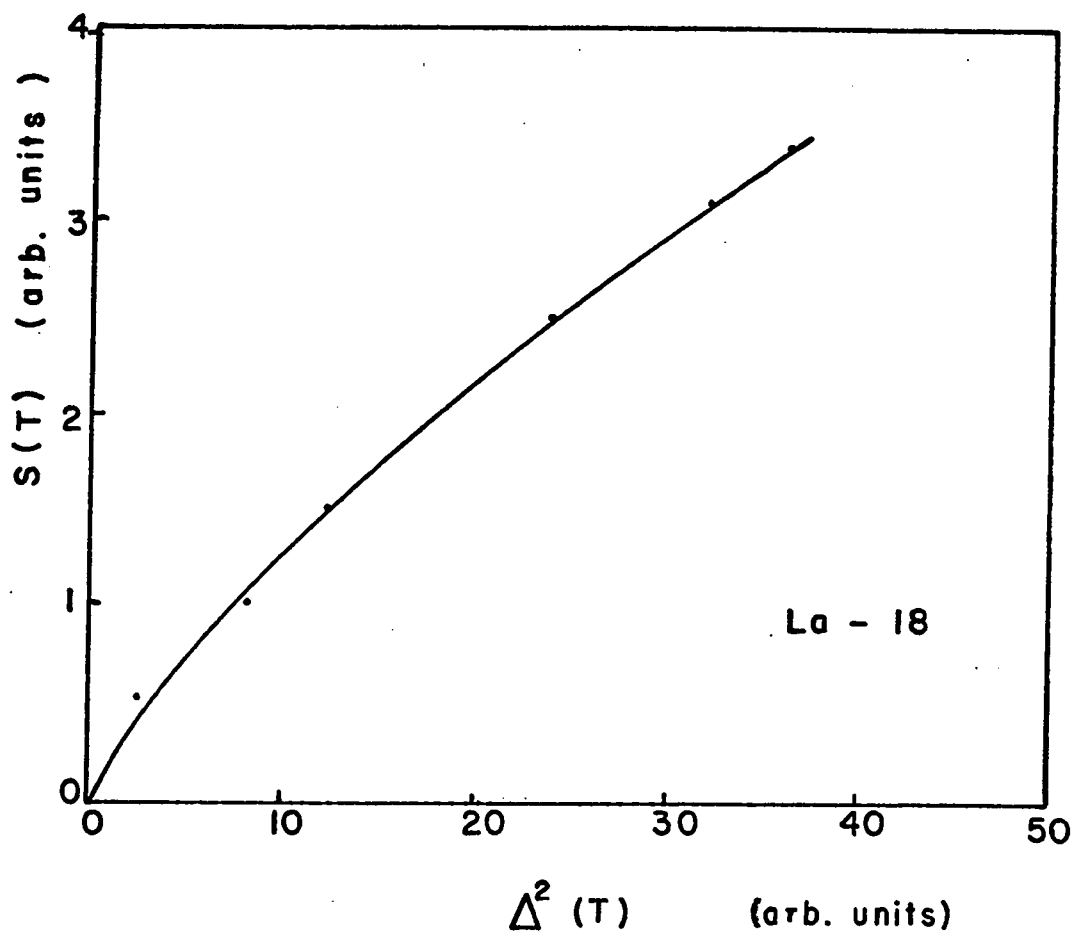


Figure 5.3

S (as defined in Eqn. (5.1 -1)) vs.  $\Delta^2$  plot for the specimen La - 18.



other metals. Lattice distortion in thin films in all the following cases was achieved by evaporating the films on substrates at helium temperatures.

Zavaritskii (1967 b) has studied the influence of lattice distortion on the superconducting properties of lead films and has observed that the phonon structure in  $\sigma - v$  and  $\frac{dg_{ns}}{dv} - v$  plots become smoother. Phonon effects are, however, definitely present in these junctions. Annealing the junctions at  $80^{\circ} \text{K}$  and  $300^{\circ} \text{K}$  increasingly sharpened this structure and the tunnel characteristics of the junction annealed at  $300^{\circ} \text{K}$  agree with the results of junctions where the Pb films were deposited at  $300^{\circ} \text{K}$ .

Structure in the  $\sigma - v$  plots have been observed by Zavaritskii (1967 a) and by Chen et al. (1967) in amorphous bismuth films. More recently, phonon effects have also been observed in amorphous gallium films (Wühl et al., 1968). In both cases, there is no sharp structure and the  $\sigma - v$  plots are quite similar in nature to those observed in La. On annealing the Al-I-Ga junctions at temperatures between  $15^{\circ} \text{K}$  and  $60^{\circ} \text{K}$ , sharp structure appears in  $\sigma - v$  plots. This structure is associated with the phonon peaks in the crystalline phase,  $\beta - \text{Ga}$ .

Al-I-La junctions deteriorate unless stored at or below liquid nitrogen temperatures. Attempts to anneal the La films by allowing the fabricated diodes to remain at  $300^{\circ}\text{K}$  in a vacuum or a pure helium atmosphere for even a few hours caused a marked deterioration of the tunnel junction as observed from the  $g_{\text{ns}} - v$  plots before and after the annealing treatment. In particular,  $2\Delta_0$ ,  $T_{\text{c}\Delta}$  and the ratio  $2\Delta_0/k_{\text{B}}T_{\text{c}\Delta}$  became smaller; the factor  $(1-\sigma_0)$ , where  $\sigma_0$  is the normalized dynamic conductance at zero-bias, increased by a few times and the conductance at higher bias voltages became erratic. The annealing attempts did not cause any appreciable change in the film resistivity. The junction fabrication technique, which was used in this work was accordingly a compromise between deposition onto a cold substrate which would smear the phonon spectrum, and deposition onto a hot substrate, which would destroy the junction.

The  $\sigma - v$  and  $\frac{dg_{\text{ns}}}{dv} - v$  results in Fig. 5.1 are thus suggestive of a phonon spectrum consisting of transverse and longitudinal peaks at  $\sim 4.5$  and  $10$  meV, respectively. The Debye temperature  $\theta_{\text{D}}$  (at  $\theta_{\text{D}}$ ) affords an approximate ( $\pm 20\%$ ) cross check on the longitudinal energy in that this energy is usually  $(1.1 - 1.4) k_{\text{B}}\theta_{\text{D}}$ . Our results would therefore suggest  $\theta_{\text{D}} \approx 100^{\circ}\text{K}$  at  $100^{\circ}\text{K}$ ; the specific-heat results of Johnson and

Finnemore yield  $\theta_D \approx 120^\circ \text{K}$  at  $10^\circ \text{K}$  for d-hcp or fcc La.

In conclusion, we have observed structure in the tunneling characteristics of La thin film diodes which is attributed to a broad phonon spectrum in the material sampled by the tunneling measurements, but in view of the differences in values of  $T_c$  and  $2\Delta_0/k_B T_c$  obtained from thin film tunnel diode measurements and the bulk values (cf., Table 2), we expect this spectrum to be only an approximate representation of pure bulk La.

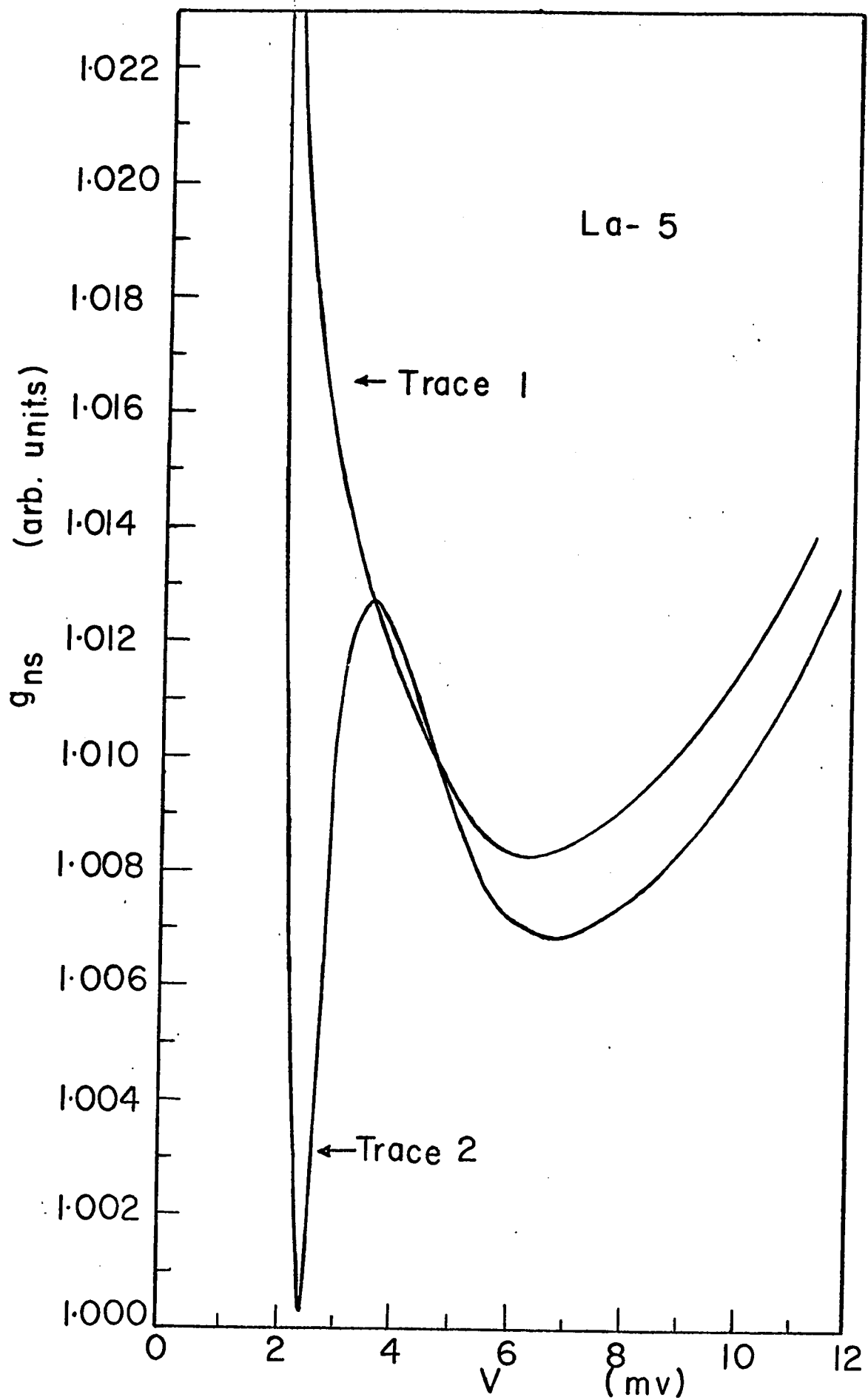
No structure, which could be associated with a second energy gap predicted by Kuper et al. (1964) was observed in  $\sigma - v$  characteristics. Fig. 5.4 shows the  $g_{ns} - v$  plots of an Al-I-La junction at two temperatures. The aluminum probe is normal in trace 1 and superconducting in trace 2. The structure near 2.5 meV in trace 2 is probably due to the superconducting aluminum probe. Such structure has been observed in junctions composed of alloys with multiple gaps and aluminum (Adler, 1968) but much more detailed work would be necessary to confirm the existence of multiple gaps in La.

Our results on the structure in the tunneling density of states of La are in accord with the present



Figure 5.4

$g_{ns} - v$  plots for an Al-I-La tunnel junction at two different temperatures. The aluminum probe is normal in trace 1 and superconducting in trace 2.



theories of superconductivity which are based on an electron-phonon interaction. The values of the various parameters of superconducting La as measured by electron tunneling in thin films diodes are lower than the corresponding bulk values. The structure in  $\sigma - v$  plots is also not fully resolved. Thus the possibility, that some other mechanism may be responsible for superconductivity of La, cannot be entirely excluded. It would appear, however, that any alternate theory must predict a departure (or departures) in the tunneling density of states near the Debye energy which is not much different in amplitude from those given by the present theories.

Johnson and Finnemore have drawn similar conclusions regarding the mechanism for superconductivity of La from the results of specific heat measurements of both phases of La which are in agreement with the BCS theory. From  $2\Delta_0/k_B T_C$  and critical field measurements of La, Johnson and Finnemore classified it as an intermediate-coupling superconductor.

## 5.2. The Energy Gap in Superconducting Lanthanum

Table 1 gives the summary of the results for several Al-I-La thin film diodes.

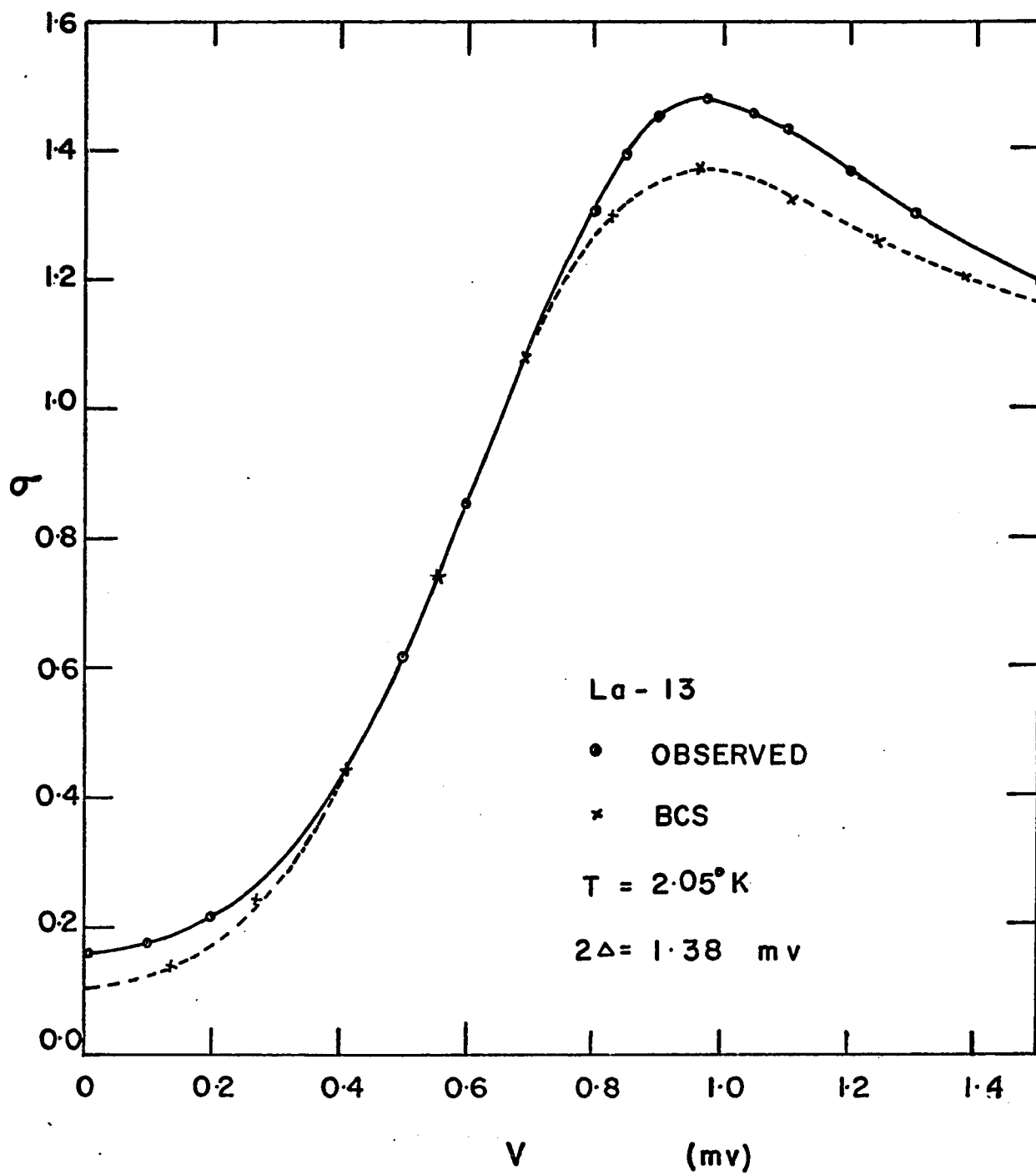
Table 1  
Properties of Superconducting Lanthanum Films. (1)

Tunnel junction	La film thickness ( $\text{\AA}$ )	Resistivity ratio	$T_{c\Delta}$ ( $^{\circ}\text{K}$ )	$2\Delta_0$ (meV)	$2\Delta_0/k_B T_{c\Delta}$
Ia-18	28,000	4.41	4.83	1.25	3.00
Ia-17				1.25	
Ia-14	17,000	4.61	5.39*	1.40	3.01
Ia-12	29,000	5.15	5.07	1.32	3.02
Ia-11			5.06	1.32	3.03
Ia-2	3,700	1.2	4.47	1.25	3.24

(1) Two tunnel junctions were prepared for each run and were given consecutive numbers. In some runs, only one member of the junction pair was studied in detail for the measurements of the various superconducting parameters. These parameters were expected to be nearly the same for the two members of the junction pair, as in La 11 and La 12.

\* Estimated value obtained by comparison with Ia-12.

The energy gap was determined by fitting the calculated normalized dynamic conductance  $\sigma$  of a tunnel junction as a function of bias voltage  $v$  to the experimental  $\sigma - v$  curve in the energy gap region. Bermon's tables (1964) were extended to obtain the calculated  $\sigma - v$  curves. These calculations are valid for a weak-coupling BCS superconductor having a single energy gap parameter. This is a reasonably accurate method for determining the energy gap of a superconductor from a n-s junction, specially at temperatures near the transition temperature of the superconductor. The experimental and the calculated curves are not expected to match in case of superconductors e.g., La, which do not have an exact BCS density of states. Fig. 5.5 shows a plot of  $\sigma - v$  in the energy gap region for a typical junction. The dashed curve is the calculated curve and it represents the best overall fit to the experimental curve. The measured normalized dynamic conductance at zero bias,  $\sigma_0$ , and the peak value of  $\sigma$ ,  $\sigma_{\max}$ , are always higher than the corresponding calculated values at low temperatures. The fit at zero bias can be improved by decreasing the estimated value of  $\Delta$ , but this will shift the calculated  $\sigma_{\max}$  to a lower bias. Similarly the experimental and the calculated values of  $\sigma_{\max}$  can be made to coincide by increasing the estimated value of  $\Delta$ , the two curves will



then not fit at zero bias and the  $\sigma_{\max}$  in the two curves will occur at different bias values. Similar results have been obtained by Edelstein in Al-I-La junctions and by Bermon and Ginsberg in Al-I-Hg junctions. An error of 5% is estimated for the energy gap values reported here.

The tunneling transition temperature  $T_{c\Delta}$  for the La film was determined by measuring the temperature at which  $\sigma_0$  began to decrease below unity. The transition was rather broad and the presence of ZBA further complicated its accurate measurement. We place an error estimate of 1% on the  $T_{c\Delta}$  of La films. In La films, the transition temperature  $T_{cr}$  as measured by the disappearance of resistance in the film was always higher than the corresponding temperature  $T_{c\Delta}$ . In most cases, it was above  $5.1^\circ\text{K}$  and could not be measured due to our experimental limitations. Accurate determination of  $T_{cr}$  was, however, not necessary for this work.

The electron mean free path in the La films is estimated to be  $\sim 50\text{\AA}$  corresponding to the resistivity ratio equal to 4. Since the bulk starting material had a resistivity ratio of  $\sim 20$ , we believe the short free path is caused by lattice defects in the films.

Before further discussing these results, it is perhaps appropriate to compare the corresponding results in La obtained by different techniques. These results are summarized in Table 2.

There is good agreement between the specific heat and the electron-tunneling results for bulk lanthanum. The transition temperature  $T_c$ , the energy gap  $2\Delta_0$  and the gap ratio  $\frac{2\Delta_0}{k_B T_c}$  for the superconducting bulk lanthanum are respectively,  $4.9^\circ \text{K}$ ,  $1.56 \text{ meV}$  and  $3.7$  for d-hcp La and  $6.0^\circ \text{K}$ ,  $1.91 \text{ meV}$  and  $3.7$  for fcc La (Johnson and Finnemore, 1967). Far-infrared measurements by Leslie et al. and microwave absorption measurements by Thompson yield lower values of  $2\Delta_0$  and  $2\Delta_0/k_B T_c$  for La. There is reasonable agreement now between the results, obtained by different workers using electron tunneling, for  $T_{c\Delta}$ ,  $2\Delta_0$  and the gap ratio  $2\Delta_0/k_B T_{c\Delta}$  for vapour deposited lanthanum films.

Electron tunneling measurements are known to determine an energy gap characteristic of the surface layer, having a thickness of the order of the coherence length, adjacent to the barrier in a tunnel junction. If the various parameters measured in a tunneling experiment are to correspond to the bulk values, the surface layer next to the barrier should be pure and be characteristic



Table 2 (See text for references)

Superconducting Properties of Lanthanum from Different Measurements.						
Technique	Phase	Film thickness ( $\text{\AA}$ )	Resistivity ratio	$T_c$ ( $^{\circ}\text{K}$ )	$2\Delta_0$ (meV)	$2\Delta_0/k_B T_c$
Far-Infrared absorption	95% fcc	Bulk		6.06	1.49	2.85
Microwave absorption	95% fcc	60,000	5.2 to 45	5.40 to 5.95	0.76 to 1.47	1.64 to 2.87
Point Contact tunneling	fcc	Bulk	17 and 21	6.2	2.14	3.7
	d-hcp	Bulk	17 and 21	5.0	1.60	3.7
Specific heat	91% fcc	Bulk		6.0	1.91	3.7
	96% d-hcp	Bulk		4.9	1.56	3.7
Tunneling in thin films						
Edelstein and Toxen (1966)	95% fcc	14,000	3.13	5.08	0.72	1.65
Hauser (1966)		2,000 - 10,500	2.8 - 7.1	4.95 - 5.0	1.375 - 1.400	3.18 - 3.28
Edelstein (1967)	90% fcc	11,000 - 26,000	3.5 - 3.7	4.69 - 4.97	1.38 - 1.526	3.41 - 3.58
	d-hcp	1,600 - 2,200	1.33 - 1.78	3.28 - 4.37	0.98 - 1.29	3.43 - 3.47
This Work		17,000 - 29,000	4.41 - 5.15	4.83 - 5.39	1.25 - 1.40	3.00 - 3.03

of the bulk metal under study.

Table 3 includes the results that are typical of the Al-I-La junctions in which the properties of superconducting La have been deteriorated purposely or inadvertently. From the results in Table 1, one finds that thick films yield a higher resistivity ratio than thin films and thick films generally have higher values of  $T_{c\Delta}$  and  $2\Delta_0$ . The resistivity ratio, however, does not appear to be the only factor affecting the parameters measured in an electron tunneling experiment. Thus in Table 3, La 9 with 30,000 Å<sup>0</sup> thick La film and resistivity ratio of 3.32 has a lower energy gap than La 5 with a 7700 Å<sup>0</sup> thick La film and resistivity ratio of 1.74. The role of the surface layer adjacent to the barrier in electron tunneling measurements becomes more clear from the results of annealing attempts on Al-I-La junctions discussed in Section 5.1. These results can be explained by assuming the deterioration of the La film adjoining the barrier, due to the interaction of Al<sub>2</sub>O<sub>3</sub> in the barrier by La. Edelstein has also suggested the possibility of reaction between Al<sub>2</sub>O<sub>3</sub> and La from the free energy data on Al<sub>2</sub>O<sub>3</sub> and La<sub>2</sub>O<sub>3</sub>.

Qualitatively similar results for the energy gap measurements in La thin films have been reported by

Table 3

Additional Measurements of Superconducting Properties of Lanthanum Films

Tunnel junction	La film thickness ( $\text{\AA}$ )	Resistivity ratio	$T_{c\Delta}$ ( $^{\circ}\text{K}$ )	$2\Delta_0$ (meV)	$2\Delta_0/k_B T_{c\Delta}$
La-9	30,000	3.32	4.90	0.95	2.25
La-5	7,700	1.74	4.95	1.12	2.62
La-4	2,500	0.58	4.33	0.70	1.88

Hauser and by Edelstein. Edelstein and Toxen were first to report the tunneling measurement of the superconducting energy gap in La thin films. The low values (see Table 2) of the energy gap  $2\Delta_0$  and the ratio  $2\Delta_0/k_B T_C$  obtained in their work, were assumed at the time to support the model of Kuper et al. for La. Further results discussed in this chapter make it seem more probable that the reactivity of La is responsible for the low values of these parameters in La thin films. Hauser prepared Al-I-La junctions by evaporating La onto a substrate which was at  $\sim 80^\circ \text{K}$  before the start of La evaporation. It was observed that  $T_{c\Delta}$ ,  $2\Delta_0$  and  $2\Delta_0/k_B T_{c\Delta}$  had no correlation with the thickness of the La films over a range of  $(2000 \text{ to } 10,500) \text{ \AA}$ . The corresponding values of the resistivity ratios for these films ranged from 2.8 to 7.1. Hauser observed that the temperatures  $T_{cr}$  and  $T_{c\Delta}$  agree fairly well when the La film is about  $2000 \text{ \AA}$  thick. However for about  $10,000 \text{ \AA}$  thick films,  $T_{cr}$  is nearly  $1^\circ \text{K}$  higher than  $T_{c\Delta}$ . Hauser attributed these results to surface effects on the first deposited layers of La (such as contamination with the substrate). No experiments were done to check these suggestions. Edelstein has later reported further results on La which are similar to those reported here. The resistivity ratios of the La films studied in this

work are about 30% higher than those reported by Edelstein; the temperatures  $T_{c\Delta}$  are almost identical but Edelstein has reported about 10% higher values for the energy gap. Such variations in the results would arise due to the differences in junction preparation in the two cases.

Another experiment showing the importance of the surface layer adjoining the barrier on the superconducting properties of La is discussed in Section 5.3. It is shown that two Al-I-La junctions, which are identical except for the nature of the barrier layer, may have their tunneling transition temperatures differing by nearly  $1.5^{\circ}$  K.

Lanthanum was not superconducting above  $1.8^{\circ}$  K as measured by tunneling in La-I-Al junctions. The barrier layer was prepared by oxidizing La in dry oxygen atmosphere. On the other hand, lanthanum was superconducting at  $4.2^{\circ}$  K in such junctions if the barrier layer was prepared by oxidizing La in air. The resistivity ratio of La films was  $\sim 3.2$ .

These results on Al-I-La and La-I-Al junctions demonstrate clearly that an important reason for the differences in the properties of superconducting La, as

measured by electron tunneling in thin film diodes, and the corresponding bulk values is the contamination of the La surface layer, mainly by its interaction with the barrier layer. Factors such as grain size and crystal structure of the La, first suggested by Hauser, may also be important in this regard but we have no evidence that the La films differed in these respects.

Thompson, using microwave absorption has studied the effect of an annealing treatment on the ratio  $2\Delta_0/k_B T_C$  of a lanthanum film. The increase in this ratio with the increase in resistivity ratio, as shown in Table 2, indicates the importance of annealing. We have annealed La films immediately after preparation in a pressure of  $\sim 5 \times 10^{-7}$  mm Hg without breaking the vacuum. The films were heated to  $\sim 225^\circ \text{C}$  for nearly 2 hours by passing a suitable amount of current through them. The resistivity ratio of the film increased from 3.5 to 21 by this annealing process. However, it was not possible to anneal the La film in an Al-I-La junction for reasons which have been discussed earlier.

It is interesting to recall the parallel stages of the energy gap measurements in superconducting  $\text{Nb}_3\text{Sn}$  (see, for example, Bosomworth and Cullen, 1967 and other references mentioned in this paper). Electron tunneling

measurements, with the exception of point contact tunneling, yielded values of  $\frac{2\Delta_0}{k_B T_c}$  significantly less than the BCS value. Vapour deposited  $\text{Nb}_3\text{Sn}$  films yielded  $\frac{2\Delta_0}{k_B T_c} = 1.3$ , single crystal  $\text{Nb}_3\text{Sn}$  yielded an anisotropic energy gap with  $\frac{2\Delta_0}{k_B T_c}$  ranging from 1.0 to 2.8. In comparison, point contact tunneling, thermal conductivity and specific heat measurements all gave  $\frac{2\Delta_0}{k_B T_c} \geq 3.5$  for  $\text{Nb}_3\text{Sn}$ . By infrared reflectivity measurements, the energy gap of as-deposited  $\text{Nb}_3\text{Sn}$  films was  $3.77 k_B T_c$ . After the sample was mechanically polished, it gave  $\frac{2\Delta_0}{k_B T_c} = 1.9$ . The original value of the energy gap was restored by etching away the damaged surface of the sample. The small gap observed with the polished sample was attributed to surface damage. It was also suggested that the surface properties of superconducting  $\text{Nb}_3\text{Sn}$  may differ from the bulk properties and the energy gap may be intrinsically smaller within a mean free path of the  $\text{Nb}_3\text{Sn}$  surface.

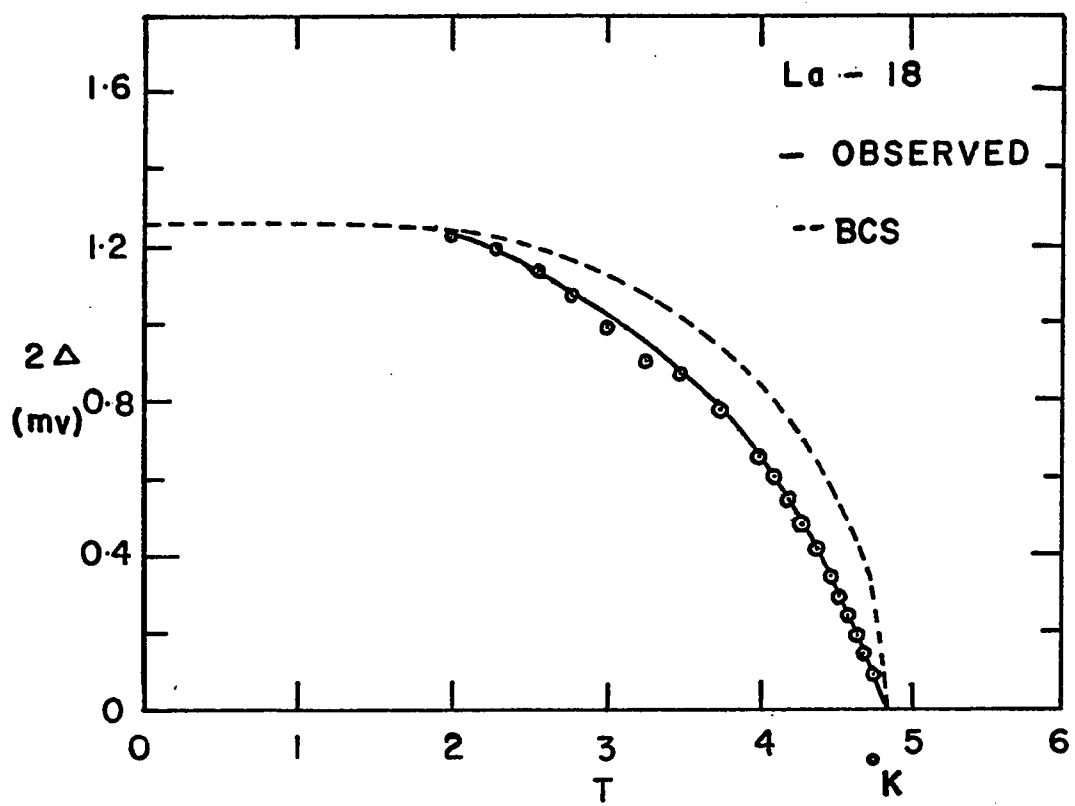
Fig. 5.6 shows the temperature variation of the energy gap in La. The differences in the experimental and calculated results indicate that the weak coupling BCS theory is not applicable to La. These results could be expected in a two-band superconductor (cf., Fig. 2.4). Similar results would also be expected if a fraction of the total current is due to non-tunneling processes in the junction. Edelstein has also studied the energy gap varia-

Figure 5.6

Temperature variation of the energy gap for lanthanum.

The dashed curve is the BCS prediction.





tion with temperature for La. He found that if one fits the low temperature data to a BCS curve, the values at higher temperature fall below the BCS curve.

Further study of the energy gap variation with temperature is thus necessary to reach definite conclusions regarding the multiple gaps in lanthanum. It is desirable to use s-s tunnel junctions for this purpose. The transition temperature of the superconducting probe should be more than the transition temperature of La for accurate determination of the  $\Delta - T$  plot. Thus Pb-I-La junction would be quite appropriate for this work. The problem of deterioration of the surface layer of La adjoining the barrier will have to be overcome.

### 5.3. Zero-Bias Tunneling Anomalies in the n-n Tunnel Junctions

Zero-bias anomalies in normal metal tunnel junctions were discussed earlier in Sections 3.3 and 3.4. Studies of the ZBA are attracting increasing attention of many workers and interesting results have been published while this thesis was under preparation. In this respect, the problem is still open and the conclusions drawn here should be considered to represent the present state of an active field.

Tunnel junctions composed of aluminum and

lanthanum are perhaps the only known tunnel junctions which exhibit such a variety of zero-bias anomalies. The properties of the metal-metal oxide interfaces are believed to be responsible for these anomalies. Small ZBA are well explained by the Appelbaum-Anderson theory of scattering by localized magnetic impurities in the interfaces between the barrier and the metal layers on its opposite sides (Appelbaum, 1966, 1967; Anderson, 1966). The origin of the 'giant' anomaly in the form of a resistance peak is not well understood at present.

#### A. ZBA in Al-I-La Junctions

In most junctions, a temperature dependent peak in conductance at zero bias was observed. Although the magnitude of the ZBA in most cases was  $\sim 2\%$ , junctions having the ZBA ranging from about  $1\%$  to  $20\%$  were also studied. In a few Al-I-La junctions, a small ( $>2\%$ ) resistance peak was observed instead of a conductance peak. Edelstein has earlier reported the presence of about  $2\%$  ZBA in Al-I-La and in manganese doped-aluminum-insulator-lanthanum junctions.

The following experiment was performed to confirm the role of the barrier layer in ZBA in La junctions. A pair of Al-I-La junctions was prepared as described in Section 4.1. Aluminum films for the two

junctions were deposited simultaneously in one evaporation. These films were located in different positions with respect to the discharge electrodes and were oxidized in a glow discharge at the same time. This resulted in a more intense glow during the oxidation process over one Al film than the other. A cross strip of lanthanum was finally evaporated to complete the two junctions. These junctions should thus differ only in the nature of the barrier layer. The resistive transition temperature  $T_{cr}$  of the portion of the La film corresponding to each of the two junctions was above  $5.1^{\circ}$  K. Both junctions showed a zero-bias conductance peak at helium temperatures. At  $4.2^{\circ}$  K, the junction in which the oxidation was done at a fast rate had 18.2% ZBA as compared to 1.9% ZBA in the other junction. The tunneling transition temperatures of La in these junctions were  $3.40^{\circ}$  K and  $4.98^{\circ}$  K respectively. The simultaneous occurrence of a larger ZBA and a smaller  $T_{c\Delta}$  for La in a junction in which the oxide layer was prepared in a more intense discharge is interesting. These effects could arise either from the reaction of La with the barrier layer or from impurities from the electrodes which were introduced in the barrier layer during the oxidation process. Shen has recently reported results in which the magnitude and the sign of the ZBA was found to depend on the impurity concentration sputtered from the electrodes onto the

oxide layer during an ac glow discharge.

Fig. 5.7 shows the voltage dependence of conductance of a tunnel junction showing ZBA at different temperatures. (cf. Fig. 3.2 ). Only a somewhat arbitrary estimate of the background conductance can be made from such plots. At zero bias, the excess conductance above the background varied as  $-\ln T$ . The voltage dependence of the excess conductance was also logarithmic. Similar results have been reported in Ta-I-Al (Wyatt, 1964) and Sn-I-Sn junctions (Shen and Rowell, 1968). The temperature dependence of the conductance at zero bias in Al-I-La junctions was two orders of magnitude stronger than results reported for Ta-I-Al junctions.

The conductance peak shown in Fig. 5.7 changed to a temperature-dependent dip in conductance as the junction temperature was increased. Fig. 5.8 shows the dip in conductance in this junction. The corresponding resistance peak decreased with increase in temperature. The junction temperatures could not be measured above  $5.1^{\circ}\text{K}$  due to experimental limitations. It is clear that both kinds of anomalies were present in this junction with different strengths. This was the first observation of both a conductance peak and a small resistance peak in a single tunnel junction. Structure in the 4 to 10 mv region in Fig. 5.8 should be ignored. Such polarity

Figure 5.7

Voltage dependence of conductance for an Al-I-La tunnel junction showing zero-bias anomaly at different temperatures.

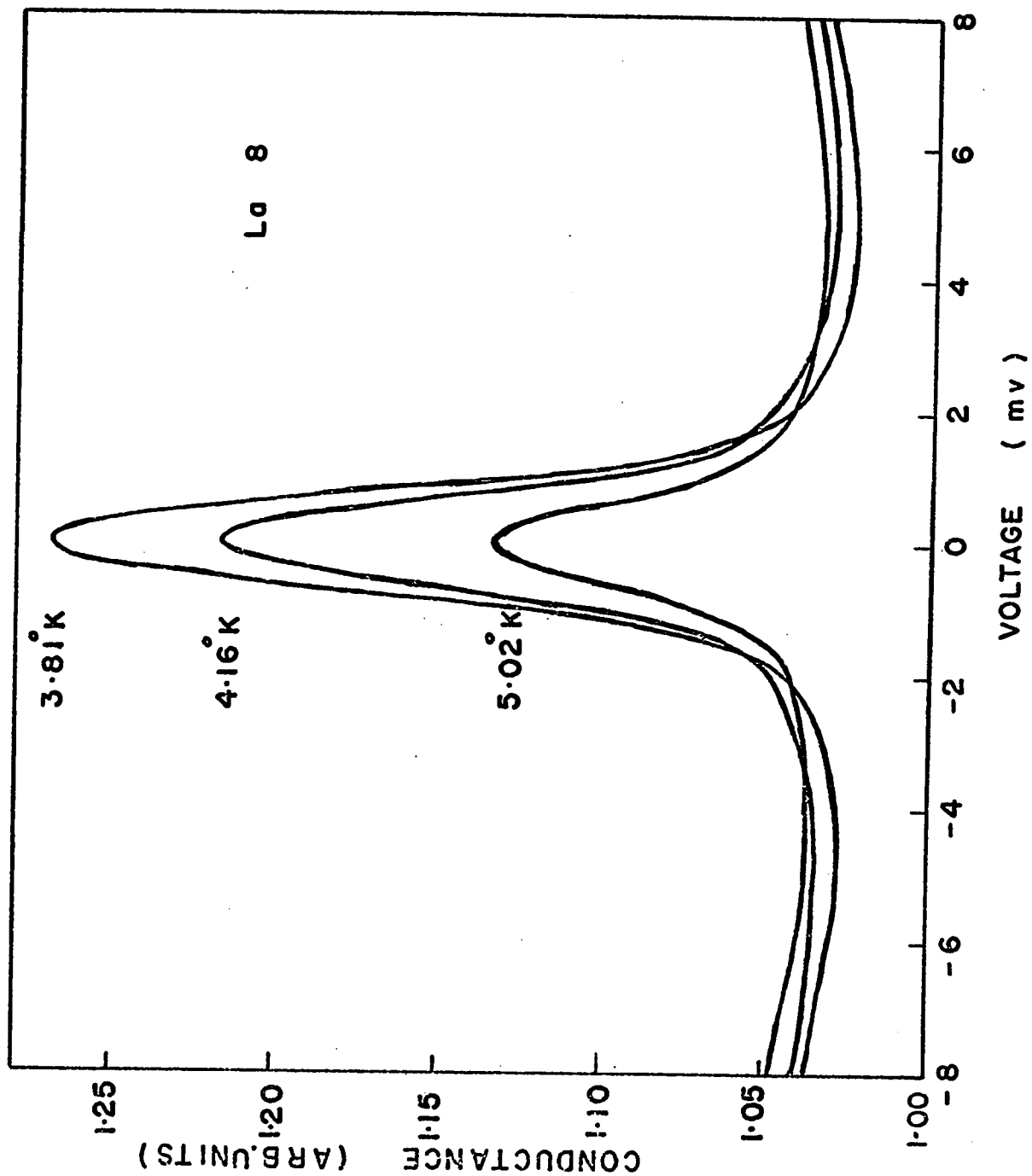
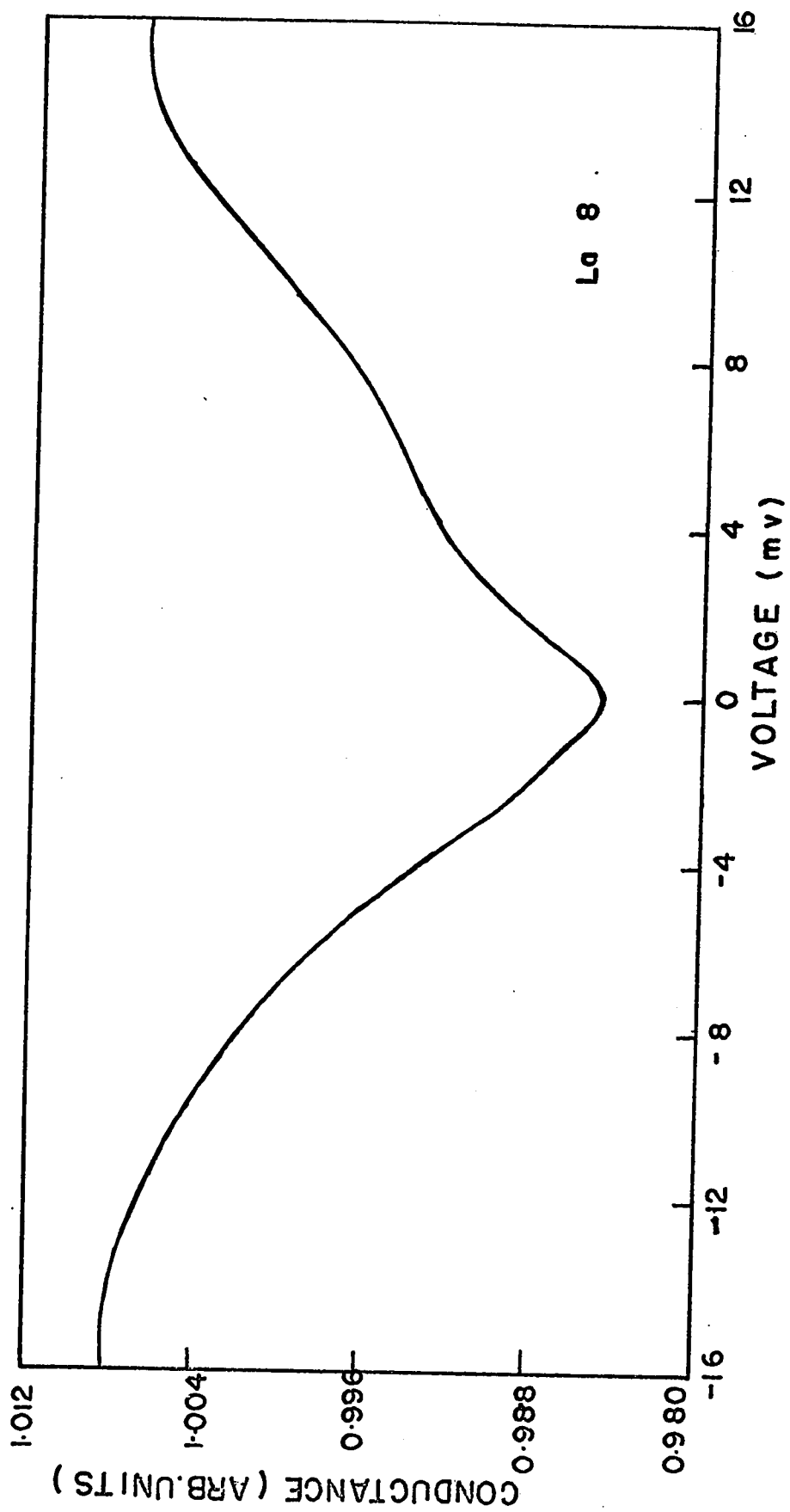


Figure 5.8

Voltage dependence of conductance for an Al-I-La tunnel junction. As the temperature is decreased, the dip in conductance at zero bias changed to a temperature dependent peak in conductance at zero bias as shown earlier in Figure 5.7. The temperature for the plot in Figure 5.8 is above  $5.1^{\circ}\text{K}$ .





dependent structures generally occur with barrier layers of poor quality.

In June 1968, Lythall and Wyatt reported the observation of both a giant resistance peak and a small conductance peak in a single Ti-doped  $\text{Al-Al}_2\text{O}_3\text{-Ag}$  tunnel junction. In a magnetic field, the conductance peak first decreases and at high fields splits into two peaks just as it does in junctions showing the conductance peak alone. The resistance peak increased with increase in Ti impurities and no conductance peak was observed in junctions showing large resistance peak.

We have studied the effect of magnetic field on conductance at zero bias in  $\text{Al-I-La}$  junctions which showed about 2% conductance peak. The conductance at zero bias decreased by 0.05% at a field of 20 kG applied parallel to the metal films at  $4.13^\circ \text{K}$ . No splitting of the conductance peak was observed at this field. Following the results in  $\text{Ta-I-Al}$  junctions, we believe that still higher magnetic fields would be necessary to split the conductance peak in these junctions.

#### B. ZBA in $\text{La-I-Al}$ Junctions

Zero-bias anomalies of much larger magnitude were observed in  $\text{La-I-Al}$  junctions. When the barrier was obtained by oxidizing La in air drawn from the

laboratory, a  $\sim 20\%$  conductance peak at zero bias was observed. However, when the barrier was prepared in pure dry oxygen, a peak in resistance of the tunnel junction was observed at zero bias. This resistance anomaly was two orders of magnitude larger than the corresponding conductance peaks observed in other Al-I-La or La-I-Al junctions. Fig. 5.9 shows the voltage dependence of conductance of such a junction. The variation of the dynamic resistance with voltage for two such tunnel junctions is shown in Fig. 5.10. The resistance at 90 mV is 0.06 times that at zero bias which indicates that there is practically no background conductance in these junctions and the entire tunneling current is involved in this anomalous process. Fig. 5.11 shows the empirical plots of  $r(v) - \ln v$  and  $\sqrt{r(v) - \ln v}$  for such a junction where  $r(v)$  is the resistance of the junction at bias  $v$ . Almost similar results have been reported in Cr-I-Ag and V-I-Ag junctions (Shen and Rowell, 1968).

The origin of the 'giant' resistance anomaly is not well understood. From the results of addition of paramagnetic impurities to the tunneling barrier, there can be little doubt that it is a result of magnetic scattering (Wyatt and Lythall, 1967; Lythall and Wyatt, 1968). Giaever and Zeller (1968) have recently suggested that it is an electrostatic-capacitance effect resulting

Figure 5.9

Voltage dependence of conductance for a La-I-Al tunnel junction.

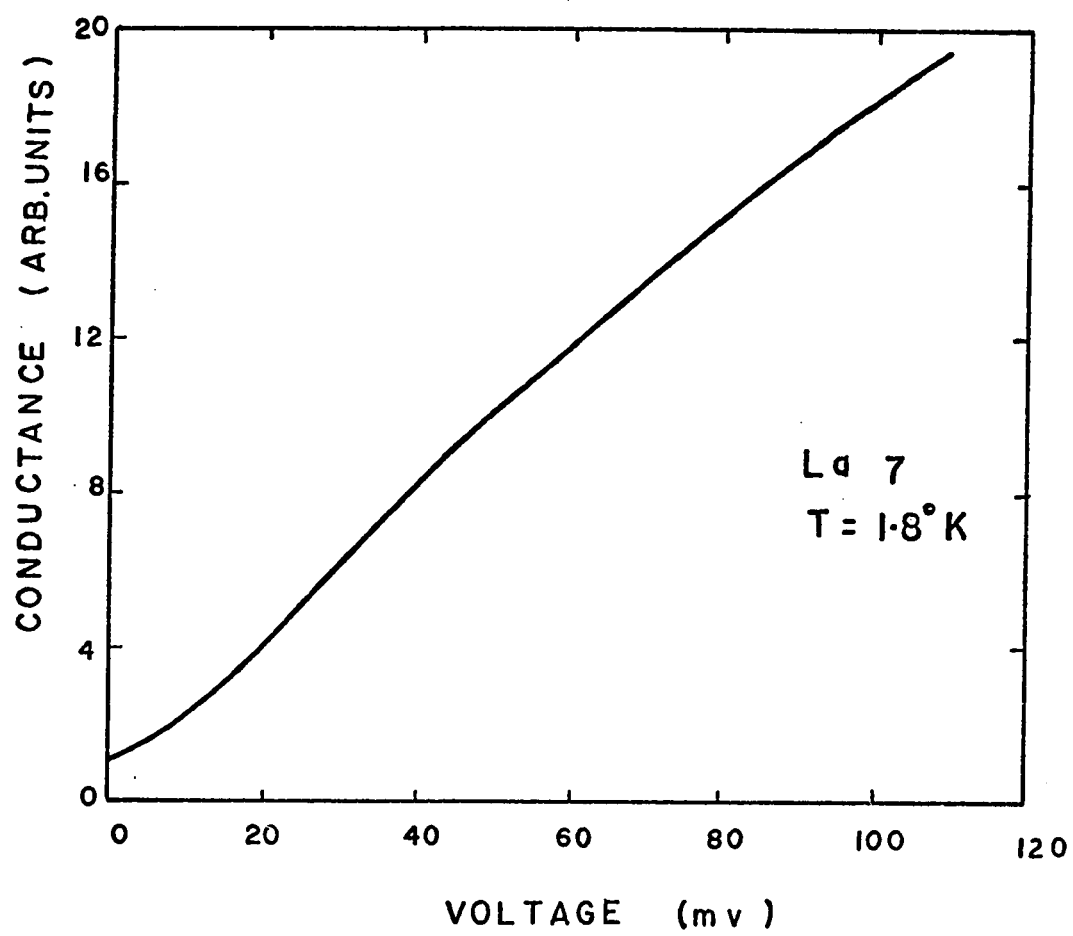


Figure 5.10

Voltage dependence of dynamic resistance for two  
La-I-Al tunnel junctions.

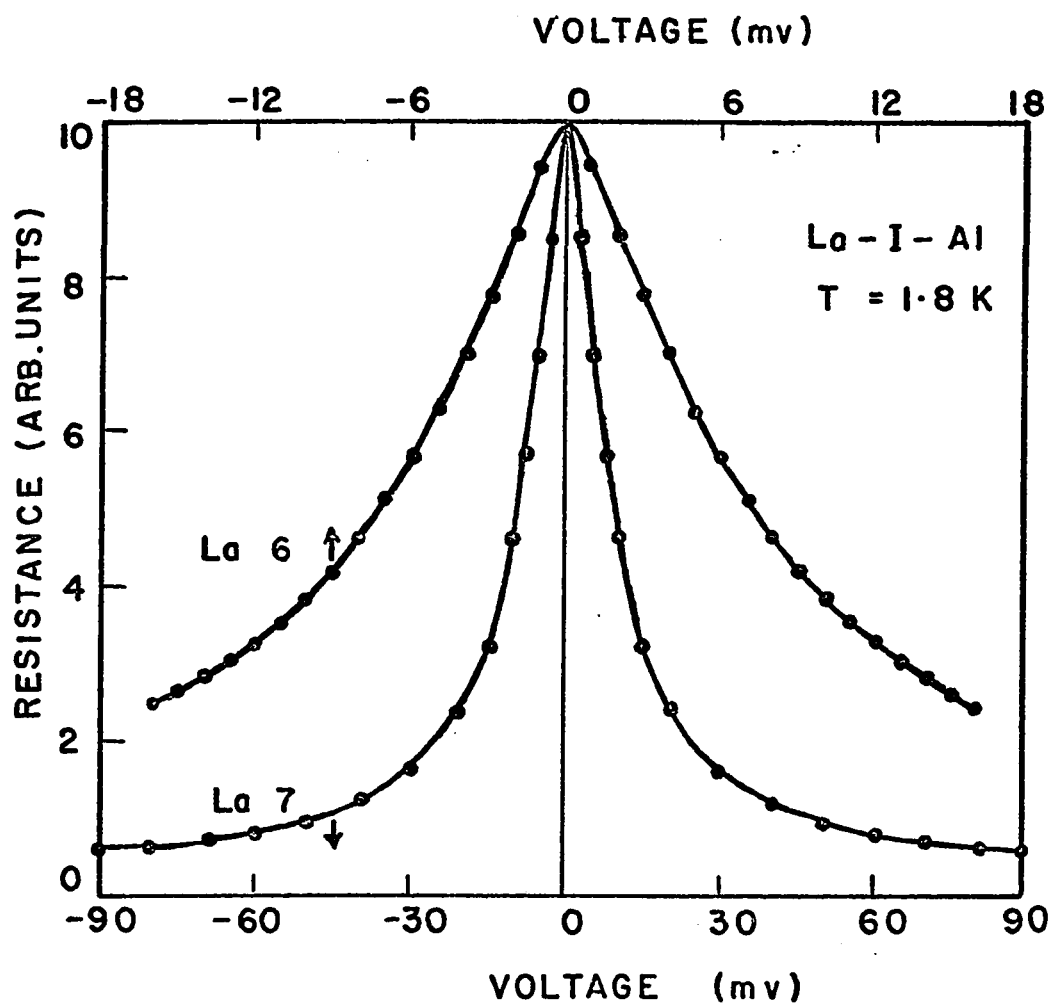
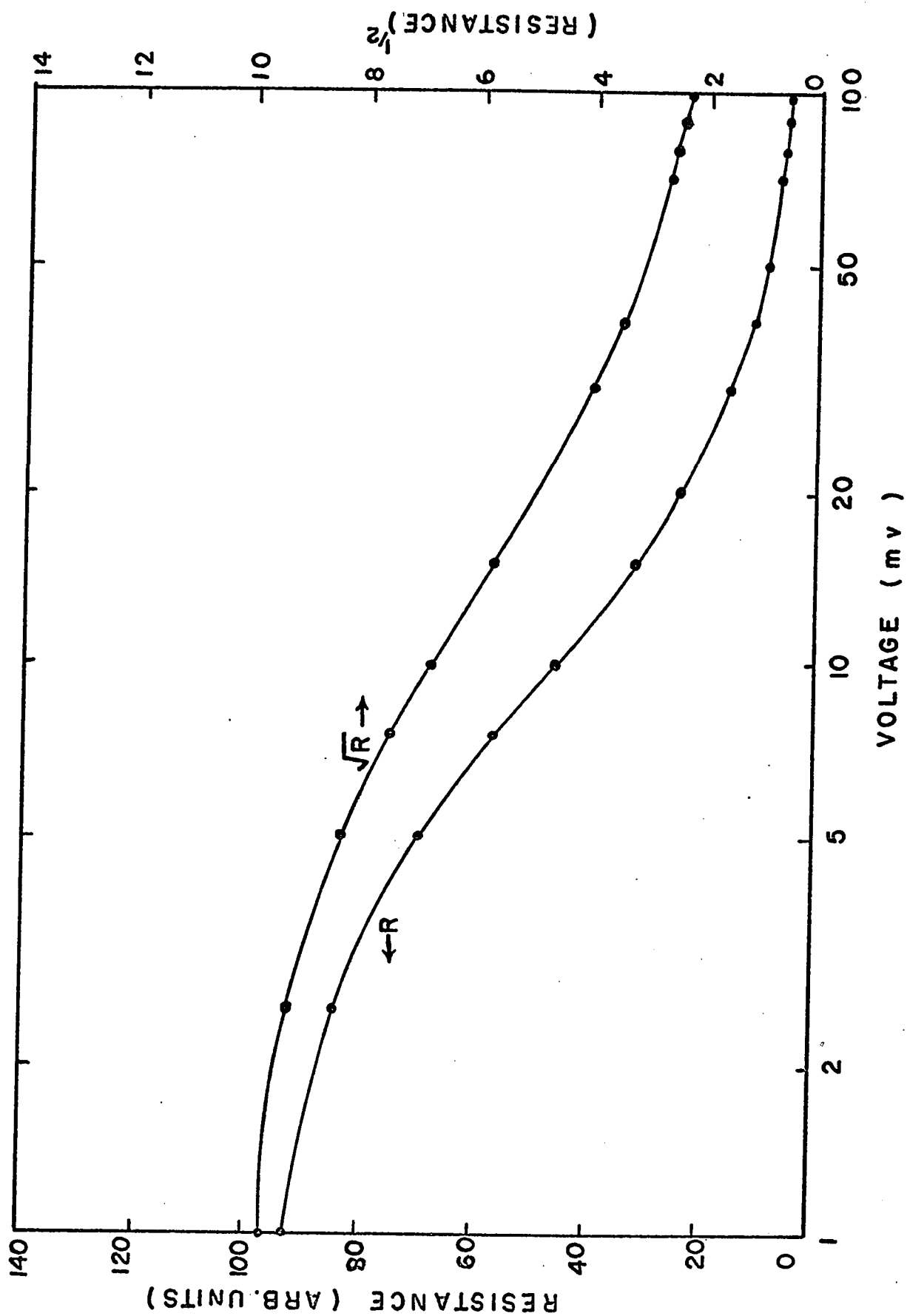
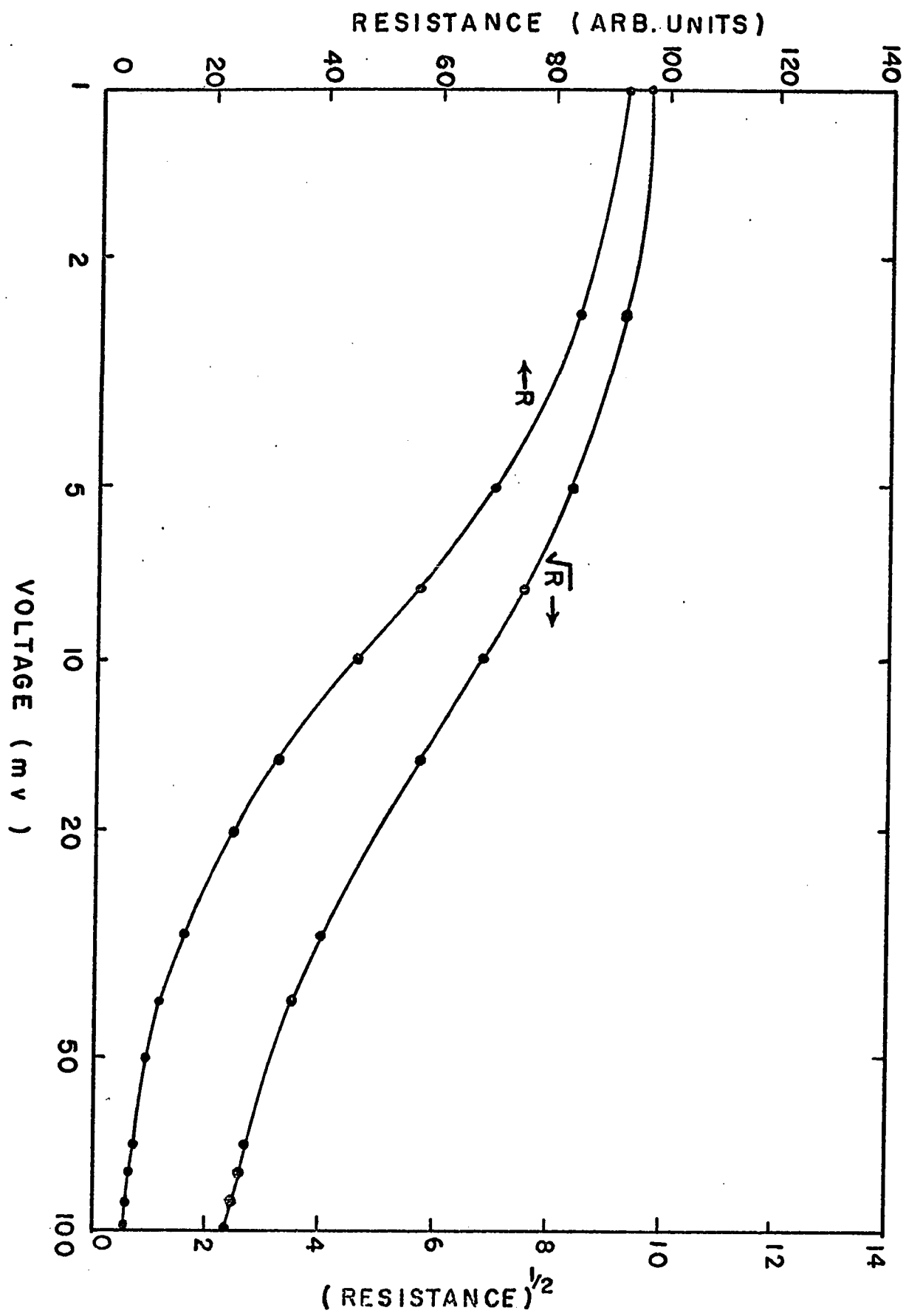


Figure 5.11

Resistance and  $(\text{resistance})^{\frac{1}{2}}$  vs.  $\ln v$  for a La-I-Al tunnel junction.







from a certain distribution of metal particles trapped in the oxide layer. This explanation does not agree with the results reported by Shen.

The effect of the ZBA on the properties of the superconductors constituting the tunnel junction was discussed in Section 3.4. We have earlier seen the effect of the ZBA on  $T_{c\Delta}$  of La in Al-I-La junctions. In La-I-Al junctions showing  $\sim 20\%$  ZBA, the  $T_{c\Delta}$  of La was about  $4.2^\circ$  K. In similar junctions which had 'giant' resistance anomalies, La was not superconducting above  $1.8^\circ$  K. From the resistivity ratio measurements and comparison with other Al-I-La junctions, the  $T_{c\Delta}$  for La was expected to be close to  $5^\circ$  K in these junctions. These results indicate that presence of the ZBA markedly affects the transition temperature  $T_{c\Delta}$  of La. We know that the superconducting properties of La, as measured in an electron tunneling experiment, are highly dependent on the purity of the surface layer of La adjoining the barrier. More detailed work is necessary to understand the effects of this surface layer and those of the ZBA separately, on electron tunneling measurements in general and the superconducting properties of La in particular.

## CHAPTER VI

### CONCLUSIONS

#### 6.1. Results for Superconducting Lanthanum

Structure has been observed in the tunneling density of states of superconducting lanthanum using thin film diodes. Although the structure is broad, the strength of the structure  $S$  scales approximately as the square of the energy gap  $\Delta^2(T)$ , similar to other superconductors e.g., Pb, In, and it is of the order of magnitude ( $\sim 1\%$ ) which one would expect if lanthanum were a phonon-mediated superconductor. The structure in the first and second derivative results may be attributed to a poorly developed phonon spectrum, with transverse and longitudinal peaks at  $\sim 4.5$  meV and 10 meV respectively, in the portion of the lanthanum film sampled by the tunneling experiment. Our results would suggest the Debye temperature  $\theta_D \approx 100^\circ\text{K} \pm 20^\circ\text{K}$  at  $\theta_D$  for the lanthanum material sampled by the experiment. These results should only approximately represent the corresponding features of the phonon spectrum of pure bulk lanthanum. These are the first published data on structure in the tunneling density of states of lanthanum.

The energy gap of lanthanum has been measured using thin film diodes and the results are in reasonable

agreement with similar published results. Our values of the energy gap, the transition temperature and the gap ratio of lanthanum are respectively,  $2\Delta_0 \approx 1.32$  meV,  $T_{c\Delta} \approx 5.1^\circ\text{K}$  and  $2\Delta_0/k_B T_{c\Delta} \approx 3.0$  and are lower than the reported bulk values (see Table 2). The surface layer of lanthanum adjoining the barrier was found to play an important role in these measurements and the differences in these results and bulk values are attributed to contamination of this surface layer, mainly by interaction of La with the barrier layer in the tunnel junction. There was little evidence for the second energy gap in lanthanum as envisaged by Kuper et al. (1964) and more work is necessary to check this prediction.

These results for the energy gap and the structure in the tunneling density of states of lanthanum are in accord with the present theories of superconductivity and indicate that the electron-phonon interaction may be largely responsible for superconductivity of La. However, in view of the lower values of the various parameters of superconducting lanthanum from measurements on thin film diodes, it is not possible to entirely exclude the possibility that some other mechanism(s) may be responsible for the superconductivity of this element.

## 6.2. Results on Zero-Bias Anomalies

Zero-bias anomalies have been observed in Al-I-La and La-I-Al junctions. Although a ~2% ZBA was reported by Edelstein (1967) in Al-I-La junctions, these results are the first report of much larger ZBA in these junctions. It was observed that both types of ZBA viz, in form of a conductance or a resistance peak, could be observed in a single tunnel junction. Recently Lythall and Wyatt (1968) have reported the presence of a resistance peak along with a small conductance peak at zero bias in a single junction as compared to our results. It was shown that these anomalies arise due to the impurities in the metal-metal oxide interface in the junction. The ZBA was also found to affect the superconducting properties of lanthanum. At present, there is no single theory which can explain all the results. The small ZBA in these junctions are similar to those observed in Sn-I-Sn (Shen and Rowell, 1968) or Ta-I-Al (Wyatt, 1964) junctions which can be explained by the Appelbaum-Anderson model of scattering by localized magnetic impurities in the metal-metal oxide interfaces (Appelbaum, 1966, 1967; Anderson, 1966). 'Giant' ZBA in form of a resistance peak were observed in La-I-Al junctions similar to those observed in Cr-I-Pb junctions (Shen and Rowell, 1968). The origin of the 'giant' anomaly is not clearly understood. Much more work has to be done for better understanding of zero-bias anomalies in tunnel junctions.

## STRUCTURE IN THE TUNNELING DENSITY OF STATES OF SUPERCONDUCTING La†

J. S. Rogers and S. M. Khanna

Department of Physics, University of Alberta, Edmonton, Alberta, Canada

(Received 8 April 1968)

Structure has been observed in the tunneling characteristics of La thin-film diodes which may be attributed to a poorly developed phonon spectrum in the portion of the La film sampled by the experiment.

It has frequently been suggested that a magnetic interaction may be primarily responsible for the superconductivity of some of the transition metals. Such ideas would gain considerable impetus if experimental data were available which were at variance with existing formalisms of superconductivity,<sup>1</sup> and it would help considerably if the experiments were ones which portrayed the electron-phonon interaction in a fairly direct manner so that any variance would be readily recognized.

The electron-tunneling experiment is one of this type,<sup>2</sup> and Wyatt<sup>3</sup> has demonstrated phonon effects in Ta and Nb in this manner. The posi-

tion of La is less certain. Levinstein, Chirba, and Kunzler<sup>4</sup> have reported seeing phonon effects of amplitudes intermediate between those for Sn and Pb during the course of preliminary point-contact tunneling measurements with La, but Edelstein<sup>5</sup> has reported seeing no such effects with La thin-film tunnel diodes. The lack of sharp phonon effects in thin films may be attributed to lattice disorder, but in view of the results of Chen *et al.*,<sup>6</sup> who observed phonon effects in amorphous Bi, or of Zavaritskii,<sup>7</sup> who observed phonon effects in Pb films having a deliberately distorted lattice, one would not expect phonon effects to be totally absent in La thin films. This

conjecture is confirmed by the results reported here.

The diodes were formed by evaporating La from a Ta boat onto an Al film which had previously been subjected to a glow discharge in oxygen at  $\sim 0.1$ -Torr pressure. The La deposition rates were  $\sim 500$  Å/sec, the substrates were glass at 300°K, and the system vacuum prior to La deposition was  $\sim 10^{-7}$  Torr. Masking definition and film widths were such that we believe over 90% of the tunneling was into La film regions of thickness  $\geq 1$   $\mu$ . The resulting residual resistivity ratios for the La films were only 5 or 6 however, corresponding to an electron free path of  $\sim 50$  Å. Since the bulk starting material had a resistivity ratio of 20, we assign this short free-path value to lattice defects.

Attempts to anneal the films by allowing the fabricated diodes to remain at 300°K in a vacuum or a pure He atmosphere for even a few hours caused a marked degradation of all parameters measured by tunneling. In particular, the energy gap  $2\Delta_0$ , the transition temperature  $T_C$ , and the ratio  $2\Delta_0/kT_C$  all became smaller, while positive zero-bias conductance anomalies of  $\sim 1\%$  amplitude became larger and the conductance at high bias voltages became erratic. The annealing attempts did not cause any appreciable change in the film resistivity ratios or the transition temperatures determined by film resistance measurements.

Taken collectively, these results suggest that thermal energy promotes a degradation of the oxide-La interface, and that the degradation influences the superconducting state of the tunneling-sampled La material immediately behind this interface.

The fabrication technique which we have adopted is accordingly a compromise between deposition onto a cold substrate,<sup>8</sup> which would smear the phonon spectrum, and deposition onto a hot substrate, which would destroy the tunneling barrier. Since this fabrication method has resulted in reasonably reproducible tunneling results on three successive attempts, only the results obtained from one diode are presented.

The energy gap value  $2\Delta_0 = 1.4$  meV was obtained by fitting the Bermon calculations to the experimental data. The fit was not good in the sense that the same difficulties were encountered as those reported by Edelstein.<sup>5</sup> Our assignment of a single energy-gap value to the tunneling results is therefore only an approximation, but it is quite adequate in view of the extreme variability

of results which may be obtained with these diodes if fabrication parameters are altered. In this sense, our values for the transition temperature and gap ratio,  $T_C \approx 5.0^\circ\text{K}$  and  $2\Delta_0/kT_C \approx 3.2$ , are in reasonable accord with those obtained by other workers, but they are not representative of bulk hcp La ( $T_C = 4.9^\circ\text{K}$ ,  $2\Delta_0/kT_C = 3.7$ ), or bulk fcc La ( $T_C = 6.0^\circ\text{K}$ ,  $2\Delta_0/kT_C = 3.7$ ).<sup>9</sup>

Results which have been obtained at higher energies are shown in Fig. 1. The dynamic conductance  $g(v) = di/dv$  was measured with an ac bridge technique, due care having been taken with regard to modulation levels and normalization procedures. The normal-state first-derivative characteristic  $g_n(v)$  which enters Fig. 1 was obtained with the aid of a magnetic field rather than an increase in temperature. This was done because the zero-bias anomalies present were observed to exhibit some temperature dependence but negligible magnetic field dependence at high bias values.

While it is true that sharp structure of amplitude  $\approx 0.1\%$  is not present in the first-derivative results, the overall results do show some resemblance to the phonon structure for In.<sup>10</sup> The normalized results were also independent of bias polarity, the gross first-derivative departure from BCS scaled approximately as  $\Delta(T)^2$ , and the amplitude of the gross structure is of the order of magnitude ( $\sim 1\%$ ) which one would expect if La were a phonon-mediated superconductor.

The first- and second-derivative results are thus suggestive of a phonon spectrum consisting of transverse and longitudinal peaks at  $\sim 4.5$  and 10 meV, respectively. The Debye temperature  $\Theta_D$  (at  $\Theta_D$ ) affords an approximate ( $\pm 20\%$ ) cross check on the longitudinal energy in that this energy is usually  $(1.1-1.4)\kappa\Theta_D$ . Our results would therefore suggest  $\Theta_D \approx 100^\circ\text{K}$  at  $100^\circ\text{K}$ ; the specific-heat results of Johnson and Finnemore<sup>9</sup>

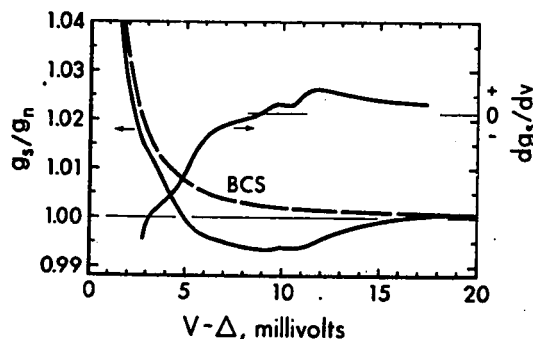


FIG. 1. Normalized first-derivative ( $g = di/dv$ ) and second-derivative results for an Al-Al<sub>2</sub>O<sub>3</sub>-La tunnel diode at 2.05°K.



yield  $\Theta_D \approx 120^\circ\text{K}$  at  $10^\circ\text{K}$  for hcp or fcc La.

In conclusion, we have observed structure in the tunneling characteristics of La thin-film diodes which may be attributed to a broad phonon spectrum in the material sampled by the tunneling measurement, but we do not expect this spectrum to be a good representation of pure bulk La.

Thus, while our results are in accord with the present theories of superconductivity which are based on an electron-phonon interaction, the resolution obtained is not sufficient to rule out the possibility that some other mechanism may be responsible for the superconductivity of La. It would appear, however, that any alternative theory must predict a departure (or departures) in the tunneling density of states near the Debye energy which is not much different in amplitude from those given by the present theories.

We would like to thank Professor S. B. Woods, Professor J. P. Franck, and Professor S. S. Shein-in for many interesting discussions relevant to

this work.

---

†Work supported, in part by the National Research Council of Canada.

<sup>1</sup>P. W. Anderson and B. T. Matthias, *Science* **144**, 373 (1964).

<sup>2</sup>J. M. Rowell and L. Kopf, *Phys. Rev.* **137**, A907 (1965).

<sup>3</sup>A. F. G. Wyatt, *Phys. Rev. Letters* **13**, 160 (1964).

<sup>4</sup>H. J. Levinstein, V. G. Chirba, and J. E. Kunzler, *Phys. Letters* **24A**, 362 (1967).

<sup>5</sup>A. S. Edelstein, *Phys. Rev.* **164**, 510 (1967).

<sup>6</sup>J. T. Chen, T. T. Chen, J. D. Leslie, and H. J. T. Smith, *Phys. Letters* **25A**, 679 (1967).

<sup>7</sup>N. V. Zavaritskii, *Zh. Eksperim. i Teor. Fiz. - Pis'ma Redakt.* **6**, 668 (1967) [translation: *JETP Letters* **6**, 155 (1967)].

<sup>8</sup>J. J. Hauser, *Phys. Rev. Letters* **17**, 921 (1966).

<sup>9</sup>D. L. Johnson and D. K. Finnemore, *Phys. Rev.* **158**, 376 (1967).

<sup>10</sup>J. G. Adler, J. S. Rogers, and S. B. Woods, *Can. J. Phys.* **43**, 557 (1965).

BIBLIOGRAPHY

- Adler, J.G., (1963) Electron Tunneling into Superconductors. Doctoral Thesis (unpublished), University of Alberta, Edmonton.
- Adler, J.G., (1968) (Private communication).
- Adler, J.G. and Rogers, J.S., (1963) Phys. Rev. Letters 10, 217.
- Adler, J.G., Rogers, J.S. and Woods, S.B., (1965) Can. Jour. Phys. 43, 557.
- Anderson, P.W., (1966) Phys. Rev. Letters 17, 95.
- Anderson, P.W. and Matthias, B.T., (1964) Science 144, 373.
- Appelbaum, J., (1966) Phys. Rev. Letters 17, 91.
- Appelbaum, J.A., (1967) Phys. Rev. 154, 633.
- Appelbaum, J.A., Phillips, J.C. and Tzouras, G., (1967) Phys. Rev. 160, 554.
- Bardeen, J., (1961) Phys. Rev. Letters 6, 57.
- Bardeen, J., Cooper, L.N. and Schrieffer, J.R., (1957 a) Phys. Rev. 106, 162.
- Bardeen, J., Cooper, L.N. and Schrieffer, J.R., (1957 b) Phys. Rev. 108, 1175.
- Bermon, S., (1964) University of Illinois Technical Report No. 1, Grant No. NSF-GP 1100 (Unpublished).
- Bermon, S. and Ginsberg, D.M., (1964) Phys. Rev. 135, A306.
- Blandin, A., (1961) J. Phys. Radium 22, 507.
- Bogoliubov, N.N., (1958) Soviet Phys.-JETP 7, 41.
- Bosomworth, D.R. and Cullen, G.W., (1967) Phys. Rev. 160, 346.
- Chen, J.T., Chen, T.T., Leslie, J.D. and Smith, H.J.T., (1967) Phys. Letters 25A, 679.
- Cohen, M.H., Falicov, L.M. and Phillips, J.C., (1962) Phys. Rev. Letters 8, 316.
- Cooper, L.N., (1956) Phys. Rev. 104, 1189.

- De Sorbo, W., (1963) Phys. Rev. 132, 107.
- Edelstein, A.S., (1967) Phys. Rev. 164, 510.
- Edelstein, A.S. and Toxen, A.M., (1966) Phys. Rev. Letters 17, 196.
- Eliashberg, G.M., (1960) Soviet Phys.-JETP 11, 696.
- Fowler, R.D., Lindsay, J.D.G., White, R.W., Hill, H.H. and Matthias, B.T., (1967) Phys. Rev. Letters 19, 892.
- Garland, J.W., (1963) Phys. Rev. Letters 11, 111.
- Gerstenberg, D. and Hall, P.M., (1964) J. Electrochem. Soc., 111, 936.
- Giaever, I., (1960 a) Phys. Rev. Letters 5, 147.
- Giaever, I., (1960 b) Phys. Rev. Letters 5, 464.
- Giaever, I., Hart, H.R. Jr. and Megerle, K., (1962) Phys. Rev. 126, 941.
- Giaever, I. and Zeller, H.R., (1968) Phys. Rev. Letters 20, 1504.
- Ginsberg, D.M., Richards, P.L. and Tinkham, M., (1959) Phys. Rev. Letters 3, 337.
- Hall, R.N., Racette, J.H. and Ehrenreich, H., (1960) Phys. Rev. Letters 4, 456.
- Hamilton, D.C. and Jensen, M.A., (1963) Phys. Rev. Letters 11, 205.
- Harrison, W.A., (1961) Phys. Rev. 123, 85.
- Hauser, J.J., (1966) Phys. Rev. Letters 17, 921.
- Johnson, D.L. and Finnemore, D.K., (1967) Phys. Rev. 158, 376.
- Khanna, S.M., (1965) Recombination Effects on Electron Tunneling into Superconducting Lead, M.Sc. Thesis (unpublished), University of Alberta, Edmonton.
- Kondo J., (1963) Prog. Theor. Phys. 29, 1.
- Kuper, C.G., Jensen, M.A. and Hamilton, D.C., (1964) Phys. Rev. 134, A 15.

- Kunzler, J.E., (1968) (Private Communication).
- Leslie, J.D., Cappelletti, R.L., Ginsberg, D.M., Finnemore, D.K., Spedding, F.H. and Beaudry, B.J., (1964) Phys. Rev. 134, A 309.
- Levinstein, H.J., Chirba, V.G. and Kunzler, J.E., (1967) Phys. Letters 24A, 362.
- Logan, R.A. and Rowell, J.M., (1964) Phys. Rev. Letters 13, 404.
- London, H. and Clark, G.R., (1964) Rev. Mod. Phys. 36, 320.
- Lythall, D.J. and Wyatt, A.F.G., (1968) Phys. Rev. Letters 20, 1361.
- Matthias, B.T., (1957) Prog. in Low Temperature Physics (Ed. C.J. Gorter, North-Holland Publishing Company, Amsterdam) 2, 138.
- Maxwell, E., (1950) Phys. Rev. 78, 477.
- Miles, J.L. and Smith, P.H., (1963) J. Electrochem. Soc. 110, 1240.
- Onnes, H.K., (1911) Leiden Comm. 122b, 124c.
- Rairden, J.R. and Neugebauer, C.A., (1964) Proc. IEEE 52, 1234.
- Reynolds, C.A., Serin, B., Wright, W.H. and Nesbitt, L.B., (1950) Phys. Rev. 78, 487.
- Rogers, J.S., (1964) Phonon Effects on Electron Tunneling into Superconductors, Ph.D. Thesis (unpublished), University of Alberta, Edmonton.
- Rogers, J.S., Adler, J.G. and Woods, S.B., (1964) Rev. Sci. Instr. 35, 208.
- Rowell, J.M., (1968) (Private communication).
- Rowell, J.M., Anderson, P.W. and Thomas, D.E., (1963) Phys. Rev. Letters 10, 334.
- Rowell, J.M. and Kopf, L., (1965) Phys. Rev. 137, A 907.
- Rowell, J.M. and Shen, L.Y.L., (1966) Phys. Rev. Letters 17, 15.

- Scalapino, D.J. and Anderson, P.W., (1964) Phys. Rev. 133, A 921.
- Scalapino, D.J., Wada, Y. and Swihart, J.C., (1965) Phys. Rev. Letters 14, 102.
- Schrieffer, J.R., Scalapino, D.J. and Wilkins, J.W., (1963) Phys. Rev. Letters 10, 336.
- Shapiro, S., Smith, P.H., Nicol, J., Miles, J.L. and Strong, P.F., (1962) I.B.M. Jour. Research and Development 6, 34.
- Shen, L.Y.L., (To be published).
- Shen, L.Y.L. and Rowell, J.M., (1968) Phys. Rev. 165, 566.
- Shen, L.Y.L., Senozan, N.M. and Phillips, N.E., (1965) Phys. Rev. Letters 14, 1025.
- Shewchun, J. and Williams, R.M., (1965) Phys. Rev. Letters 15, 160.
- Suhl, H., Matthias, B.T. and Walker, L.R., (1959) Phys. Rev. Letters 3, 552.
- Thompson, W.A., (1967) Phys. Letters 24A, 353.
- Toxen, A.M., Burns, M.J. and Quinn, D.J., (1965) Phys. Rev. 138, A 1145.
- Van Hove, L., (1953) Phys. Rev. 89, 1189.
- Woods, S.B. and Rogers, J.S., (1966) Proceedings of the Tenth International Conference on Low Temperature Physics, Moscow., (To be published).
- Wühl, H., Jackson, J.E. and Briscoe, C.V., (1968) Phys. Rev. Letters 20, 1496.
- Wyatt, A.F.G., (1964 a) Phys. Rev. Letters 13, 401.
- Wyatt, A.F.G., (1964 b) Phys. Rev. Letters 13, 160.
- Wyatt, A.F.G. and Lythall, D.J., (1967) Phys. Letters 25A, 541.
- Zavaritskii, N.V., (1967 a) Soviet Phys.-JETP Letters 5, 352.
- Zavaritskii, N.V., (1967 b) Soviet Phys.-JETP Letters 6, 155.